ARAB ACADEMY FOR SCIENCE, TECHNOLOGY & MARITIME TRANSPORT

College of Engineering and Technology
Department of Mechanical Engineering

Ocean Current Estimation and Mapping Using Autonomous Underwater Vehicle

By

Omar Hesham Ahmed Ezzat Rashed

A thesis submitted to AASTMT in partial fulfillment of the requirements for the award of the degree of

MASTER OF SCIENCE

in

MECHANICAL ENGINEERING

Supervised by

Prof. Dr. Abdelaziz Morgan
Professor in Mechanical Engineering Dept.
Ain shams University, Cairo, Egypt

Prof. Dr. Mohamed Abdellatif
Professor in Mechanical Engineering Dept.
Future University in Egypt, Cairo, Egypt

Prof. Dr. Sameh Shaaban
Professor in Mechanical Engineering Dept.
Arab Academy for Science and Technology, Cairo, Egypt

2019

Declaration

I certify that all the material used in this thesis which is not my own work has been identified, and that no material is included for which a degree has previously been conferred on me.

The contents of this thesis reflect my own personal views, and are not necessarily endorsed by the university.

Eng. Omar Hesham Ahmed Ezzat Rashed

Signature ………….

Date / / 2019

We specify that we have read the present work and that in our opinion it is fully adequate in scope and quality as thesis towards the partial fulfillment of the Master Degree requirements in

Specification ……………………

From

College of Engineering and Technology (AASTMT)

Date …………………………

Supervisors:

Name: **Prof. Dr. Abdelaziz Morgan**

Position: Professor in Mechanical Engineering Dept., Ain shams University, Cairo, Egypt

Signature: ………………………………..

Name: **Prof. Dr. Mohamed Abdellatif**

Position: Professor in Mechanical Engineering Dept., FutureUniversity, Cairo, Egypt

Signature: ………………………………..

Examiners:

Name:

Position: .

Signature: ………………………………..

Name:

Position:

.

Signature: ………………………………..

Name: **Prof. Dr. Sameh Shaaban**

Position: Professor in Mechanical Engineering Dept., Arab Academy for Science and Technology.

Signature:……

Abstract

Autonomous Underwater Vehicles (AUVs) have been a trending research field in the last three decades due its wide range of applications such as oceanography, oil and gas field, geoscience, weather prediction, search and rescue, and military applications. Therefore, the technology behind the AUVs become more intelligent to perform the required complicated missions without human intervention. One of the main challenges of the AUV technology is the environmental disturbances such as ocean currents, waves, winds which disturb the AUV to complete its mission perfectly. Here, the unknown ocean current is considered as the only main disturbance that acts on the AUV. The main objective is to identify the current disturbance parameters and work under this disturbance without deviating from the planned mission path. So, the unknown ocean current is estimated using nonlinear observer and mapped along the scanned area by the AUV. Then, this estimation is used in guiding and controlling the vehicle to maintain the desired mission trajectory. In addition, the mapping of the ocean current is important in planning the AUV missions and avoiding vortices and violent currents that could losen the control of the vehicle. Also, the generated map is used in the ocean current surveillance that helps in oceanography studies and ocean weather prediction. In this research, a complete 6 DOF nonlinear model is derived and implemented in Matlab software using Hydrographic Research Centre (HRC)-AUV parameters and validated using experimental trial provided by the literature. Then, the nonlinear observer and guidance control system are designed to deal with v ocean current disturbance. Line Of Sight (LOS) guidance law is used in path following mission however it cannot be applied to the ocean current disturbance case. Adaptive LOS guidance that depends on the ocean current estimation is implemented and compared to the old integral LOS method. The comparison shows that the adaptive LOS increased the tracking performance in variable ocean current case with 32.27% compared to the traditional LOS guidance and with 30.5% compared to ILOS guidance. Different simulation cases are applied to the system to evaluate the performance of the observer which show a successful estimation and mapping. So, the estimated ocean current improves the tracking performance of the adaptive LOS guidance compared to the traditional LOS and Integral LOS methods.

Acknowledgement

First of all, thanks to ALLAH for aiding, guiding and giving me power to accomplish this work.

I wish to express my greatest appreciation and deepest gratitude to the thesis supervisors. My sincere thanks to Prof. Dr. Mohamed Abdellatif for the invaluable guidance and unrelenting support he showed. His discussions, suggestions and keen follow-up made the realization of this study possible.

My sincere gratitude is going to Prof. Dr. Abdelaziz Morgan and Prof. Dr. Sameh Shaaban for their grateful support and assistance in making this thesis. Discussions with them have been very practical and gave me the engineering feeling and sense.

Special Thanks to Dr. Mostafa Rostom, and Dr. Amany Khaled for their grateful help and support throughout this work.

My deep appreciation and gratefulness are to all the people at Mechatronics Program, professors, colleagues, and the whole staff, for their endless support and help in all my work.

Last and not the least, I'm so grateful to my great family and my wonderful friends for their patience, continuous encouragement, and their endless prayers through the progress of this work. No words can do them true justice.

Table of Contents

List of Figures

LIST OF TABLES

NOMENCLATURE

BG	Distance between centre of gravity & centre of bouncy [m]
C_{RB}	Coriolis and centripetal vector of rigid body [N.s/m]
C_a	Coriolis matrix including added Coriolis [N.s/m]
CE	Cross track error [m]
$D_l(V) = \{X_u, Y_v, Z_w, K_p, M_q, N_r\}$	1st order damping parameters [N.s/m]
$D_c(V)$	2nd order damping parameters [N.s/m]
e	Eccentricity [m]
g (η):	vector of gravitational forces and moments “hydrostatic term” [N]
I	Moment of inertia [Kg.m]
IAE	integral absolute error [m.s]
k	Observer gain
L	AUV length [m]
m	Mass [Kg]
m_e	mass of the prolate spheroid [Kg]
M	inertia matrix including the added mass [kg, kg.m]
M_{RB}	inertia matrix of rigid body [kg, kg.m]
$M_A = \{X_{\dot{u}}, Y_{\dot{v}}, Z_{\dot{w}}, K_{\dot{p}}, M_{\dot{q}}, N_{\dot{r}}\}$	added mass inertia matrix [kg, kg.m]
n	Propeller revolution speed [rpm]
$P(t) = [x, y]^T$	instantaneous position of the AUV [m]
P_{int}	point of interest [m]

R	AUV radius [m]
$r_G = [x_G\ y_G\ z_G]^T$	distance between the origin (OB) and the centre of gravity (GC) [m]
S	long track error [m]
SD	standard deviation [m]
T_A	Fluid Kinematics [J]
t	Time [s]
ts	Sampling time [s]
V=[u,v,w,p,q,r]	Velocity vector in 6 DOF [m/s]
Vr	Relative velocity [m/s]
$V_c = [u_c \quad v_c \quad w_c \quad 0 \quad 0 \quad 0]^T$	Ocean current velocity [m/s]
V_c^E	Current velocity relative to earth frame [m/s]
W	Path waypoints [m]
$\mathbf{x}_1$	State space vector of attitude
$\mathbf{x}_2$	State space vector of velocity
β_c	Current angle [deg]
τ=[X Y Z K M N]	vector of control input forces [N, N.m]
η=[x,y,z, ϕ, θ, ψ]	Vector of attitude in 6 DOF [m, deg]
ω	Rotation angle [rad/s]
μ_{roll} and μ_{pitch}	relative damping ratios
∇	Volume of the vehicle[m^3]

$\boldsymbol{\varepsilon}$	the difference between system dynamics and system model
γ_p	angle between any two waypoints [deg]
ψ_{los}	deriving yaw angle for the vehicle [deg]
α	the integral gain in ILOS guidance law [deg]

List of Abbreviations

ADCP	Acoustic Doppler Current Profiler
AGV	Autonomous Ground Vehicles
AI	artificial intelligence
ATT	Acoustic Travel Time
AUV	Autonomous Underwater Vehicles
BC	Buoyancy Center
CB	constant bearing
CFD	Computational Fluid Dynamics
CTD	Conductivity Temperature Depth sensor
CURV	Cable-controlled Underwater Recovery Vehicles
DOF	Degree Of Freedom
DVL	Doppler velocity log
GC	Gravity Center
GPS	Global Positioning system

HRC-AUV	Hydrographic Research Centre “type of AUVs”
HRI	Human Robotic Interface
HUGIN	High Precision Untethered Geo-survey and Inspection system
ILOS	Integral Line Of Sight
IMU	Inertial Measurement Unit
INS	Inertial Navigation system
IoUT	Internet of Underwater Things
KF	Kalman Filter
LBS	Long Base Bine
LOS	Line Of Sight
NIST	National Institute of Standards and Technology
NTNU AMOS	Norwegian University of Science and Technology Centre for Autonomous Marine Operations and Systems
OB	origin of the vehicle body

OE	origin of earth
PID	Proportional Integral Derivative
PP	Pure Pursuit
REMUS	Remote Environment Monitoring Units
ROV	Remotely Operated Underwater Vehicle
SLAM	Simultaneous Localization And Mapping
SMC	slide mode control
SPURV	Special Purpose Underwater Research Vehicle
TMS	Tether Management System
UGAS	uniform global asymptotic stability
ULES	uniform local exponential stability
USBL	Ultra-Short Base Line
UUV	Unmanned Underwater Vehicle

CHAPTER ONE:

INTRODUCTION

1.1 Background

Autonomous Underwater Vehicles (AUVs) have become one of the revolutionary technologies in recent years. Since the early 1970s, AUVs have shown significant development in the oceanography and in-depth study of oceans due to the measurement instrumentations that AUVs are equipped with. According to Technavio analysists, the AUV market is expected to grow with 12% by 2021 [1]. Different underwater projects depend on the AUV surveillance information and its assistance in handling deep operations side by side the Remotely Operated underwater Vehicles (ROVs). Oil and gas field is the major contributor in the underwater vehicle technology as the onshore field is declining while the offshore is increasing its production. Offshore oil production contribute with about 33% of the world oil production and about 9% is coming from deep water as in the Fig 1.1 [2]. So the development of underwater vehicles is highly demanded especially in deep waters. One of the new offshore discoveries is the Zohr gas field in Egypt that considered as the largest gas reservoir in Mediterranean Sea with an estimation of 850 billion cubic meters of gas in place. In this project, the AUVs are deployed to execute the surveillance missions related to the project [3]. In this kind of projects the data collected by different tools is a play factor in determining the location of the rich areas. So, the underwater vehicle is playing an important role not only in exploration but also for the operations and production.

Hence, many researches are engaged in developing the AUVs different features; such as, navigation, control, planning, and ocean current measurements.

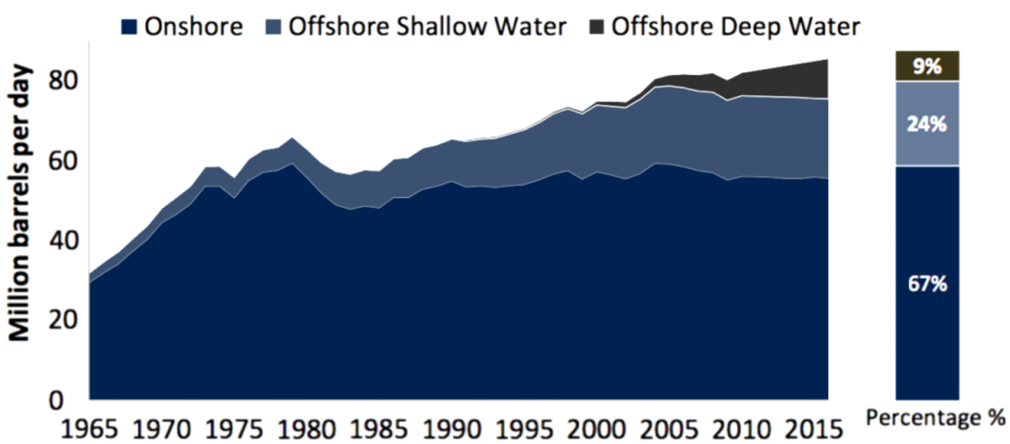

Fig 1.1 Onshore versus offshore oil production map [2]

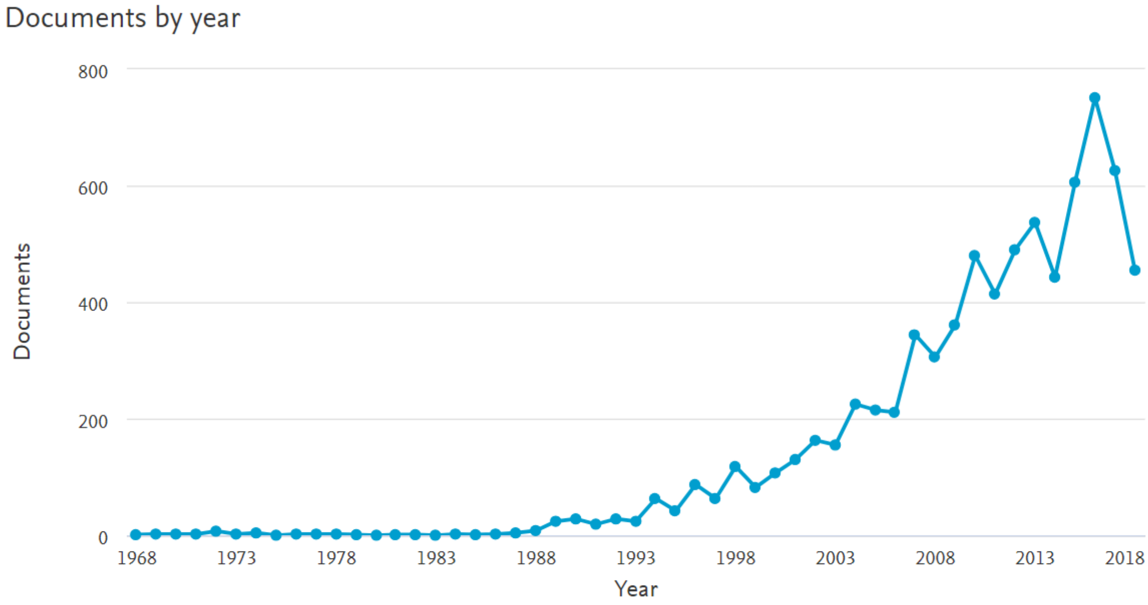

Fig 1.2 Publication trend in underwater vehicle field according to SCOPUS[4]

According to SCOPUS research engine, there are 7643 published researches of the underwater vehicle until 2018 and the analyses given by the research engine show a tendency in this field in the last three decades as shown in the Fig 1.2 [4]. Besides, many research institutes and projects concerns about the underwater research field and its influence in different disciplines. One of these projects is Norwegian University of Science and Technology Centre for Autonomous Marine Operations and Systems (NTNU AMOS) research program. This program, which started in 2013 and will continue until 2022, is oriented to challenges subjected to autonomous marine operations such as maritime transportation, fisheries and aquaculture, oceans science, oil and gas exploration, offshore renewable energy and marine mining. Using their theoretical and experimental fundamental knowledge, this research program is developing the autonomous underwater systems including navigation, control, guidance and modelling to solve multiple case studies that enhance the underwater field. In their annual review, different solutions are addressed and discussed related to real field problems. Case studies include developing the ROV manipulation systems for oil and gas companies to enhance the mission handling, field surveillance using multiple vehicles for biological, archaeological and geological research, and investigations in Arctic to understand the biodiversity and food web structure through the polar night including ecological processes, reproduction, and growth. All of these studies benefit from the technology within underwater vehicles and give the opportunity to solve the challenges subjected to it [5], [6].

This main technical challenges that faces the AUVs are related to energy, actuation, navigation, and autonomy of the vehicle. The limitation in the power due to batteries capacities leads to develop this technology and also develop low consumption sensors and actuators. The development of actuators also concerned with developing new mechanisms of thrusting and movement in the water to increase the manipulation of the underwater vehicles [7], [8]. In the navigation system, the main challenge is the absence of direct positioning sensor such as GPS, so the combination of indirect measurement tools and advanced algorithms is used to achieve higher accuracy which increase the AUVs dependency. In addition, the autonomy of the vehicle requires an intelligent mission planner combined with efficient guidance controller and actuation controllers to deal with the environmental difficulties. So, the vehicle main controller should be able acquire useful feedback from multi sensors and uses a sensor fusion techniques to estimate the vehicle states. In this research, an environmental disturbance which induced by the ocean currents, waves, or winds information is required to enhance the vehicle decision making and the mission tracking. Also, some missions such as geoscience applications require a certain speed of the vehicle to correctly collect the data and the ocean current disturbance could affect this kind of missions. So, this disturbance should be measured and the controller have to use this information to apply the right actuation orders to avoid the disturbance influence. Direct measurement sensors have disadvantages of high cost, difficult to implement in small vehicles, and reliance on external information such as scatters of the water to measure current velocities. So, an alternative methods is introduced to enhance the disturbance estimation to use it in enhancing the intelligence and controllability of the vehicle. This research discusses the usage of observers as an alternative or a redundant technique in ocean current estimation to enhance the guidance control system.

1.2 Problem definition

The ocean current measurement and estimation is an essential task not only for oceanography but also for the navigation and control missions. The direct measurement tools are not available for all AUVs and require a technique to avoid errors of measurement or sudden failure. In addition, mapping of estimated ocean current is very important for oceanography, surveillance studies, and mission planning. Then, guidance control under the non-uniform ocean current disturbance gives a low accuracy and high cross track error that could cause failure of the mission or even loses of the AUV itself.

1.3 Aim of the work

The objective of this research is to enhance the autonomy of the vehicle and provide an alternative way of ocean current measurements. The AUV operates in a complex and uncertain environment where the vehicle is subjected to ocean currents, waves, and wind disturbance. However, this research considers only the ocean current disturbance to be estimated and mapped in order to be used in other systems or in the oceangraphical analysis. The guidance controller should track the vehicle along the mission path under this disturbance without deviation. So, the ocean current information is used to modify the controller in order to compensate the disturbance effect and maintain the desired path.

1.4 Methodology

The methodology used in this work is described as follows:

- Construct and validate the dynamic model of the AUV and implement this model in Matlab software in order to test and evaluate the system.
- Design an observer to estimate the non-uniform ocean currents
- Enhance the guidance controller with the ocean current components feedback
- Evaluate the system with different scenarios.

1.5 Thesis outline

The thesis consists of six chapters and is arranged as follows:

Chapter 2: Literature Review

In this chapter, the full description of the AUV system is discussed mentioning the different designs and approaches used to implement the AUV in practice. Also, a comprehensive study of the recent observation methodology usage of the AUV and the trajectory tracking control techniques is presented.

Chapter 3: AUV System Modelling

This chapter provides the architecture of the HRC-AUV and the derivation of the dynamic model of the vehicle within the ocean current disturbance. Also, the derivation of the model parameters is provided.

Chapter 4: Control System Design

This chapter introduces the guidance controller algorithm used to track the AUV along the desired path with the ocean current observer. Firstly, two kinds of observers are described and implemented. Then, the LOS guidance algorithm is derived and implemented to the AUV system combined with the integral action to compensate the variable ocean current disturbance. The low level control is then used in order to control the vehicle actuators to follow the guidance controller set points.

Chapter 5: Simulation Results

This chapter shows the implementation of the AUV dynamic model in the Matlab software and combines the ocean current observer and the guidance controller to represent the full system. Then, the validation of the derived model is discussed regarding similar literature experimental tests. The ocean current estimation is consequently represented with different cases to show their influence. Finally, the modified guidance controller is tested under the ocean current disturbance to illustrate the controller performance.

Chapter 6: Conclusion

This chapter discusses the results and how far it meets the desired objectives. Besides, the recommendations of the future work are presented in order to enhance the AUV autonomy and also to use this system in other scoops and applications.

CHAPTER TWO:
LITERATURE REVIEW

2.1 Introduction

This chapter discusses the AUV research field. It starts with the history of the underwater vehicles and the key factors behind the development in this field followed by the types of underwater vehicles and their applications. Then, the AUV architecture is explained including the modelling, planning, navigation, guidance, and control with several research work on each category. Finally, the ocean current estimation is discussed with several approaches used and focusing on the observer technique.

2.2 Underwater vehicle History

Generally, Unmanned Underwater Vehicle (UUV) term is used for ROVs and AUVs which differ from the normal submarines as there is no crew on it. It was firstly designed in 1868 by Whitehead in Austria as a self-propelled torpedoes for military usage as shown in Fig 2.1 and it was classified as an AUV. However, the UUV was not commercially used and manufactured until 1970s when the oil and gas discovered in the North Sea. So, countries began to research and develop the UUV technology. Although of initial trials of the AUVs was performed in 1960s but it was for specific applications such as data collection and a few of papers about these designs was published. The first AUV was developed in 1957 in University of Washington and named SPURV (Special Purpose Underwater Research Vehicle) that was designed to research in the Arctic waters [9]. During 1970-1980s, the offshore oil and gas were discovered and the ROVs was extensively used to perform the underwater missions. On the other hand, the usage of AUVs was limited and constrained within on-board computers which were too big, power consuming, and the limitation on the memory to handle the AUV tasks compared to the ROVs which did not have the same issues as it is controlled remotely.

At the beginning of 1990s, computer technology showed a great development that enhanced the AUVs technology respectfully. So, the AUVs moved from 1980s conceptual designs and prototypes into a commercial industry. The first processor based AUV was deployed in 1987 using a 32-bit Motorola processor to allow real time interface between the operators and the vehicle for 35 hours mission [9].

Fig 2.1 First AUV developed by Whitehead [8]

Different AUVs were developed for varied applications including military and marine fields with different types and models. However, AUVs were still had problems and challenges related to hardware optimization and autonomy level. The first problem stated as an AUV operation needs a long term sufficient batteries, different sensors, and powerful thrusting while the design requires low weight equipment. Secondly, low human intervention requires higher autonomy level and intelligence in order to learn from the surrounding environment and take decisions [8][10].

2.3 Underwater vehicle types

The UUV could be classified into two main categories as in the Fig 2.2;

- The cruising type which uses a propeller thruster and control fins to thrust and steer. This kind of UUV is mostly a torpedo shaped and used in applications including survey and data collection. The main disadvantage of this type is the difficulty to control in low speed and in tight places
- The box design type which uses multiple thrusters in different locations in the vehicle to steer and move. This configuration provides a low speed manoeuvring to the vehicle in order to work in narrow places. This enables

the vehicle to handle missions that require robotic actions. However, it is difficult to operate in high speed because of the high drag forces subjected to the wide angle of attack area. Also, the small motion correction is not efficient because of the steering mechanism which suffers from controlling the propulsion in inconstant rotational speed.

So, according to this classification, the types of UUV depends on the application and the basic design of the vehicle [8][11].

2.3.1 Remotely Operated underwater Vehicles

ROVs are known as tethered operated vehicle. The surface vessels are controlling the ROVs which allows the ROV to communicate, assign a real time stream monitoring, and consume more power from the surface vessel to execute more tasks. The main components of standard ROV are sturdy frame, a floatation unit for buoyancy supply (typically, ROVs are slightly positively buoyant), a number of thrusters to enable manoeuvrability in three dimensions, and a tether. The tether is usually used to connect the system to the host ship; however, it can be connected to a Tether Management System (TMS).

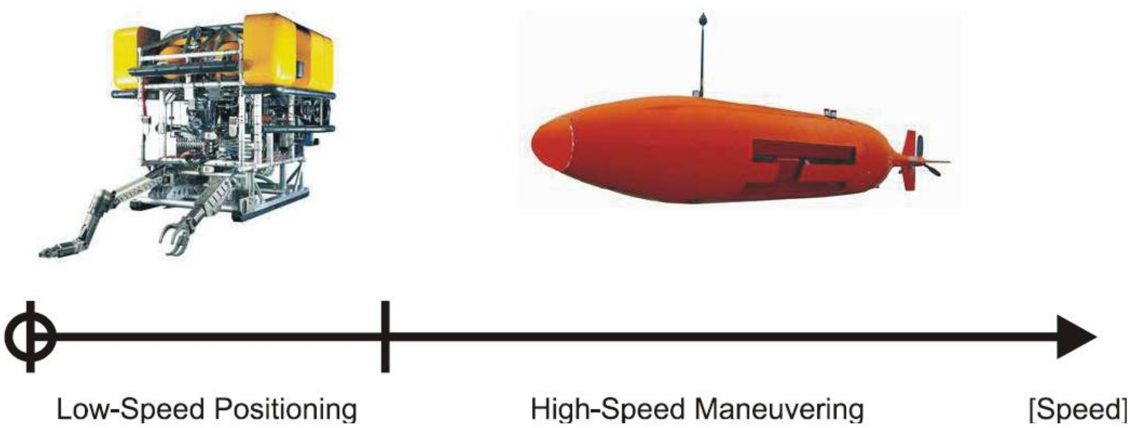

Fig2.2 UUV types: ROVs and AUVs [10]

The TMS is a separate non-buoyant unit to lessen the impact generated by the ship's movement on the ROV, so it should be attached to the ROV on an armoured cable from the ship. In 1960s, the military used the ROV under the name of CURV: "Cable-controlled Underwater Recovery Vehicles" for recovery operation, mine clearing, etc. [12]. In the late 1970s and 1980s, the industrial domain used this technology to perform some operations beyond depths instead of the divers. Currently, ROVs are used in the fields of Oil and Gas. Not only that but also they are diffused for scientific research and salvage operations.

Providing an ROV with sensors, instruments and tools, should be based on many factors such as the frame size, the operational specifications and the vehicle's depth rating. In the primitive layouts, the real time data is transferred to the on-board operator using one or more video cameras that are carried on an ROV. Also, the ROV could be provided by one or two manipulator arms with multi levels of functionality, in addition to a storage device to store tools and samples. Moreover, advanced configurations can be upgraded by integrating other sensors and equipment into the system, such as small CTDs, optical sensor, chemical sensors, HD cameras, sector scanning sonars, multi-beam echo-sounders, and suction samplers.

ROVs are usually introduced in various capabilities. They could be categorized depending on their depth-rating but also on their size. The work-class ROVs are known as large and powerful vehicles – up to 2 m high and 4 m long – and are equipped with two 5 or 7 function manipulator arms. Therefore, they are used for complex operations like carrying several instruments or large volume samples. However, in the scientific aspect, the perfectly known ROVs are the Jason ROV from the Woods Hole Oceanographic Institution (WHOI), the Isis ROV from the National Oceanography Centre (NOC), and the ROV Victor from the Institut Français de Recherche pour l'Exploitation de la Mer (IFREMER), which can all operate down to 6000 m water depth [13]. Another class of ROVs, used for inspection or observation, are smaller in size (metre-size), have one manipulator arm, and commonly used for video surveys. By comparing this inspection class with the previous work-class, the inspection class vehicles have more sufficient power to work in full marine conditions down to 3000 or 4000 m water depth despite their compact size. In addition to video surveying, they can perform other tasks. Furthermore, a single suitcase can easily contain an Eyeball class ROVs that are also known as mini- and micro-ROVs, and can be deployed by a single person. These ROVs are dedicated to inspection work in relatively calm and shallow water that is lower than 200m. Nowadays, the users may build their own mini-ROV using the assembly kits that are available online [14].

2.3.2 Autonmous Underwater Vehicles

AUVs are unmanned self-propelled vehicles that deployed from surface ships and can operate from few hours into several days and normally follows a predefined mission and navigate using a set of sensors which are suitable for the geoscience applications. The operational depth ranges of AUV varies from few hundreds of meters to more than 6000 meters. Most of the AUVs are cruising type with torpedo shape and containing single thruster which enables it to operate in large areas with average speed 2 m/sec. This type is widely commercial and carries on the major oceanography surveillance missions. The other type is the hovering one which be could categorised under the box design UUVs. Hovering AUVs includes several thrusters to allow it to move in any direction and give the vehicle high manoeuvrability in slow missions such as seabed photography. Besides, it could work in distinctly 3-dimensional terrains, such as around coral reefs or hydrothermal vents [14], [15]. Fig 2.3 shows the difference between the cruising and hovering AUVs.

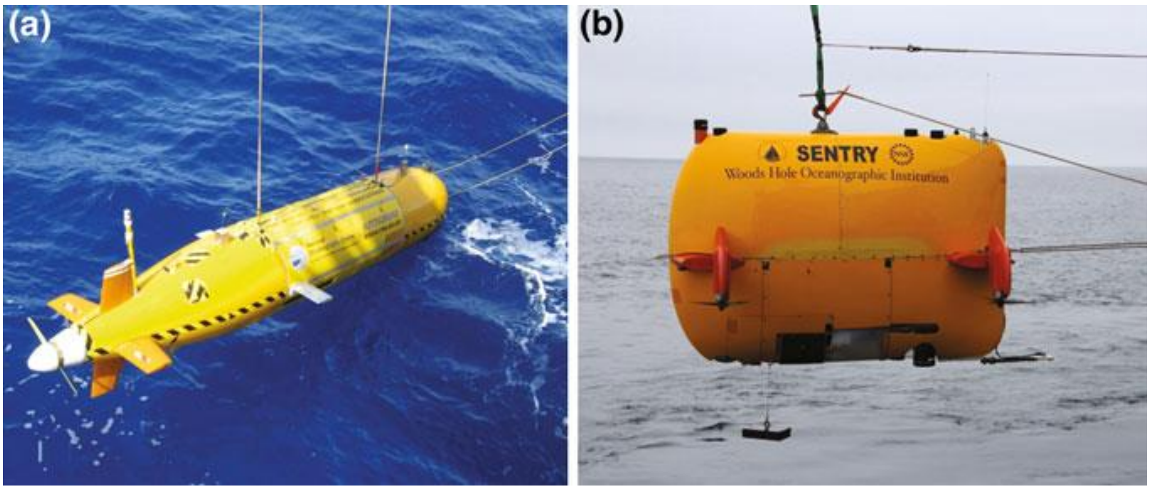

Fig 2.3 Examples of AUV types: the torpedo-shaped survey AUV Autosub6000 and the hovering AUV Sentry from WHOI [14].

According to [16], AUVs normally consist of basic modules and function modules. The basic module includes the power supply, control, navigation, and communication systems of the vehicle. In the control system, the main processor unit responsible of controlling the steering and thrusting actuation systems according to the sensor feed-back to maintain the desired trajectory. The navigation system includes positioning sensors such as Global Positioning System (GPS) for surface navigation and Inertial Navigation System (INS), Ultra Short Base Line (USBL), or Doppler Velocity Logger (DVL) for underwater navigation.

On the other hand, functional modules represent the auxiliary sensors such (altimeter/single-beam probe, Doppler Velocity Log, acoustic modem, Conductivity Temperature Depths sensor (CTD), Obstacle avoidance sonar and lights) and survey equipment (multi-beam bathymetry, side scan sonar, sub-bottom profiler, magnetometer, water quality sensor, and camera).

The main struggles that affect the AUV are the deep-water pressure acting on the vehicle and the power limitation problem due to using batteries. So, the AUVs are designed in a compact shape and neutral buoyancy body characteristics which reduces the thrusting power consumption. Also, the sensors are isolated to resist the water pressure using resisting materials.

One of the most popular AUV series is the HUGIN AUV illustrated in Fig 2.4 that stands for 'High Precision Untethered Geo-survey and Inspection system' and developed jointly by Kongsberg Maritime and the Norwegian Defence Research Establishment. The first trials of HUGIN were in 1996 using HUGIN 3000. The 5 meters length, 1-meter diameter, and 1450 Kg mass was equipped with side-scan sonar, multi-beam echo sounder, sub-bottom profiler, camera, CTD and volume search sonar with depth range up to 3000 meters and endurance of 60 hours. These specifications attracted the surveying companies to benefit from HUGIN capabilities so it covered about 120000 KM of commercial survey work. Another development for HUGIN was demonstrated to generate other classes of HUGIN AUVs such as HUGIN 1000, HUGIN 4500, and HUGIN 6000. HUGIN 1000 is a reduction of weight and volume HUGIN 3000 by 50% which increased the manoeuvrability of HUGIN AUV but with low depth range not exciding 1000 meters.

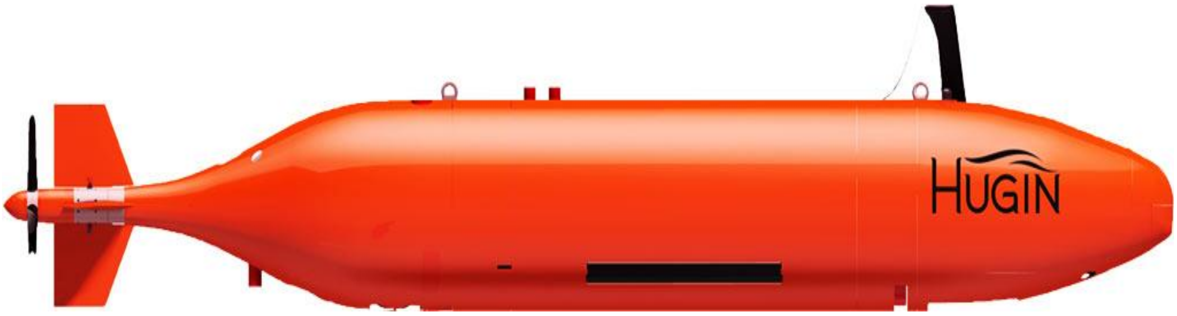

Fig 2.4 HUGIN AUV [17]

HUGIN 4500 and HUGIN 6000 are a high depth ranges classes with 4500 and 6000 maximum depths respectively and also with high endurance batteries up to 100 hours combined with intelligent systems for navigation and control [10], [11], [16]–[18].

Another popular series of AUVs are REMUS (Remote Environment Monitoring Units) which developed in 2001 by the Woods Hole Oceanographic Institute (WHOI), the Naval Oceanographic Office, and the Office of Naval Research. It was designed for reconnaissance inspection and mine works of shallow water. REMUS uses a large number of sensors and measuring devices and the data collected are transmitted using acoustic communication system. This enables the REMUS AUV to be used in applications such as Hydrographic surveys, environmental monitoring, debris field mapping, search and salvage operations, fishery operations and scientific sampling and mapping[9], [10]. REMUS AUVs are used widely in military applications which contributed by 82 vehicles in 2007 as shown in Fig 2.5.

Fig 2.5 REMUS 6000 used by the U.S. Navay [18].

REMUS 6000 as in the Fig 2-5 is the most recent developed model of this series which could reach depths up to 6000 with livestreaming communication to the surface [19].

Besides the commercial AUVs, a lot of research AUVs are constructed and developed to be used in scientific purposes. One of this model is the HRC-AUV project which developed by researchers from the Universidad Central de Las Villas (UCLV) and the Hydrographic Research Centre. The aim of this project was to establish a low cost AUV platform that could be used for scientific research. This AUV is similar to popular commercial AUVs such as HUGIN, REMUS, and STARFISH AUVs. Basically, this design was influenced by Fossen's dynamic model of the AUV in order to simulate the AUV behaviour and tune its performance and intelligent systems. A set of experimental tests has been conducted in order to estimate the vehicle model coefficients and the necessary equations to be used [20].

2.3.3 Glider AUVs

Gliders considered as a low power consuming AUV that designed for investigations. Unlike the normal AUVs, it works in small depths with an average 200 meters but for long periods with an average 1 month of operation. It uses different actuation mechanism for heave motion by changing its buoyancy [10]. The demand of high cruising ranges influenced the research and military fields to develop a new type of AUVs that has the ability to operate for weeks and months. The concept of the gliders was founded by Henry Stommel and Doug Webb in 1955. However, gliders did not appear in the field until 1999 by IRobot Company that introduced the sea glider. In order to develop the gliders depth range, a carbon fiber used to construct the vehicle body hull which enabled a Deepglider to reach a 6000 m depth at 2006. Other development and researches conducted to minimize the energy consumption such as thermal and electric buoyancy control mechanisms that showed a great achievement by reducing the consumption with more than 3 times as the SLOCUM glider fulfill [9]. The military field benefits from the gliders technology in reconnaissance and detection applications due to the gliders ability to stay underwater for several thousands of hours. One of the military gliders that used in this kind of applications is the Liberdade XRAY which equipped with lot of measuring tools and could work up to 6 months [21]. Fig 2.6

shows different designs of gliders that presented by Wood who reviewed gliders types and features extensively [21]. The main difference between these three designs is the actuating mechanism or the glide control. The glide control in Spray is achieved exclusively by axial translation and rotation of internal battery packs. Pitch is controlled simply by moving the center of gravity in the manner of a hang glider. Turning is initiated by rolling. Seaglider uses a hydrodynamic aluminum pressure hull that is contained within a free-flooded fiberglass fairing that supports the wings. The flooded aft section is used to carry self-contained instruments on the vehicle. The Slocum Thermal glider uses the change in volume from a material's (ethylene glycol) freezing and melting as the means of vehicle propulsion.

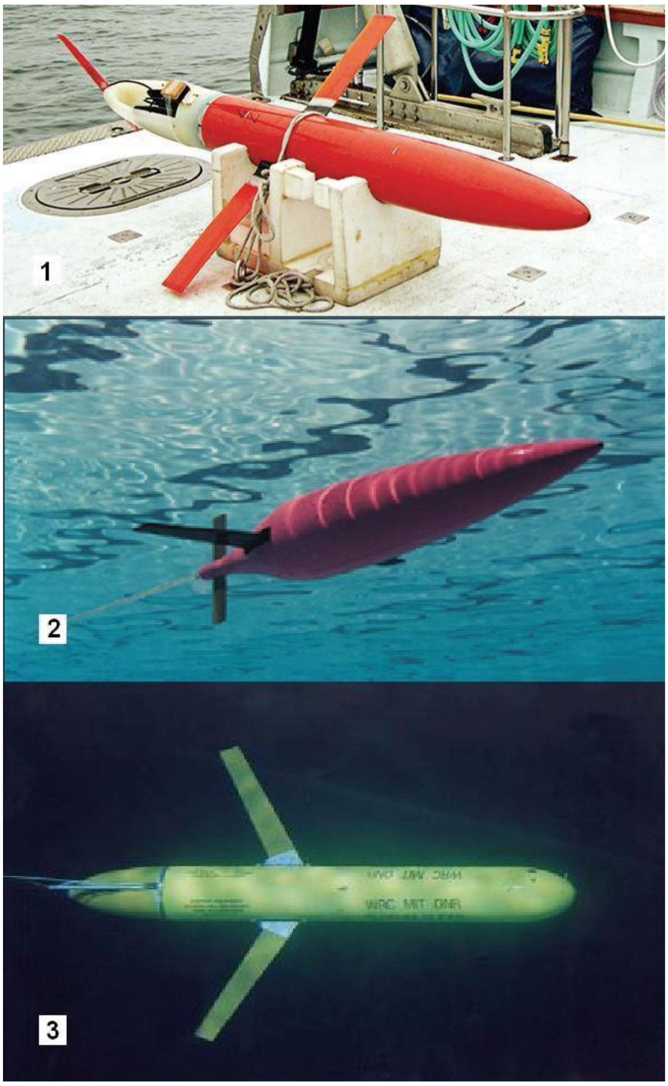

Fig 2.6 1) Spray, 2) Seaglider, 3) Slocum Glider [21]

2.4 AUV applications

AUVs are generally used in surveying applications for both marine, military, and scientific purposes. In marine applications, the AUVs are equipped with different sensor platforms to collect data related to different fields. In oil and gas field, the AUVs are used in explorations of oil wells and provide a bathymetry map around these wells [2]. Also, AUVs are used to map the operation field before the drilling and production operations. In addition, AUVs could be used to inspect the production pipes along the seabed and detect the failures or cracks.

In marine geoscience, the AUVs are used to study submarine volcanism and hydrothermal, map and monitor low-temperature fluid escape features and chemosynthetic ecosystems, map benthic habitat in shallow and deep water environments, and a map of seafloor morphological features (e.g. bedforms generated beneath ice or sediment-gravity flows). Also, AUVs are used in new geoscience studies such as multi-frequency acoustic imaging of trawling impacts on deep-water coral mounds, collection of high-resolution seafloor photomosaic at abyssal depths, and velocity measurements of active submarine density flow [15].

On the other hand, military applications require more navigational accuracy and obstacle avoidance besides the strong target identification and the capabilities to attack. The main military usage of the AUVs are hydro acoustic and electronic reconnaissance, detection of submarines, naval mines and other objects and destroying them using torpedoes or missiles carried by the AUV [9].

2.5 AUV architecture

The main difference between the AUV and the ROV is the type of operation which depends on the autonomy level of the vehicle. The autonomy levels range from human remotely control to full autonomous according to the Human Robotic Interface (HRI), environmental complexity, and mission complexity. As illustrated in the Fig 2.7, the National Institute of Standards and Technology (NIST) divided the autonomy into ten levels with five main regions that are declared as following [6], [22]:

0. Human control: means that human is performing low and high level actions without any kind of computer control.
1. Remotely control: means that although the actions are executed automatically, the human must perform high level tasks and missions without computer assistance.
2. Tele-operated: means that computer assists in controlling and makes recommendation related to missions.
3. Semi-autonomous: means that the computer performs the tasks and mission automatically under the human supervision who controls the parameters and choose between alternatives.
4. Highly autonomous: means that the intelligent computer is performing all missions specified in a very complex environment and has the ability to re-plan the missions according to the information collected. The human maybe informed by the progress of the mission which the computer is fully independent.

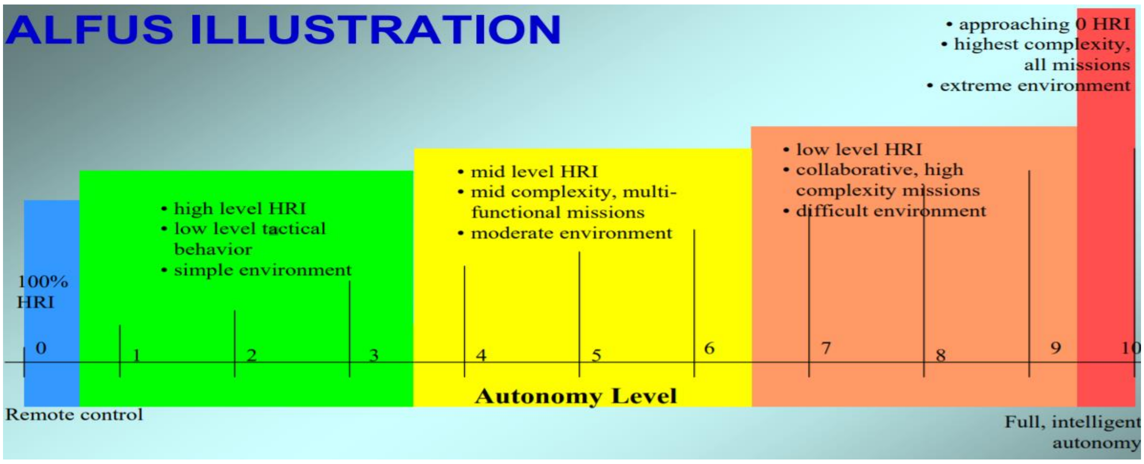

Fig 2.7 Automation levels for unmanned systems[22]

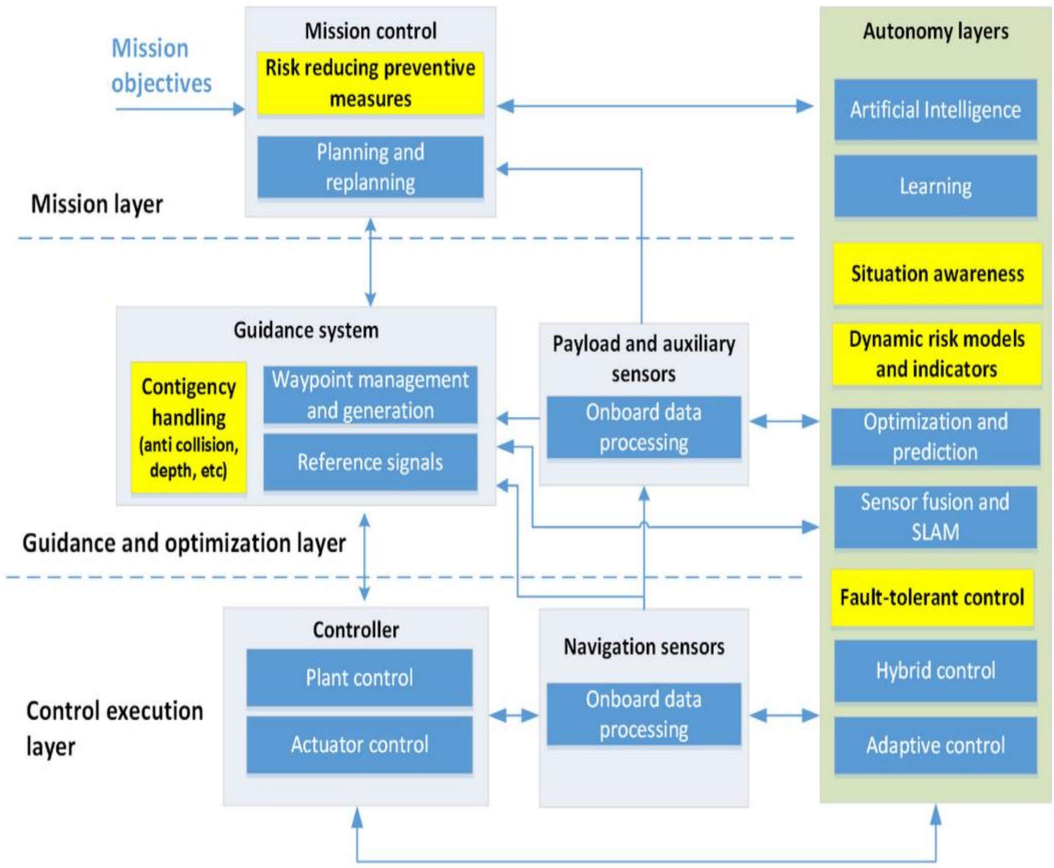

Fig 2.8 AUV Architecture [5].

AUV is considered as a highly autonomous system due to its structure and complex working environment that the system has to deal with. Based on Fossen's description of the autonomous underwater vehicles, the structure of the AUV consists basically of guidance, control, and navigation systems [23]. However, this elementary description could be extended into multi layers including advanced mission planning techniques and intelligent control system that uses the artificial intelligence tools as illustrated in Fig 2.8. Guidance system includes mission planner that determine the mission way points and the necessary velocities and path following controller to convert these way-points into controlled actions for the controller. Then, the controller is responsible of determining the required input signal to achieve the desired set points provided by the guidance system. Finally, the navigation system is responsible of sensing the position, speed, and orientation of the vehicle. This main system components discussed branch into several layers according to the used components, mission and environmental complexity, and the intelligence of the system. Also, the system modeling has a significant importance in the control, navigation, and system simulation and testing.

2.6 Modelling of the AUV

The modelling of the underwater vehicles was firstly introduced firstly by Gertler and Hagen. In this model, the second order nonlinear differential equations considered as the basics of the submarine equations which helped in building the modelling and control of underwater vehicles [24]. Later, Fossen derived the equations of motion of the marine vehicle in his book entitled "Guidance and Control of Ocean Vehicles" which is considered as a guiding technique of underwater vehicle modelling [7], [10], [25], [26]. These equations are derived using either Newton-Euler equations or Lagrangian form. Also, the equations are represented in the vector form. To calculate the underwater vehicle model coefficients, experimental or Computational Fluid Dynamics (CFD) approaches are used based on the geometrical parameters of the vehicle [20], [27]. Then, the numerical simulation of the model is tested using simulation software such as Matlab with marine vessels toolbox or special underwater vehicle simulation software [23], [26].

2.7 Mission Planning

The purpose of the mission planner is to provide mission waypoints that the AUV has to cover in order to perform the provided task. This mission maybe re-planned according to the environmental disturbances during the vehicle motion [6]. So, the planning system is required to find the optimal path between alternative feasible paths to lead the AUV from its starting location to the target destination using minimal time and energy costs [28]. Then, the real time path planner uses the sensing and navigational system to take action decisions to avoid obstacles or disturbances within short time and limited manoeuvrability. Morten D. Pedersen used re-planning method in order to avoid the obstacles during the travel of the AUV using the feedback of the potential flow around these obstacles [29]. Also in Kai-Chieh Ma work, the navigational data was integrated with ocean current monitoring information to obtain the optimal re-planned path during the traveling of the AUV in order to cover the most uncertainty regions [30]. The main problem that faces the planning task in the AUV is the large geographical area to be covered that considered as a large scale optimization problem taking into account the variable environmental disturbances. So, several optimization algorithms are used to solve the path planning problem such as A*, RRT, and evolutionary algorithms. More details about the techniques used and the differences between each technique are presented in the Z. Zeng, K. Sammut, L. Lian, F. He, and A. Lammas work [28].

2.8 Guidance control

The guidance system is responsible of supplying the controller with the set point steering, velocities and acceleration based on the predefined path and trajectory from the planner. According Charles Stark Draper who stated that "Guidance depends upon fundamental principles and involves devices that are similar for vehicles moving on land, on water, under water, in air, beyond the atmosphere within the gravitational field of earth and in space outside this field" [31]. For underwater vehicles, guidance control could be classified into different main motion scenarios; path following, trajectory tracking, path manoeuvring, and target tracking. In the path following scenario, the vehicle has to converge to the path between pre-defined waypoints without any velocity constraints. While in the trajectory tracking, the vehicle is required to follow the path with specified velocities within mission time limit. Path manoeuvring, in contrast, gives the priority to the geometric of the path before the velocity which the vehicle is supposed to steer on the pre-defined curves between points. Target tracking scenario is to track a motion of a target where the target instantaneous position is known [11]. Missile guided community, the first contributor in this field, provided three main guidance laws for an object. First, Line Of Sight (LOS) guidance which consists of three points; interceptor, target, and reference points and the interceptor is guided through the line of sight between the reference point and the target point as illustrated in the Fig 2.9. This method is commonly used in the literature due to its stability. Secondly, the Pure Pursuit (PP) which considered as a two point guidance system where the interceptor is align its velocity on the line of sight between interceptor and target points. This technique is widely used in tracking target applications and Autonomous Ground Vehicles (AGV) systems.

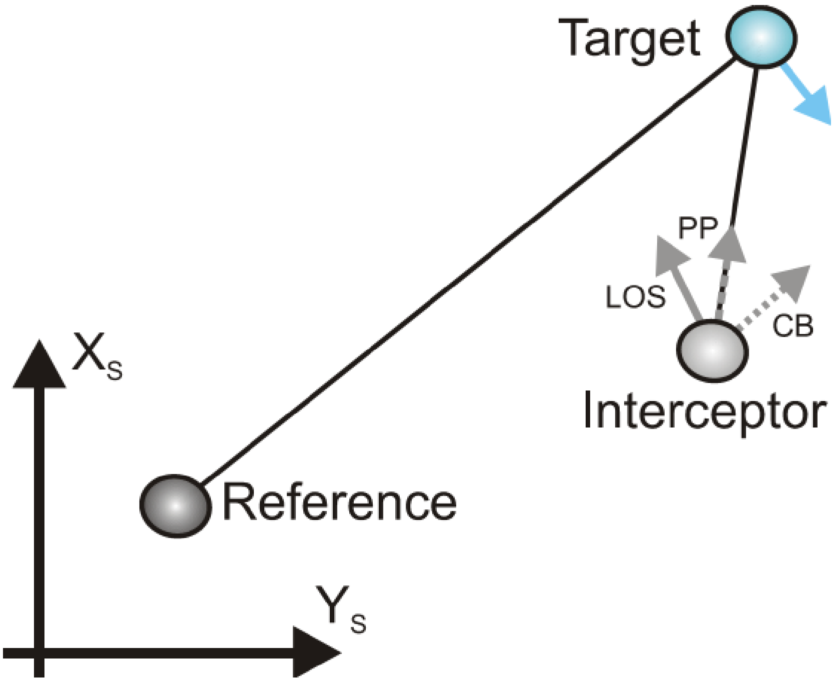

Fig 2.9 Guidance laws: LOS, PP, and CB[11]

Although PP technique is less addressed in the marine systems, but some works have used it such as Sfahani work [32]. The third technique is the constant bearing (CB) guidance which also classified as two point guidance system. However, the main difference between PP and CB is that in CB the interceptor aligns the relative interceptor-target velocity on the line of sight between the interceptor and the target. This technique is used in the collisions avoidance applications such as steering away from a situation where another vessel approaches at a constant bearing [11]. In Morten Breivik work, the CB method was used in the AUV target torching scenario [33].In addition to these three techniques, there are some other strategies influenced by the Autonmous Ground Vehicle (AGV) systems such as hand position strategy which is introduced by K. Ytterstad and C. Paliotta [34].

The LOS strategy is the popular method used in AUVs guidance system due to its stability which has been studied extensively in different works such as Fossens line of sight study [35]. It was initially presented by A. J. Healey and D. Lienard in their work [36]. LOS derived for the straight line path following scenario by Fossen and Lekkas for the underwater vehicles [35], [37]–[40]. For the manoeuvring scenario where the vehicle has to follow a curved path, different researches have been conducted in this problem to derive the suitable formula that guides the vehicle along the path [40]–[43]. LOS has been extended into 3D path following by decoupling the heave and sway motion equations. However, Breivik introduced a coupled LOS technique for 3D path following [44]. Then, many researchers motivated this technique and developed it by intelligent controllers [45].

The main problem that faces the guidance system is the environmental disturbances (mainly the ocean currents) that prevent the vehicle from converging the desired path. So, an integral control action is supplied to the controller in order to minimize the cross track error that induced by this disturbance. Different researches provided solutions to this problem using different methods and techniques to improve the guidance algorithms. The initial solutions were very simple such as Aguiar and Pascoal work in which the guidance depends on the AUV velocity measurements [46]. Bakaric suggested a direct control of the relative speed of the vehicle by estimating the necessary crab angle [47]. The integral LOS was introduced by Børhaug which considered as a turning point solution for the ocean current disturbance that inspired the researchers to enhance the LOS guidance [48]. Based on this solution, many researchers provided studies on counteracting the ocean current disturbance for different cases and scenarios [42], [49]–[51]. Although these solution have a significant enhancement on the AUV guidance, but it is considered a constant irrotational current acts on the vehicle. This assumption was minimized in later works [52], [53]. On the other hand, not only the adapting of ocean current disturbance is the main difficulty, but also the estimation of this disturbance is considered as an additional problem. The estimation of ocean current disturbance techniques will be discussed later.

2.9 Control

The controller is responsible of determining the necessary forces in order to achieve the desired set points provided by the guidance controller to track the path. Also, the navigation system feedbacks the controller to correct the control output signal. The main difficulty that faces the AUV controller is the model uncertainty and the ocean current disturbances. So, the controller should be self-tuned and robust to counter the variations in parameters and stand with the disturbances [54].

Different kinds of controllers have been suggested by authors through the previous decades including several techniques and aiming different objectives. One of the simplest controllers are the linear controllers which show a decent satisfactory which has been described by several works [25], [55]. Although the simplicity to implement and maintain this kind of controllers, it has a drawback of disability to account the system nonlinearity and instability in high manoeuvres. Also, a slide mode control (SMC) is implemented which considered as an earlier way to solve the system nonlinearity but it could cause chattering on actuators, waste energy, and make fault on fins [56]. So, the adaptive controllers are required in this situation and implemented by different works [57]–[59]. The adaptive controller is a nonlinear control method that applied on the system with uncertainty. It is useful on the AUV system because of variation in the model parameters and the environmental disturbances acting on this model.

Also, intelligent controllers such as fuzzy logic control are applied on the AUV system. Fuzzy logic control is used extensively by authors in AUVs system. In Xiang work, different types of fuzzy controller is described including conventional, adaptive, and hybrid techniques [60]. Furthermore, neural network based control has been implemented and has shown good robustness and tuning ability [61]. However, neural network could suffer from long training time.

Among all of these strategies, the combination of conventional controllers such as PID controller with intelligent adapting technique could easily implemented and achieve robust and stable performance without high processing time [54].

2.10 Navigation system

Navigation system is considered one of the main challenges of underwater vehicles. Compared to the surface vehicles where the GPS system provides an accurate solution to the navigational issues, there is no similar solution for the underwater applications and the GPS signal cannot transmitted for similar depths. However, navigation is a critical task for the AUVs which travels for long distances and periods besides the autonomy of the vehicle depends on it [62]. So, navigation literature provides an alternative aiding techniques in order to achieve more accurate navigation.

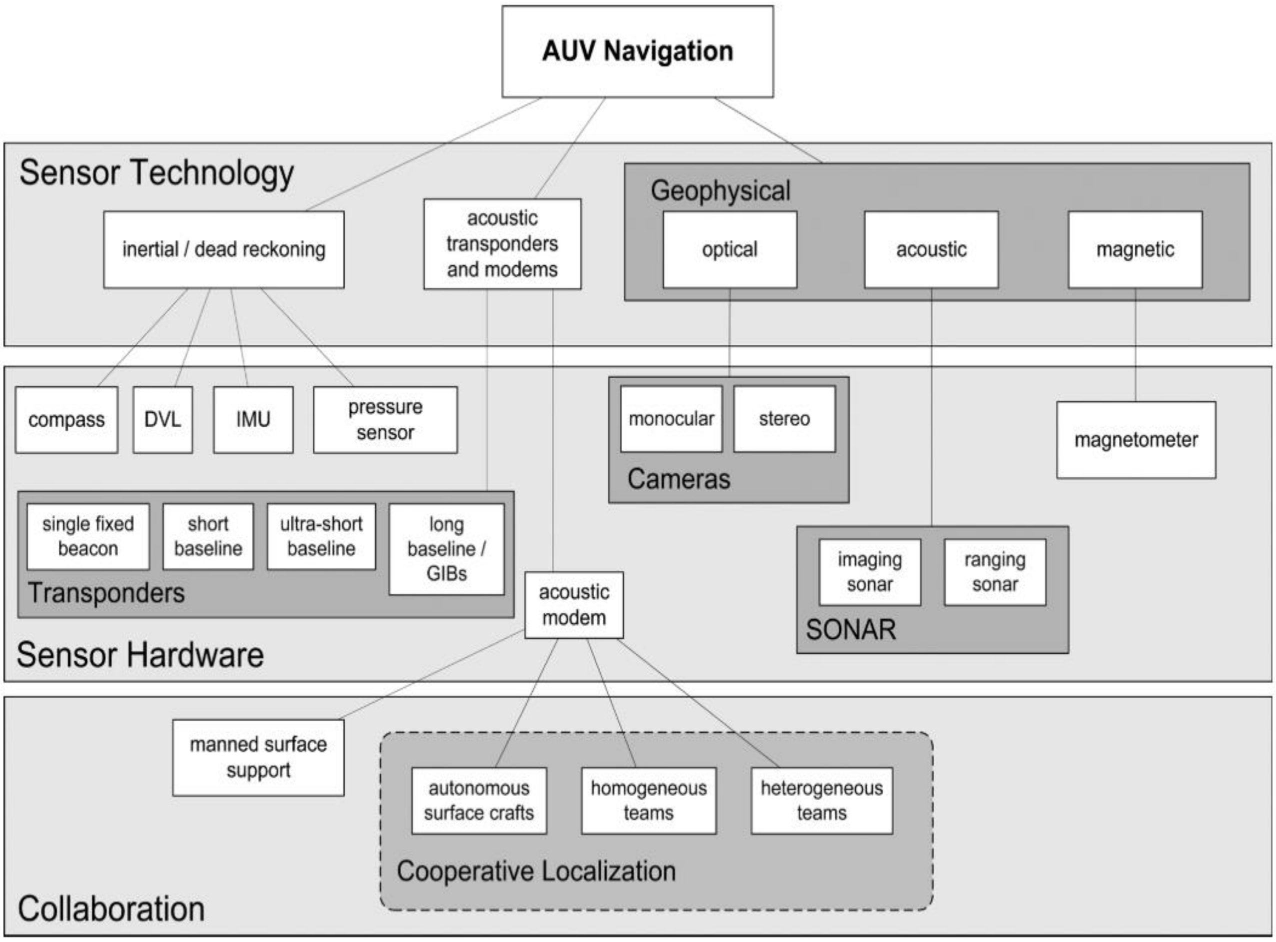

Fig 2.10 Navigation categories and technologies [63].

According to Paull, navigational sensors in the underwater vehicles categorized into three main systems as in Fig 2.10 [63].

- **Inertial/dead reckoning:** INS uses accelerometers, compass, and gyroscopes to estimate the acceleration and rate of change of orientation to provide the velocity, position, and orientation values. The problem of the INS is the error growth with time depending on the class of the sensor due to the dead-reckoning nature of the method [62]. So, this system needs a redundant or an aiding sensors to correct this error. The poplar aiding technique is to use the Doppler velocity log (DVL) which measures Doppler shift in the incoming signal reflected off the seabed (bottom track mode) or particles in the water (water track mode) column using the same principles as ADCP. Having several transducers pointing in different directions – velocity of all three axes is observable [6].

- **Acoustic transponders and modems:** For several decades, acoustic baseline sensors like long base line (LBL) and ultra-short base line (USBL) have been the preferred positioning sensors for underwater operations. These systems measure the time of flight for the signals, and by applying the speed of sound, the range is calculated. USBL also measures the phase of the incoming signal to determine direction. The result is a position derived from range and phase angle. Their advantage is that the errors are observable and bounded and the disadvantages are the required installations on the seabed (LBL) or on the vessel (USBL). For ROV operations, this might be acceptable. However, for AUVs, one of the prime arguments has been lower dependence on pre-installed infrastructure and vessels [6].
- **Geophysical:** This technique uses environmental features as a navigational reference. Camera images and sonar images are used in this technique based on processing these images and identify features to extract positioning information. Different algorithms used in this process based on Simultaneous Localization And Mapping (SLAM) to estimate the positioning of the vehicle [63], [64].

All of these techniques cannot be used separately but combined in order to achieve higher performance. Different aiding techniques are used by combining a group of sensor to get a good estimation of the navigational data. Besides, one of the trending techniques is the model aided navigation system where the dynamic model of the vehicle is considered. The Kalman Filter (KF) is implemented to filter the navigational data online and also to provide the optimal estimation [65], [66]. Model aiding technique could be used with only the INS navigation or also combined with aiding sensors such as DVL, USBL, and pressure sensors which provide a better estimation of the navigational data.

2.11 Ocean current estimation

Ocean current measurements are considered as a critical task of the AUV not only for the oceanography study, but also for the planning and controlling of the AUV itself. Besides, integrating the current measurements with internet of underwater things (IoUT) will enhance the environmental monitoring and disaster prevention.

2.11.1 Ocean current measurement sensors

There are different ways to measure the ocean currents such as using Acoustic Travel Time (ATT) sensors which measure the travel time of sound between a pair of probes. This method can be affected by air bubbles, biofouling, and are somewhat intrusive in the flow field. Secondly, the Acoustic Doppler Current Profiler (ADCP) sensor which is the popular technique of measuring current profile. In this method, the current wave induces the acoustic signal generated by the sensor causing the Doppler shift and reflected back to the receiver which surmises the velocity profile. The main disadvantages of the ADCP, its dependency on the scatters presence in the water column, can suffer from signal interference, and it's significantly affected from low energy level and deeper in water column [67]–[69].

2.11.2 Ocean current observation

Another technique used in estimation of the ocean current is the observation method. According to Ogatta [70], in practical application not all the system states are measureable. However, observation can estimate the unmeasured system states by using limited information or measureable states. In marine applications, observation is used to estimate the environmental disturbance, construct unmeasured states based on the available inputs, and filter the measured signals. In this research, the observation is used in ocean current estimation as an enhancement for the guidance controller and also for mapping ocean currents.

a) Linear observer technique

In this technique the ocean current considered irrotational and acting on the 2D frame. Besides, the current direction assumed to be constant as in the short term experiments the average speed considered slowly varying. This technique depends on the linear navigation model of the vehicle which uses KF to give the optimal estimation of navigation parameters including positioning and speed. Then, using statistical algorithms, the ocean current parameters could be estimated before and during the navigation mission.

In [71], a 3 DOF linear model of the HRC-AUV is developed and deployed a model aided inertial navigation system to improve the navigation system and estimate the ocean current parameters. Based on the non-linear equation of motion of the AUV, the model linearization was derived upon the perturbations from the operational point. Then, the linear state space representation of the model was obtained and the ocean current and waves state variables were considered also. The main problem was to determine the initial values of the disturbance as in the position and velocity initialization can be settled using the GPS values. Besides, wrong initialization of current parameters could affect the dynamic model performance. So, it was considered that the ocean current parameters were constant and a pre-mission experiment was applied to overcome the wrong initialization problem. This experiment used an open loop control strategy to the AUV in which the vehicle was introduced to a constant rudder angle that provokes a turning manoeuvre.

The manoeuvring pattern affected with the presence of the ocean current since in the absence of the motion current it produces a constant circle but with the presence of the ocean current a sliding pattern was obtained. The estimated centre of each sliding circle allows the estimation of the drift angle introduced by the ocean current using a least square line fitting over the centres. This strategy was conducted by simulation with less than 10% error in the simulation depending on the samples created. The real experiments are executed with same procedures using GPS and INS measurements. The results with two sensors show bigger error while using low cost INS decreases the performance over the time compared with GPS data [65]. The average current speed is estimated using the dynamic navigation vehicle model (DNVM) and the measurements of the INS sensor. This observation is initialized with incorrect value of the speed and then the observer corrects the estimation value. This technique of observation and estimation of the navigation parameters and ocean current disturbance parameters shows significant robustness with less complex model. Similar approach used has been reported in [66], [72]. In these researches, the kinematic technique of HUGIN 4500 AUV used to implement the navigation model. The deterministic least squares method was applied to the model in order to obtain the navigation parameters of the AUV and the unknown ocean current disturbance. Using experimental trials was the evaluation of this algorithm and its functionality. The results satisfy the physical interpretation and give a good post processing criteria to identify the manoeuvring characteristics including ocean current parameters. This old method was modified in the later work of Hegrenæs were the kinetic used and integrated with the navigation system. Additional sensors including USBL, pressure sensor and DVL used to validate the proposed algorithm. To filter and estimate the unknown navigation parameters of the system, the EKF was selected due to its flexibility and modest computational burden. Here, ocean current estimation depends on the DVL sensor which measures the vehicle absolute velocity and compares it with the kinetic model measurements that measure the vehicle relative velocity to the ocean current. This estimation of current depends on the DVL sensor and it's not possible to estimate the ocean current without this aiding sensor.

b) Non-linear Observers technique

Non-linear observer is commonly used on ocean current estimation especially in guidance control application to counter act the ocean current disturbance in purpose to maintain the desired planned path.

In S. Fan, W. Xu, Z. Chen, and F. Zhang work, a proposed high gain non-linear observer was implemented based on the dynamic model of the vehicle[73]. The observer designed to estimate the relative velocity of the AUV and the ocean current was considered as system uncertainties. This method benefits from the high gain observer robustness and the estimated flow velocity is more important than the usual ADCL flow gradient. The derived model based on the full dynamic equation of the AUV in terms of relative velocity of the vehicle and operate in unsteady and non-uniform flow field. The dynamic model used was based on the underwater glider architecture. The observer estimation of vehicle relative velocity used to calculate ocean current velocity in an indirect way. It is assumed that the vehicle absolute velocity vector and Euler angles are measured. Euler angles could be calculated using an electronic compass or INS and the absolute velocity could be calculated using DVL or the position differentiating. This strategy was validated using the numerical simulation and the results show a good agreement between the true and estimated current velocities, except some transient burrs during heading control [73]. Underwater glider used in this research is quietly different to the popular AUVs. This kind of underwater vehicle is a small low weight winged type and have different actuating mechanism that depends on variable buoyancy to rise or sink the vehicle. Servo actuators are used to shift the centre of mass relative to the centre of buoyancy to control pitch and roll attitude which changes the vehicle direction accordingly [74].

High gain observation could be found in different works concerned with minimum phase nonlinear system and demonstrate the robustness of this observer strategy. The influence of this kind of observer in control systems has been discussed and extended in Khalil and Praly work [75].

From the guidance control point of view, the current observation is an essential task used to take on account in control the vehicle. To overcome the current disturbance effect on the vehicle tracking control system, the controller must know the ocean current parameters. On the contrary, vehicle will diverge from the desired path and the controller will give an oscillatory behavior. The use of nonlinear observers to develop the guidance controllers appeared in different researches. In Aguiar and Pascoal work [76], the guidance of underwater vehicles has been demonstrated in the presence of ocean currents. Aguair's main problem was to track the AUV in horizontal plane and influenced by the constant ocean currents as well as combining the guidance controller and control system to achieve way point tracking. So, the guidance method chosen was the LOS technique and the controller designed was Lyapunov based adaptive controller combined with exponential observer for estimating the current disturbance. A Sirene AUV type used in this study and the kinematic model of the AUV was derived to design the controller. Resorting to integrator backstepping and Lyapunov techniques, a non-linear adaptive controller is developed that extends the kinematic controller to the dynamic case and deals with model parameter uncertainties. Then, observation of ocean currents was designed that assumes the availability of the navigation system parameters and non-variable ocean current scenario. The stability of the system has been proved through theorem 1 in the paper and the system is shown to be globally κ-exponentially stable. The performance of the system was evaluated using computer simulation that solves the mathematical frame work of the system numerically.

Using the same considerations, several works developed the guidance control system based on the nonlinear observer that has been described above. In Lekkas and Fossen work [38], [50], minimization of cross-track and along-track errors for path tracking was studied to achieve perfect tracking. Firstly, the guidance controller designed to perform a cross-track error minimization and developing a methodology for obtaining a velocity assignment that minimizes the along- track error without ocean current disturbance effect. Secondly, the ocean current disturbance considered in the system and the guidance controller used this information to correct the reference trajectory to minimize the position error caused by current disturbance. So, two adaptive nonlinear observers have been used in order to estimate current components. Based on the kinematic model of the AUV the guidance controller has been derived and the adaptive observers are deduced accordingly. The adaptive nonlinear observer assumes that the ocean current is constant and irrotational. One of the main advantages of this method is no additional absolute velocity measurement is needed.

Curved path following method also uses the adaptive nonlinear observer to estimate the current disturbance acting on underwater vehicles. The implementation of curved path following but without ocean current disturbance developed in [40] then followed by other researches conducting the presence of ocean current disturbance without estimating its parameters [43]. In [42], LOS guidance law, an adaptive current observer, and local parametrization of the path combined together to provide a curved path following in the presence of constant unknown ocean currents. In this work, it is assumed that the ocean current is constant and irrotational. Besides, the vehicle velocity is larger than the maximum ocean currents in order to overcome its effect on the vehicle.

In [77], [78], a new approach has been used to develop a control system of the AUV to reduce the effect of the destabilizing Coriolis and centripetal forces and moments which is a big challenge of controlling the AUV with high forward speed. So, the model spiltted into two separate control plant models. In this research, a nonlinear Luenberger observer has been used to estimate ocean current disturbance. The main assumptions of the observer design are the availability of the navigation parameters and considering the ocean current slowly changing. The observer provides global exponential stability of the error dynamics. Simulation results showed that the method was robust to environmental disturbance and un-modelled dynamics. The controller provided accurate tracking with the inclusion of the nonlinear Munk- moment accounting for the current velocity.

2.12 Summary

In summary, the unmanned underwater vehicle was discussed showing its history and classifying its types. Also, the different applications including oceanography, oil and gas operations, scientific analyses, weather forecasting, rescue missions, and military applications mentioned showing the importance and tendency of the underwater vehicles. AUV, which is target in this research, described comparing the different designs and versions. This chapter went through the AUV architecture and systems that determine the autonomy level of the AUV. Firstly, the AUV model techniques mentioned and concluding that Fossens technique is the reference modelling technique in the literature. Secondly, the mission planning strategies reviewed mentioning different algorithms. Then, guidance control which is the target system in this work discussed showing strategies used through the literature. ILOS guidance, the popular and effective method in different works, was chosen and reviewed for this work. Furthermore, the controlling methods sorted mentioning there advantages and disadvantages. In addition, the navigation system has been classified showing different sensors and aiding techniques that enhance the navigational performance. Finally, the ocean current estimation analyzed mentioning the importance of the observation methods as an alternative and redundant tool to estimate the current disturbance parameters.

CHAPTER THREE:

AUV SYSTEM MODELLING

3.1 Introduction

This chapter is dedicated to illustrate the HRC-AUV system used in this dissertation. It also shows the main components of the system and the use of each component. First, the dynamic model of the vehicle is derived including the main governing equations that describe the AUV motion under the water in order to simulate the behavior of the HRC-AUV under the ocean current disturbance. Then, the hydrodynamics forces that act on the vehicle underwater are detailed represented by the equation of motion. Besides, the actuation forces are derived including the coefficients of forces that describe the thruster actuator. In addition, the ocean current disturbance model is derived and represented in the equation of motion. Furthermore, the Martinez method in model parameter calculation is mentioned. Finally, the model validation is previewed comparing the simulation results with the experimental results conducted by the previous works.

3.2 HRC-AUV Architecture

The design selected in this work is the HRC-AUV model that is considered as a low cost AUV type and similar to the popular commercial and military AUV designs. It is a cigar-shaped vehicle type that has been described by Fossen's book about AUV design and modelling using the cigar-shaped type of AUV which is the standard shape and easily to construct and model mathematically [25]. This kind of AUVs is a cruising type vehicle that used in a fly-by type missions. Fly-by missions are used to surveying and gathering information using its on board sensors in long distance operations [11].

Generally, HRC-AUV consists of a single thruster and two control rudders (after rudder and stabilizing fin) for depth and heave motion. The physical and geometrical parameters of the vehicle are described in Table 3.1.

Table 3.1 AUV physical parameters [20]

Parameter	Description	Value
m	Mass	4094.56 kg
u_0	Cruise speed	1.9 m/s
N	Propeller revolution	52.36 rad/s
L	Length	9.46 m
R	Radius	0.4 m
I_{xx}	Moment of inertia	450.1 kg m^2
I_{yy}	Moment of inertia	21010.4 kg m^2
I_{zz}	Moment of inertia	20816 kg m^2
I_{xz}	Moment of inertia	275.44 Kg m^2
BG	Distance between centre of gravity & centre of bouncy	[0,0,22 mm]
δ_T	After rudder angle	+/- 30º
δ_E	Stabilizing fin angle	+/- 30º

On board components of the vehicle consist of two main industrial computers, power unit including battery, modem for communication with remote station, and sensors related to the vehicle and also for data collection. The main sensors used in the vehicle are listed as follows:

- Navigation sensors including IMU sensor for vehicles orientation and altitude, GPS sensor for vehicle localization and positioning on the surface, DVL sensor which provides the absolute velocity of the vehicle, and depth sensor.
- Operation sensors including rudders angle to feed the controller with the actual position of the rudders, thruster speed sensor, leakage sensor to alert any water leakage in the vehicle, and battery level sensor to measure the battery statues.

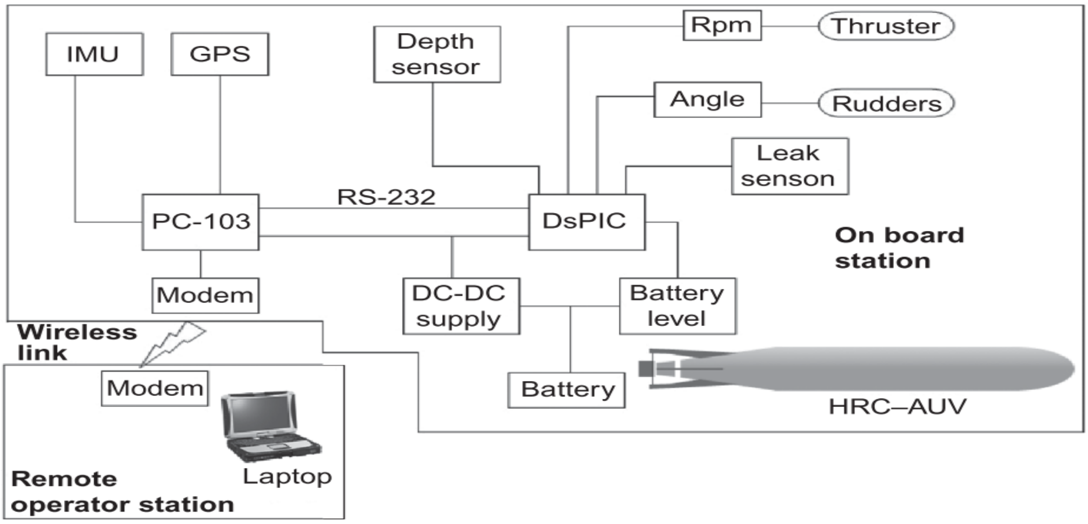

Fig 3.1 HRC-AUV architecture layout[20]

Fig 3.1 shows HRC-AUV layout architecture used in this research which is similar to the architecture used in [71],[65] and influenced by other designs like HUGIN 4500 and STARFISH AUVs [79], [80]. The model parameters and terms calculations are based on the Martinez work which have been validated experimentally [20].

The operation of the AUV consists of sequential tasks performed by the vehicle in order to achieve the user required mission as illustrated in the Fig 3.2. Firstly, the user define the target locations which the vehicle has to reach. Then, the planner defines the path and the trajectory needed regarding the time frame, minimum distance of travel, and the obstacles and dangerous regions to be avoided. Converting the defined path waypoints into velocity and direction set-points is executed by the guidance controller which is responsible of aligning the vehicle on the pre-defined path and minimizing the cross track error. The set-points provided by the guidance controller are then translated into control actions to the actuators seeking the optimal performance of this actuators. Navigation and perception system is responsible of allocating the vehicle position and measuring the vehicle velocity and orientation to feedback the vehicle control system. Besides, these sensing measurements are used to monitor the vehicle along the mission and provide the travel information to the operator and alert the controller of any danger situation. Finally, the observer provide the unmeasured states of the vehicle such as ocean current components using estimation algorithms.

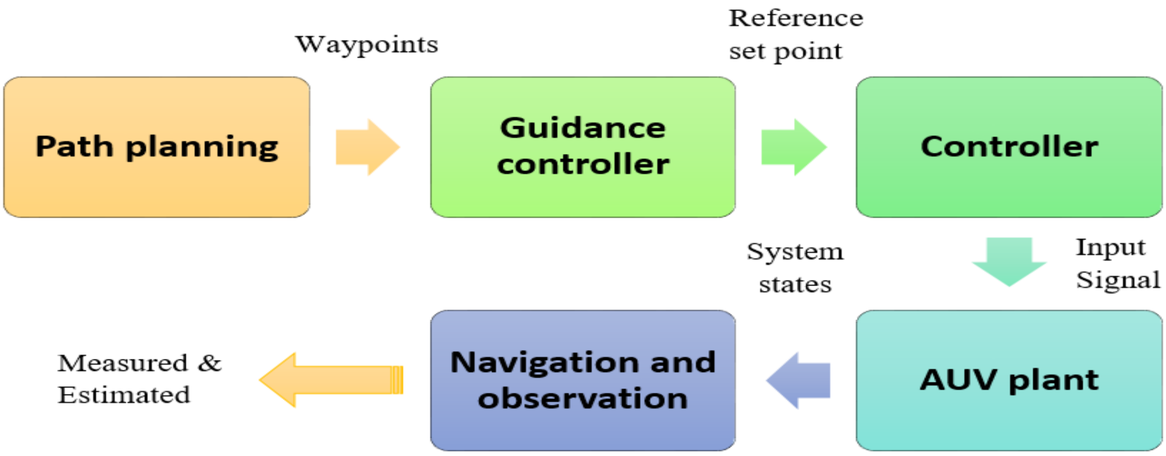

Fig 3.2 AUV operation block diagram

3.3 AUV Dynamic Modelling

The modelling method used in this work is a geometrical based analysis presenting highly nonlinear, and coupled with a dynamic relationship. The vehicle is considered as a rigid body with 6 DOF: three coordinate for displacement movement, while the other three coordinate are for the rotational movement. The motion of the vehicle at ocean is described with respect to an inertial reference system. Thus, the reference frame on the Earth fixed frame is considered as an inertial frame. Moreover, the body fixed frame where in the vehicle is considered as a moving frame that the sensors measure upon. Fig 3.3 describes the coordinate system of the vehicle responsible for defining the translational and rotational variables of the vehicle. Table 3-2 represents the nomenclature that describes mobile motion, force and moments. This is the recommended standard notation for use in maneuver applications and control of submarines[81].

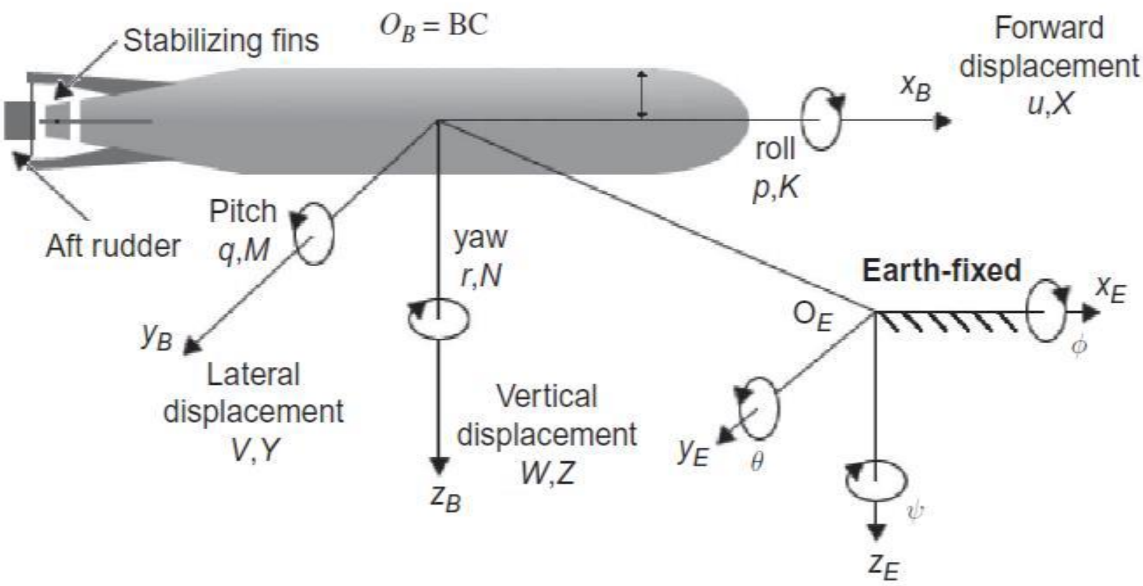

Fig 3.3 AUV reference frames

Table 3.2 Forces, moments, velocities and position notation of underwater vehicles

Motion	Forces &Moments	unit	Velocities	units	Positions	units
Surge	X	N	u	m/s	X	m
Sway	Y	N	v	m/s	Y	m
Heave	Z	N	w	m/s	Z	m
Roll	K	N.m	p	rad/s	Φ	rad
Pitch	M	N.m	q	rad/s	θ	rad
Yaw	N	N.m	r	rad/s	ψ	rad

3.3.1 Vehicle kinematics

The origin of the vehicle body (OB) coincides with the buoyancy center (BC) where the linear and angular velocities, forces, and momentum are referenced to the coordinate system (OB). However, the inertial frame with the origin of earth (OE) is used to represent the alttitude of the vehicle. The velocity and attitude vectors are defined as follows:

$$\eta = \begin{bmatrix} \eta 1 \\ \eta 2 \end{bmatrix} \quad \text{where} \quad \eta 1 = (x, y, z)^{\mathrm{T}} \tag{3.1}$$

$$\eta 2 = (\Phi, \theta, \psi)^{T}$$

$$\mathrm{V} = \begin{bmatrix} V1 \\ V2 \end{bmatrix} \quad \text{where} \quad V1 = (u, v, w)^{T} \tag{3.2}$$

$$V2 = (p, q, r)^{T}$$

The translation between body fixed frame and earth fixed frame can be obtained through the transformation of Euler angles.

$$\dot{\eta} = J(\eta)V \tag{3.3}$$

Where: $J(\eta) = \begin{bmatrix} J_1(\eta_2) & 0 \\ 0 & J_2(\eta_2) \end{bmatrix}$

$$J_1(\eta_2) = \begin{bmatrix} c\psi c\theta & (c\psi s\theta s\phi - s\psi c\phi) & (s\psi s\phi + c\psi c\phi s\theta) \\ s\psi c\theta & (c\psi c\phi + s\psi s\theta c\phi) & (s\theta s\psi c\phi - c\psi s\phi) \\ -s\theta & c\theta s\phi & c\theta c\phi \end{bmatrix} \tag{3.4}$$

$$J_2(\eta_2) = \begin{bmatrix} 1 & t\theta s\phi & t\theta c\phi \\ 0 & c\phi & -s\phi \\ 0 & \frac{s\phi}{c\theta} & \frac{c\phi}{c\theta} \end{bmatrix} \tag{3.5}$$

Where: c= cos(), s = sin() and t =tan() and θ≠0.

3.3.2 Rigid body dynamics

According to Fossen's expression of Newton's second law, the equation of motion of the underwater vehicle can be formulated as follows [25];

$$\mathrm{M}\dot{V} + \mathrm{C}\ (\mathrm{V})\ \mathrm{V} + \mathrm{D}\ (\mathrm{V})\ \mathrm{V} + g\ (\eta) = \tau \tag{3.6}$$

Where:

M: inertia matrix including the added mass.

C (V): Coriolis matrix including added coriolis.

D (V): Damping matrix.

g (η): vector of gravitational forces and moments "hydrostatic term".

τ: vector of control input.

The derivation of equation (3.6) is deduced from the Euler's first and second axioms that applied on the Newton's second law. It is considered that the body fixed is rotating about the earth fixed frame with angle $\omega = [\omega_1\ \omega_2\ \omega_3]^T$ with body mass moment of inertia I_o referred to body origin which is chosen to be at the vehicle centre of gravity .

$$I_o = \begin{bmatrix} I_x & -I_{xy} & I_{xz} \\ -I_{yx} & I_y & -I_{yz} \\ I_{zx} & -I_{zy} & I_z \end{bmatrix} \tag{3.7}$$

So the translation motion of body could be represented as:

$$m(\dot{V} + \omega \times V) = [X\ Y\ Z]^T \tag{3.8}$$

And the rotational motion could similarly expressed as:

$$I.\dot{\omega} + \omega \times (I.\omega) = [K\ M\ N]^T \tag{3.9}$$

By extending the equations (3.8) and (3.9) on the 3D, the coupled equations of motion is represented as:

$$m[\dot{u} - vr + wq - x_G(q^2 + r^2) + y_G(pq - \dot{r}) + z_G(pr + \dot{q})] = X$$

$$m[\dot{v} - wp + ur - y_G(r^2 + p^2) + z_G(qr - \dot{p}) + x_G(qp + \dot{r})] = Y$$

$$m[\dot{w} - uq + vp - z_G(p^2 + q^2) + x_G(rp - \dot{q}) + y_G(rq + \dot{p})] = Z$$

$$\begin{aligned} &I_x\dot{p} + (I_x - I_y)qr - (\dot{r} + qp)I_{xz} + (r^2 - q^2)I_{yz} + (pr - \dot{q})I_{xy} \\ &\qquad + m[y_G(\dot{w} - uq + vp) - z_G(\dot{v} - wp + ur)] = K \end{aligned} \tag{3.10}$$

$$\begin{aligned} &I_y\dot{q} + (I_x - I_z)rp - (\dot{p} + qr)I_{xy} + (p^2 - r^2)I_{zx} + (qp - \dot{r})I_{yz} \\ &\qquad + m[z_G(\dot{u} - vr + wq) - x_G(\dot{w} - uq + vp)] = M \end{aligned}$$

$$\begin{aligned} &I_z\dot{r} + (I_y - I_x)pq - (\dot{q} + rp)I_{yz} + (q^2 - p^2)I_{xy} + (rq - \dot{p})I_{zx} \\ &\qquad + m[x_G(\dot{v} - wp + ur) - y_G(\dot{u} - vr + wq)] = N \end{aligned}$$

The first three equations represent the translational motion while the last three equations represent the rotational motion and ($r_G = [x_G, y_G, z_G]^T$) is the distance between the origin (OB) and the centre of gravity (GC).

The compact vector representation of the equation of motion could be shown as:

$$M_{RB}\dot{V} + C_{RB}(V)V = \tau \tag{3.11}$$

Where $\tau = [X\ Y\ Z\ K\ M\ N]^T$ and $V = [u\ v\ w\ p\ q\ r]^T$.

The properties of the inertia M_{RB} and Coriolis and centripetal vector C_{RB} could be calculated according to the skew-symmetricity of the HRC-AUV, the distance between the GC and BC which is defined as $r_G = BG = [0\ 0\ BG_z]^T$, and parallel axis theorem. The inertia matrix according to this assumptions could be simplified into:

$$I_o = \begin{bmatrix} I_{xx} & 0 & I_{xz} \\ 0 & I_{yy} & 0 \\ I_{xz} & 0 & I_{zz} \end{bmatrix} \tag{3.12}$$

So, the inertia M_{RB} and Coriolis and centripetal vector C_{RB} is defined as:

$$M_{RB} = \begin{bmatrix} m & 0 & 0 & 0 & m\,BG_z & 0 \\ 0 & m & 0 & -m\,BG_z & 0 & 0 \\ 0 & 0 & m & 0 & 0 & 0 \\ 0 & -m\,BG_z & 0 & I_{xx} & 0 & -I_{xz} \\ m\,BG_z & 0 & 0 & 0 & I_{yy} & 0 \\ 0 & 0 & 0 & -I_{xz} & 0 & I_{zz} \end{bmatrix} \tag{3.13}$$

$$C_{RB} = \begin{bmatrix} 0 & 0 & 0 & m\,BG_z r & m\,w & -mv \\ 0 & 0 & 0 & -m\,w & m\,BG_z r & mu \\ 0 & 0 & 0 & mv - m\,BG_z p & -mu - m\,BG_z q & 0 \\ -m\,BG_z r & mw & -mv + m\,BG_z p & 0 & -I_{xz}p + I_{zz}r & -I_{yy}q \\ m\,w & -m\,BG_z r & mu + m\,BG_z q & I_{xz}p - I_{zz}r & 0 & I_{xx}p - I_{xz}r \\ mv & -mu & 0 & I_{yy}q & -I_{xx}p + I_{xz}r & 0 \end{bmatrix} \tag{3.14}$$

3.4 Hydrodynamics forces

According to Faltensin [82], the hydrodynamic forces and moments acting on a rigid body can be subjected to two sub forces:

a. Radiation induced forces

- Added mass
- Hydrodynamic damping
- Hydrostatic restoring forces

b. Environmental disturbances

- Ocean currents
- Waves
- Wind

Radiation induced forces could be described as the forces on the body when the body is forced to oscillate with wave oscillation frequency and there are no incident waves. More details could be found on [83]. In this section, the radiation induced forces will be discussed to develop the equation of motion of the 6 DOF AUV while moving underwater and the environmental disturbance will be discussed later.

3.4.1 Added mass property

Due to the rigid body movement in the fluid, an additional inertia of the surrounding fluid accelerated by this movement and it has its effect on the body. According to Fossen's definition of added mass, it is considered as pressure-induced forces and moments due to a forced harmonic motion of the body which are proportional to the acceleration of the body [25]. The added mass is a function of the object surface geometry. Using fluid kinetic energy, the added mass terms could be calculated assuming that the coefficients are constants. According to Lamb expression, the fluid kinetic energy defined as following:

$$T_A = \frac{1}{2} V^T M_A V \tag{3.15}$$

Here, the added mass inertia matrix M_A could be defined as:

$$M_A = -\begin{bmatrix} A_{11} & A_{12} \\ A_{21} & A_{22} \end{bmatrix} = -\begin{bmatrix} X_{\dot{u}} & X_{\dot{v}} & X_{\dot{w}} & X_{\dot{p}} & X_{\dot{q}} & X_{\dot{r}} \\ Y_{\dot{u}} & Y_{\dot{v}} & Y_{\dot{w}} & Y_{\dot{p}} & Y_{\dot{q}} & Y_{\dot{r}} \\ Z_{\dot{u}} & Z_{\dot{v}} & Z_{\dot{w}} & Z_{\dot{p}} & Z_{\dot{q}} & Z_{\dot{r}} \\ K_{\dot{u}} & K_{\dot{v}} & K_{\dot{w}} & K_{\dot{p}} & K_{\dot{q}} & K_{\dot{r}} \\ M_{\dot{u}} & M_{\dot{v}} & M_{\dot{w}} & M_{\dot{p}} & M_{\dot{q}} & M_{\dot{r}} \\ N_{\dot{u}} & N_{\dot{v}} & N_{\dot{w}} & N_{\dot{p}} & N_{\dot{q}} & N_{\dot{r}} \end{bmatrix} \tag{3.16}$$

Where $A_{ij}(i,j = 1,2)$

It is declared that if the body moves in the x-axis, the hydrodynamic forces due to acceleration $\dot{u}$ is defined as:

$$X_A = -X_{\dot{u}}\,\dot{u} \tag{3.17}$$

Where $X_{\dot{u}} = \frac{\partial X}{\partial \dot{u}}$,

In Newman book "Marine Hydrodynamics" [84], the added mass forces and moments are derived by applying Kirchhoff's equations which relates the fluid kinetic energy to the forces and the moments acting on the vehicle.

Added Coriolis and centripetal is also considered and can be parametrized such that $C_a(V)$ is skew-symmetrical and could be defined as Fossen's derivation and proof into the following matrix:

$$C_A(V) = \begin{bmatrix} 0_{3\times3} & -S(A_{11}V_1 + A_{12}V_2) \\ -S(A_{11}V_1 + A_{12}V_2) & -S(A_{21}V_1 + A_{22}V_2) \end{bmatrix} \tag{3.18}$$

For the fully submerged underwater vehicles, the velocities are low and the vehicle has three plans of symmetry. So, the off diagonal terms of M_A could be neglected and this will simplify the added mass matrices into:

$$M_A = dig\{X_{\dot{u}}, Y_{\dot{v}}, Z_{\dot{w}}, K_{\dot{p}}, M_{\dot{q}}, N_{\dot{r}}\} \tag{3.19}$$

$$C_A = \begin{bmatrix} 0 & 0 & 0 & 0 & -Z_{\dot{w}}w & Y_{\dot{v}}v \\ 0 & 0 & 0 & Z_{\dot{w}}w & 0 & -X_{\dot{u}}u \\ 0 & 0 & 0 & -Y_{\dot{v}}v & X_{\dot{u}}u & 0 \\ 0 & -Z_{\dot{w}}w & Y_{\dot{v}}v & 0 & -N_{\dot{r}}r & M_{\dot{q}}q \\ Z_{\dot{w}}w & 0 & -X_{\dot{u}}u & N_{\dot{r}}r & 0 & -K_{\dot{p}}p \\ -Y_{\dot{v}}v & X_{\dot{u}}u & 0 & -M_{\dot{q}}q & K_{\dot{p}}p & 0 \end{bmatrix} \tag{3.20}$$

Fossen gives a method to calculate the added mass parameters using an approximation to an ellipsoidal body with uniform mass distribution. Where a, b, and c are semi axis as in the Fig 3.4 which b and a are the largest radii of the shape and b=c.

$$X_{\dot{u}} = -\frac{\alpha_0}{2-\alpha_0}m_e \tag{3.21}$$

$$Y_{\dot{u}} = Z_{\dot{w}} = -\frac{\beta_0}{2-\beta_0}m_e \tag{3.22}$$

$$K_{\dot{p}} = 0 \tag{3.23}$$

$$M_{\dot{q}} = N_{\dot{r}} = -\frac{1}{5}\frac{\left(b^2-a^2\right)^2(\alpha_0-\beta_0)}{2(b^2-a^2)+(b^2+a^2)(\alpha_0-\beta_0)}m_e \tag{3.24}$$

Where the mass of the prolate spheroid is:

$$m_e = \frac{4}{3}\,\pi\rho a b^2 \tag{3.25}$$

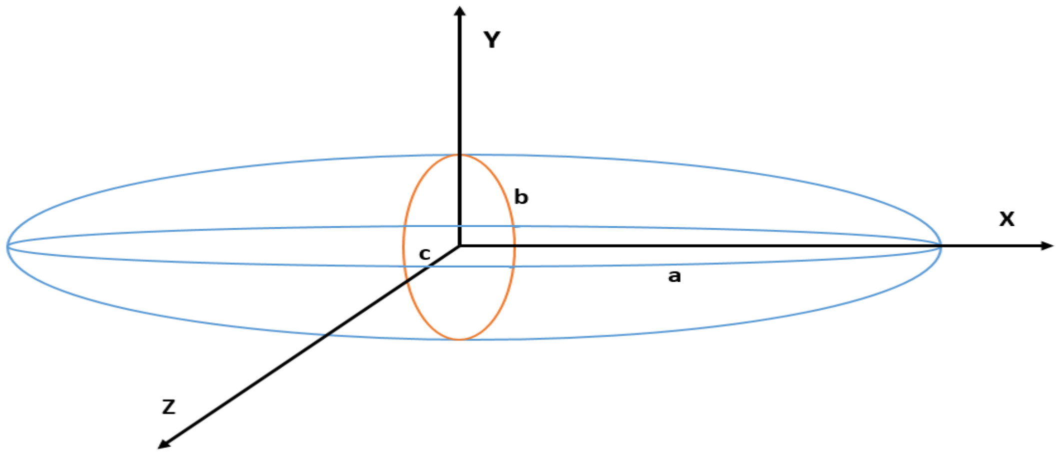

Fig 3.4 Ellipsoidal body geometry

Considering the eccentricity e to be defined as:

$$e = 1 - (^{b}/_{a})^2 \tag{3.26}$$

Hence, the constants α_0 and β_0 can be calculated as:

$$\alpha_0 = \frac{2(1-e^2)^2}{e^3}\left(\frac{1}{2}ln\frac{1+e}{1-e} - e\right) \tag{3.27}$$

$$\beta_0 = \frac{1}{e^2} - \frac{1-e^2}{2e^3}.ln\frac{1+e}{1-e} \tag{3.28}$$

On the other hand, the HRC-AUV and most of the AUVs are cylindrical not ellipsoid type. So, a methodology of finding the equivalent prolate ellipsoid is applied in HRC-AUV and different researches use the same procedures as in [10]. It is assumed that the equivalent cylinder volume to be equal to the ellipsoid volume and the equivalent ellipsoid parameters are based on the inertia moments of the AUV approximated to those in a uniformly distributed mass cylinder, where inertia moment I_x is given by $m\left(\frac{r^2}{2}\right)$ assuming r as the actual radius of the AUV. The moment of inertia $\grave{I}_x$ corresponding to the prolate ellipsoid is considered to be equal to that one of the cylinder. This moment of inertia is given by $m\left(\frac{\grave{r}^2}{2}\right)$ assuming $\grave{r}$ as the radius of the widest part of the ellipsoid [20].

3.4.2 Hydrodynamic damping property

Ocean vehicle motion is affected by the hydrodynamic damping forces acting on the vehicle. According to Fossen explanation of hydrodynamic damping, it could be summarized as follows:

- Potential damping due to forced body oscillation, $D_p(V)$.
- Linear skin friction due to laminar boundary layers and quadratic skin friction turbulent boundary layers, $D_s(V)$.
- Wave drift damping, $D_w(V)$.
- Vortex shedding damping, $D_M(V)$.

So, the hydrodynamic damping equation could be written as following:

$$D(V) = D_p(V) + D_s(V) + D_w(V) + D_M(V) \tag{3.29}$$

Due to the complexity of determining the damping parameters, a rough assumption has been considered by Fossen. It is assumed that the vehicle is performing a non-coupled motion, has three planes of symmetry and that terms higher than second order are negligible. So, diagonal structures of linear and quadratic terms are considered as follows:

$$D(V) = D_l(V) + D_c(V) \tag{3.30}$$

$$D_l(V) = -diag\{X_u, Y_v, Z_w, K_p, M_q, N_r\} \tag{3.31}$$

$$D_c(V) = -diag\{X_{u|u|}|u|, Y_{v|v|}|v|, Z_{w|w|}|w|, K_{p|p|}|p|, M_{q|q|}|q|, N_{r|r|}|r|\} \tag{3.32}$$

It is common to assume the parameters of $D_c(V)$ are zero expect the term $X_{u|u|}|u|$ which has to be calculated. This assumption is valid in case of cylindrical AUV [20].

The remaining terms could be calculated using different optimisation methods. Fossen suggested a method of identification the terms of hydrodynamic damping for control systems in surge, sway, heave and yaw using 2nd-order linear decoupled mass-damper systems formula [85]:

$$m\,\ddot{x} + d\dot{x} = \tau \tag{3.33}$$

To obtain the linear damping coefficient, a time constant is specified as following:

$$d = \frac{m}{t} \tag{3.34}$$

Where t > 0 that could be found by performing a step response in surge, sway, heave and yaw with AUV.

So the damping coefficients could be calculated as following:

$$-X_u = \frac{m - X_{\dot{u}}}{t_{surge}} \tag{3.35}$$

$$-Y_v = \frac{m - Y_{\dot{v}}}{t_{sway}} \tag{3.36}$$

$$-Z_w = \frac{m - Z_{\dot{w}}}{t_{heave}} \tag{3.37}$$

$$-N_r = \frac{m - N_{\dot{r}}}{t_{yaw}} \tag{3.38}$$

For cylindrical shape, it is assumed that:

$$N_r = M_q \; ; Y_v = Z_w \tag{3.39}$$

According to Martinez, Y_v could be simplified into:

$$Y_v \approx 12\frac{N_r}{L^2} \tag{3.40}$$

For Roll and pitch are assumed to be 2nd-order mass spring damper system:

$$m\,\ddot{x} + d\,\dot{x} + k\,x = \tau \tag{3.41}$$

Where

$$\frac{d}{m} = 2\mu\omega_n = 2\mu\sqrt{\frac{k}{m}} \text{ Or } d = 2\mu\sqrt{k.m}$$

So, the roll and pitch damping terms is calculated as following:

$$-K_p = 2\mu_{roll}\sqrt{BG_z.W(I_x - K_{\dot{p}})} \tag{3.42}$$

$$-M_q = 2\mu_{pitch}\sqrt{BG_z.W(I_y - M_{\dot{q}})} \tag{3.43}$$

Where relative damping ratios μ_{roll} and μ_{pitch} are small between 0.1 and 0.2[85]. Another approach of obtaining the hydrodynamic terms is using Lyapunov method which introduced by Lyashevskiy and Abel [86].

3.4.3 Hydrostatic restoring forces

The hydrostatic forces acting on the vehicle consist of gravitational weight forces acting on the center of the gravity GC and a buoyancy forces that act on center of buoyancy BC. For submerged bodies the weight and buoyancy forces are equal to following:

$$W = m.g \tag{3.44}$$

$$B = \rho_{water}.\, g.\nabla \tag{3.45}$$

Where ∇ is the submerged volume of the vehicle and $\rho_{water}$is the density of the water. By transforming the forces to the body fixed frame, the vector representation of the forces will be equal to:

$$f_g = J^{-1}(\eta_2)\ [0\ 0\ W]^T \tag{3.46}$$

$$f_b = J^{-1}(\eta_2)\ [0\ 0\ B]^T \tag{3.47}$$

The sign of restoring forces and moments is negative since this term is included on the left hand-side of Newton's 2nd law. So the total restoring forces could be expressed as follows:

$$g(\eta) = -\begin{bmatrix} f_g + f_b \\ r_g \times f_g + r_b \times f_b \end{bmatrix} \tag{3.48}$$

Then, the equation could be expanded into:

$$g(\eta) = \begin{bmatrix} (W-B)s\theta \\ -(W-B)c\theta s\phi \\ -(W-B)c\theta c\phi \\ -(y_gW - y_bB)c\theta c\phi + (z_gW - z_bB)c\theta s\phi \\ (z_gW - z_bB)s\theta + (x_gW - x_bB)c\theta c\phi \\ -(x_gW - x_bB)c\theta s\phi - (y_gW - y_bB)s\theta \end{bmatrix} \tag{3.49}$$

The distance between GC and BC is represented as:

$$BG = [BG_x\ BG_y\ BG_z]^T = [x_g - x_b, y_g - y_b, z_g - z_b] \tag{3.50}$$

Taking into account, for underwater vehicles $W = B$ and $BG_x = BG_y = 0$ for HRC-AUV. So the restoring forces could be represented as:

$$g(\eta) = [0,0,0, W.BG_z.c\theta\ s\phi, W.BG_z.s\theta, 0]^T \tag{3.51}$$

3.5 Actuator Modelling

The actuation forces that control the HRC-AUV are subjected to the main propeller, aft rudder, and stabilization fin. In Fossen's survey of underwater actuators, different actuation and configuration have been described and the non-rotatable thruster type has been deduced for the 6 DOF motion [87]. The input control force could be described with linear model equation:

$$F = k.U \tag{3.52}$$

And

$$F = \begin{bmatrix} f_x \\ f_y \\ f_z \end{bmatrix} = \begin{bmatrix} k_1 & 0 & 0 \\ 0 & k_2 & 0 \\ 0 & 0 & k_3 \end{bmatrix} . \begin{bmatrix} |n|n \\ \delta_T \\ \delta_E \end{bmatrix} \tag{3.53}$$

Where the k is the force coefficient matrix and U is the control input which is function of the propeller revolution speed n and rudder angles δ_T and δ_E. According to Fossen [25], the modelling of thrusting force is highly nonlinear and complicated which depends on the vehicle velocity and control variable u.

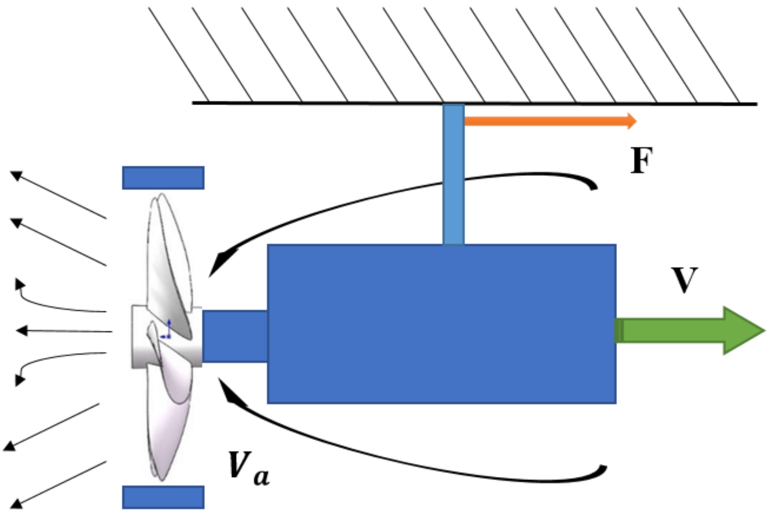

Fig 3.5 Single screw propeller

For single screw propeller as in the Fig 3.5, the developed thrust f_x can be calculated using lift force calculations as following:

$$f_x = \rho_{water}\, D^4 K_T\, J_o |n| n \tag{3.54}$$

And

$$\mathrm{J_o} = \frac{\mathrm{V_a}}{\mathrm{n.D}} \tag{3.55}$$

Where K_T is the thrust coefficient, D is the propeller diameter, and V_a is the advance speed at the propeller (speed of water going into propeller).

The forces and moments acting on the vehicle in 6 DOF based on the input force vector could be written as:

$$\tau = \begin{bmatrix} F \\ r \times F \end{bmatrix} = \begin{bmatrix} f_x \\ f_y \\ f_z \\ f_z l_y - f_y l_z \\ f_z l_y - f_y l_z \\ f_z l_y - f_y l_z \end{bmatrix} \tag{3.56}$$

Where $r_f = [I_x \quad I_y \quad I_z]$ the vector of moment arm is related the actuator location with respect to the body origin OB. In HRC-AUV, the actuators are aligned with OB which $r_f = [4 \quad 0 \quad 0.022]$. From equations (3.53) and (3.56), the total actuation force acting on the vehicle could extended into:

$$\tau = \begin{bmatrix} 1 & 0 & 0 \\ 0 & 1 & 0 \\ 0 & 0 & 1 \\ 0 & -I_z & I_y \\ I_z & 0 & -I_x \\ -I_y & I_x & 0 \end{bmatrix} \begin{bmatrix} k_1 & 0 & 0 \\ 0 & k_2 & 0 \\ 0 & 0 & k_3 \end{bmatrix} . \begin{bmatrix} |n|n \\ \delta_T \\ \delta_E \end{bmatrix} = \begin{bmatrix} k_1 & 0 & 0 \\ 0 & k_2 & 0 \\ 0 & 0 & k_3 \\ 0 & -k_2 I_z & k_3 I_y \\ k_1 I_z & 0 & -k_3 I_x \\ -k_{1_y} & k_2 I_x & 0 \end{bmatrix} \begin{bmatrix} |n|n \\ \delta_T \\ \delta_E \end{bmatrix} \quad (3.57)$$

$$\tau = \begin{bmatrix} X \\ Y \\ Z \\ K \\ M \\ N \end{bmatrix} = \begin{bmatrix} b_1 & 0 & 0 \\ 0 & b_2 & 0 \\ 0 & 0 & b_3 \\ 0 & b_4 & 0 \\ 0 & 0 & b_5 \\ 0 & b_6 & 0 \end{bmatrix} \begin{bmatrix} |n|n \\ \delta_T \\ \delta_E \end{bmatrix} \quad (3.58)$$

These gains could be calculated using experimental tests to obtain these values [20].

3.6 Numeric values of HRC-AUV

In this section, the HRC-AUV model parameters are calculated in order to solve the equation of motion to get the output states at the given inputs. After deriving the equation of motion terms, the equation (6) is extended into:

$$M_{RB}\dot{V} + C_{RB}(V)V + M_A\dot{V} + C_A(V)V + D(V)V + g(\eta) = \tau \quad (3.59)$$

Besides, the terms of the equation of motion including geometrical and inertial values could be estimated for HRC-AUV using mechanical design software such as Autodesk Inventor as mentioned in [20]. The results was represented in Table 3.1. The added mass values could be calculated using equations (21), (22), (23), and (24). So:

$X_{\dot{u}} = -250.84$ kg. $Y_{\dot{v}} = Z_{\dot{w}} = -3834$ kg, $K_{\dot{p}} = 0$ and $M_{\dot{q}} = N_{\dot{r}} = -15572$ kg m^2.

So the inertia and added mass matrices could be calculated from equations (3.13) and (3.16) by applying the previous results and expressed as follows:

$$M_{RB} = \begin{bmatrix} 4094.56 & 0 & 0 & 0 & 90.08 & 0 \\ 0 & 4094.56 & 0 & -90.08 & 0 & 0 \\ 0 & 0 & 4094.56 & 0 & 0 & 0 \\ 0 & -90.08 & 0 & 450.1 & 0 & -275.44 \\ 90.08 & 0 & 0 & 0 & 21010 & 0 \\ 0 & 0 & 0 & -275.44 & 0 & 20816 \end{bmatrix} \tag{3.60}$$

$$M_A = -dig\{-250.84, -3834, -3834, 0, -15572, -15572\} \tag{3.61}$$

Also, Coriolis and added Coriolis matrices from equations (3.14) and (3.20) could be expressed as following:

$$C_{RB} = \begin{bmatrix} 0 & 0 & 0 & 90.08r & 4094.56\,w & -4094.56v \\ 0 & 0 & 0 & -4094.56\,w & 90.08r & 4094.56u \\ 0 & 0 & 0 & mv - 90.08p & -4094.56u - 90.08q & 0 \\ -90.08r & 4094.56w & -4094.56v + 90.08p & 0 & -275.44p + 20816r & -21010.4q \\ 4094.56\,w & -90.08r & 4094.56u + 90.08q & 275.44p - 20816r & 0 & 450.1p - 275.44r \\ 4094.56v & -4094.56u & 0 & 21010.4q & -450.1p + 275.44r & 0 \end{bmatrix} \tag{3.62}$$

$$C_A = \begin{bmatrix} 0 & 0 & 0 & 0 & 3834w & -3834v \\ 0 & 0 & 0 & -3834w & 0 & 250.84u \\ 0 & 0 & 0 & 3834v & -250.84u & 0 \\ 0 & 3834w & -3834v & 0 & 15572r & -15572q \\ -3834w & 0 & 250.84u & -15572r & 0 & 0 \\ 3834v & -250.84u & 0 & 15572q & 0 & 0 \end{bmatrix} \tag{3.63}$$

The gravitational term could be calculated from equation (3.51) by applying geometrical parameters from Table 1 and is expressed as following:

$$g(\eta) = [0, 0, 0\,,\ 890.5\, c\theta\, s\phi,\ 890.5\, s\theta,\ 0]^T \tag{3.64}$$

The main problem is to calculate the damping and actuation forces terms. According to Martinez, these terms are calculated by model linearization and decoupling. Then, an experimental identification is applied to the linearized model equations to obtain the missing terms [20]. First, the system is separated into three subsystems:

a- Longitudinal linear subsystem:

The equation of motion is linearized and decoupled by stating that the variables υ= p= r = ϕ=0. The model is simplified by assuming constant forward speed ($u = 0$). So, the 3 DOF model will be simplified into:

$$\begin{bmatrix} m - Z_{\dot{w}} & 0 \\ 0 & I_{yy} - M_{\dot{q}} \end{bmatrix} \begin{bmatrix} \dot{w} \\ \dot{q} \end{bmatrix} + \begin{bmatrix} -Z_w & 0 \\ 0 & -M_q \end{bmatrix} \begin{bmatrix} w \\ q \end{bmatrix} +$$

$$\begin{bmatrix} 0 & -(m - X_{\dot{u}})u \\ (Z_{\dot{w}} - X_{\dot{u}})u & 0 \end{bmatrix} \begin{bmatrix} w \\ q \end{bmatrix} + \begin{bmatrix} 0 \\ WBG_z s\theta \end{bmatrix} = \begin{bmatrix} Z \\ M \end{bmatrix} \tag{3.65}$$

The dynamics of pitching could be expressed as:

$$(I_{yy} - M_{\dot{q}})\ddot{\theta} - M_q\dot{\theta} + WBG_z\theta = M \tag{3.66}$$

The transfer function between stabilizing angle δ_E and pitch angle θ is:

$$\frac{\theta(s)}{\delta_E} = \frac{b_5}{(I_{yy} - M_{\dot{q}})s^2 - M_q s + WBG_z} \tag{3.67}$$

b- Lateral linear subsystem:

The equation of motion is linearized and decoupled by stating that the variables u, w, p, r, ϕ and θ are small. The dynamic equation of the AUV left to the states (υ, p, and r) and (y, ϕ, ψ) is as follows:

$$\begin{bmatrix} m - Y_{\dot{v}} & 0 \\ 0 & I_{zz} - N_{\dot{r}} \end{bmatrix} \begin{bmatrix} \dot{v} \\ \dot{r} \end{bmatrix} + \begin{bmatrix} -Y_v & 0 \\ 0 & -N_r \end{bmatrix} \begin{bmatrix} v \\ r \end{bmatrix} +$$

$$\begin{bmatrix} 0 & -(m - X_{\dot{u}})u \\ (X_{\dot{u}} - Y_{\dot{v}})u & 0 \end{bmatrix} \begin{bmatrix} v \\ r \end{bmatrix} = \begin{bmatrix} Y \\ N \end{bmatrix} \tag{3.68}$$

The dynamics of yaw ψ could be expressed as:

$$(I_{zz} - N_{\dot{r}})\ddot{\psi} - N_r\dot{\psi} = N \tag{3.69}$$

The transfer function between aft rudder angle δ_T and yaw angle ψ is:

(3.70)

$$\frac{\psi(s)}{\delta_T(s)} = \frac{b_6}{(I_{zz} - N_{\dot{r}})s^2 - N_r s}$$

c- Navigational linear subsystem:

The equation of motion is established in a 3 DOF where the working plane is the x-y plane. So, the velocity and force vectors become $V = [u \quad v \quad r]^T$ and $\tau = [\tau_X \quad \tau_Y \quad \tau_N]^T$ and the following equation is obtained:

$$\begin{bmatrix} m - X_{\dot{u}} & 0 & 0 \\ 0 & m - Y_{\dot{v}} & 0 \\ 0 & 0 & I_{zz} - N_{\dot{r}} \end{bmatrix} \begin{bmatrix} \dot{u} \\ \dot{v} \\ \dot{r} \end{bmatrix} +$$
$$\begin{bmatrix} -X_u - X_{u|u|}|u| & 0 & 0 \\ 0 & -Y_v - Y_{v|v|}|v| & 0 \\ 0 & 0 & -N_r - N_{r|r|}|r| \end{bmatrix} \begin{bmatrix} u \\ v \\ r \end{bmatrix} +$$
$$\begin{bmatrix} 0 & 0 & (-m - Y_{\dot{v}})v \\ 0 & 0 & (m - X_{\dot{u}})u \\ (m - Y_{\dot{v}})v & (-m - X_{\dot{u}})u & 0 \end{bmatrix} \begin{bmatrix} u \\ v \\ r \end{bmatrix} + \begin{bmatrix} 0 \\ 0 \\ 0 \end{bmatrix} = \begin{bmatrix} X \\ Y \\ N \end{bmatrix} \tag{3.71}$$

The decoupled equation of motion for 1 DOF model for navigation when $v = r = 0$ could be expressed as:

$$(m - X_{\dot{u}})\dot{u} = X + X_u u + X_{u|u|}|u| \tag{3.72}$$

From the above equations, Martinez applied an experimental identification technique using Matlab identification toolbox software to get the missing parameters of the system [20]. So, damping values are:

$$D_l\,(v) = -diag\{-181.45, -1219.8, -1219.8, -126.62, -9096.9, -9096.9\}$$

$$\text{And } X_{u|u|} = 47.49\ \frac{N}{m^2/s^2} \tag{3.73}$$

3.7 Ocean Current Modelling

In marine vehicles, winds, waves, and ocean, currents are considered as an environmental disturbance that affect the vehicle motion. For AUVs, ocean currents can be assumed as the main disturbance on the vehicle motion. Therefore, in this research, ocean currents are considered, whereas the other environmental disturbances are neglected. Generally, ocean currents generated by different factors including atmospheric wind over the ocean surface, the heat exchange between ocean layers and zones, the salinity effect, Coriolis forces due to earth rotation which will turn the major current to right in the northern hemisphere and opposite in the southern hemisphere, and also the tidal components arising from planetary interactions like gravity [25]. Using Fossen's methodology in marine disturbance modelling, vehicle under the effect of ocean currents can be represented by the equation of motion in terms of relative velocity (V_r).

Where:

$$V_r = V - V_c \tag{3.74}$$

And $V_c = [u_c \quad v_c \quad w_c \quad 0 \quad 0 \quad 0]^T$ is the velocity vector referred to OB, assuming that the current does not generate rotational movement on the vehicle. To transform between body fixed frame OB and earth fixed frame, the Euler transformation angle is applied as following:

$$V_c^E = J(\eta).V_c \tag{3.75}$$

where V_c^E is the ocean current velocity vector with respect to the earth fixed frame.

Besides, the velocity component equation (59) can be rewritten in the new format:

$$M_{RB}\,\dot{V}_r + C_{RB}(V_r)V_r + \; M_A\,\dot{V}_r + C_A(V_r)V_r + \; D(V_r)V_r + g(\eta) = \tau \tag{3.76}$$

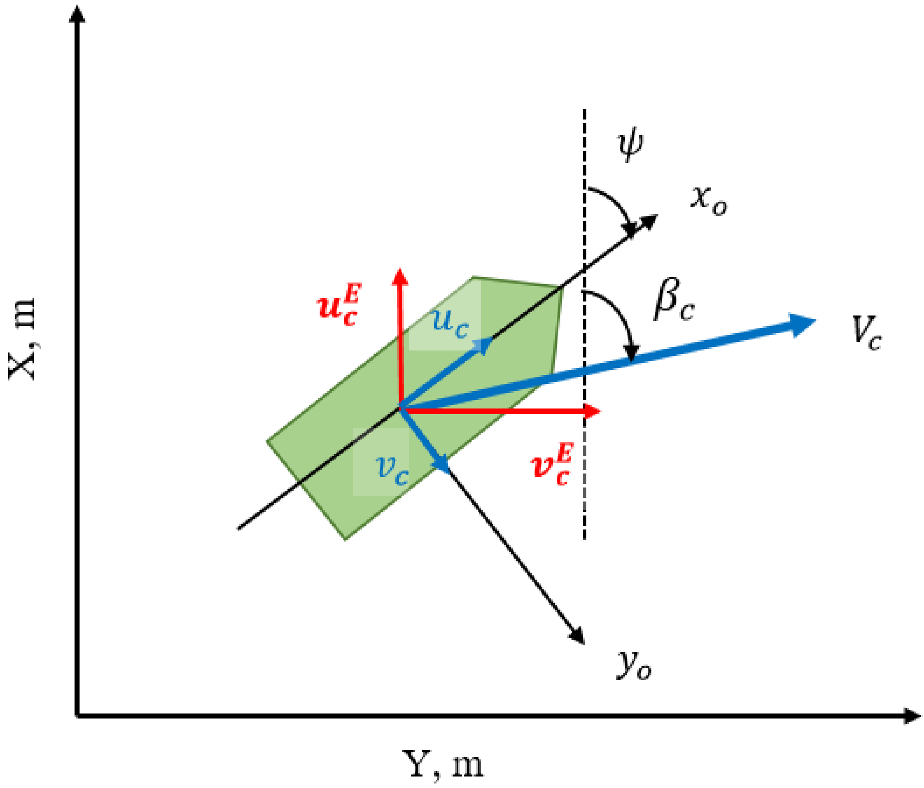

Fig 3.6 Ocean current acting on the vehicle in 2D representation

For the 2D representation, the velocity components referred to the OE are related to the V_c vector by average current speed V_{ca} the current angle (β_c) as in the Fig 3.6.

$$u_c^E = V_{ca} \cos \beta_c \tag{3.77}$$

$$v_c^E = V_{ca} \sin \beta_c \tag{3.78}$$

To refer velocity components to OB, the Euler angle transformation and the trigonometrical identities are applied according to the following equations:

$$u_c = V_{ca} \cos(\beta_c - \psi) \tag{3.79}$$

$$v_c = V_{ca} \sin(\beta_c - \psi) \tag{3.80}$$

In simulation work, the ocean current could be generated using 1st order Gauss-Markov process. Next, by the usage of the nonlinear observer, the current velocity components can be estimated and mapped.

3.8 Model validation

This model was validated experimentally with the calculated parameters on a real test conducted on March 2010. The first test was established by applying a constant deflection angle $\delta_T = 0.45\, rad$, propulsion of $n = 490\, rpm$, and initial yaw angle $\psi = 213.5°$, ocean current $V_c = 0.195\, m/sec$ $\beta_c = 260°$.The AUV operated in the surface of the water and the navigational data was measured using the GPS and compared to the simulation data. The results show that the position mean error was of 2.9 m with a standard deviation of 1.74 m as in the Fig 3.7 [20].

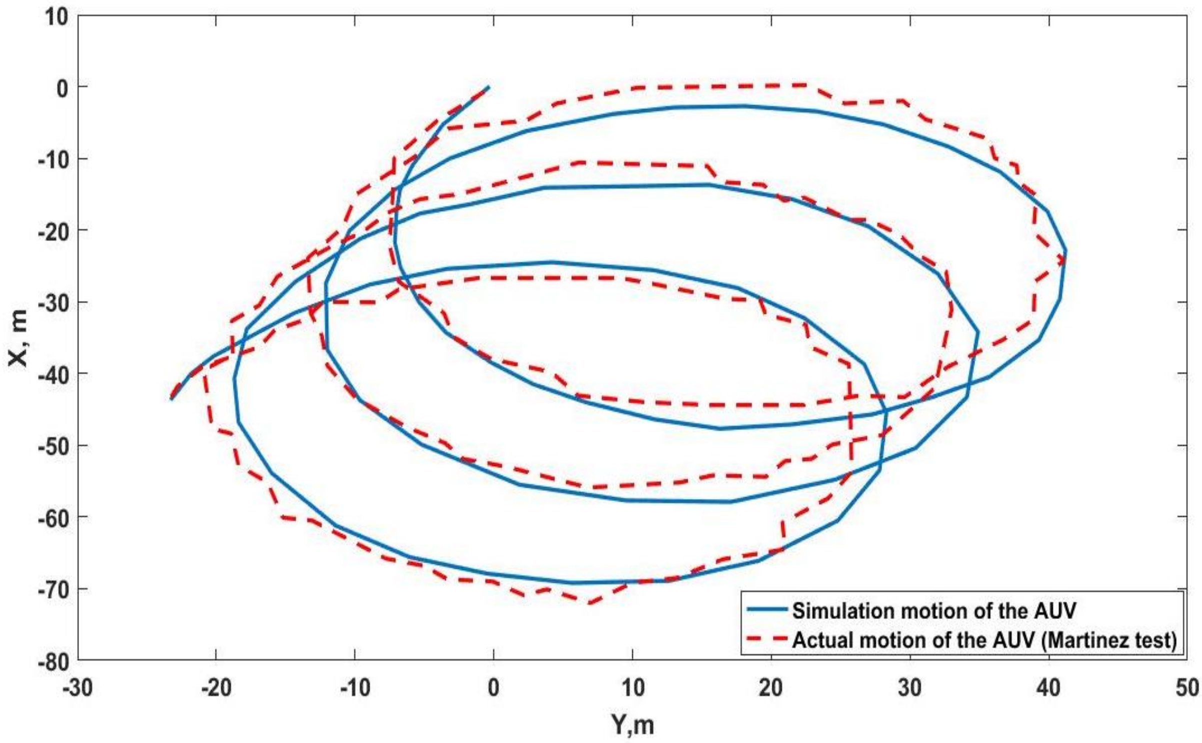

Fig 3.7 Navigational behavior of the HRC-AUV compared to the model simulation

3.9 Summary

In this chapter, the HRC-AUV is introduced considering its architecture and main hardware components. Also, the dynamic model of the HRC-AUV is derived using Fossen's modeling technique that based on Newton-Euler equation of motion. Then, the parameters of the model are derived and then calculated numerically based on the Martinez calculations. Besides, the modeling of ocean current disturbance is derived and represented in the model. Finally, the validation of the model is discussed based on the Martinez test.

CHAPTER FOUR:
CONTROL SYSTEM DESIGN

4.1 Introduction

This chapter shows the implementation of the dynamic model of the HRC-AUV in Matlab software. Then, the control system is discussed through the derivation of the ocean current observer and the guidance control system. Also, the heading controller is derived to perform the path following mission. Fig 4.1 illustrates the structure of the AUV system in which the path waypoints are generated by the mission operator and this waypoints are processed using the guidance controller to generate the reference heading angle. Then, the heading controller applies the sufficient signal to the after rudder actuator in order to hover with reference heading angle that enable the vehicle to follow the desired path.

4.2 Implementation Dynamic model of the AUV

The model is implemented by several stages to include the environment model and the AUV model. First the physical parameters of the HRC-AUV in Table 3-1 are declared in M-file as shown in Appendix.

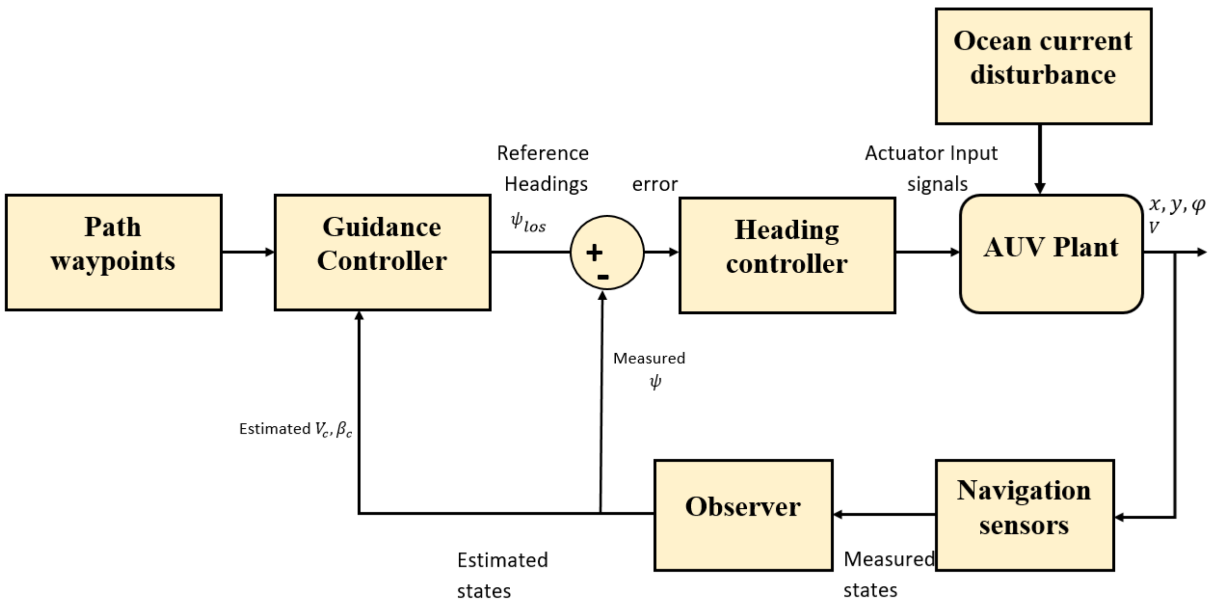

Fig 4.1 AUV control system architecture

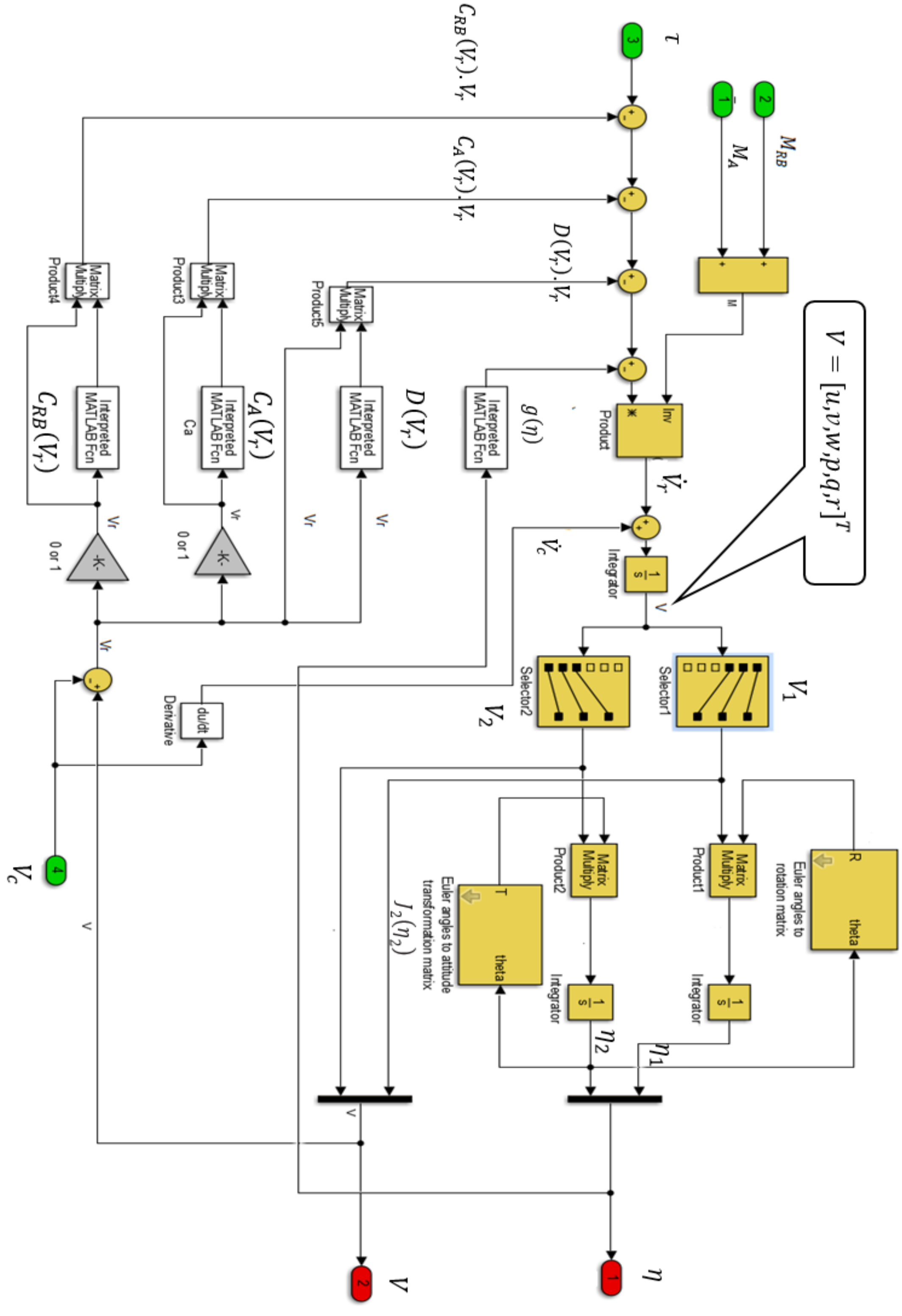

Fig 4.2 AUV equation of motion sub system in Simulink

Also the rigid body mass and added mass from equations (3.60), (3.61) are generated in the same file from the physical parameters of the HRC-AUV. According to equations (3.74) and (3.76), the system dynamic model could be written in the following form:

$$\dot{V} = (M_{RB} + M_A)^{-1}.[\tau - C_{RB}(V_r)V_r - C_A(V_r)V_r - D(V_r)V_r - g(\eta)] + \dot{V}_c \tag{4.1}$$

The generated M-file is used to construct the terms of equation (4.1) that represent the dynamic model of the AUV. So, the rigid body and added Coriolis, damping, and hydrostatic restoring forces are generated as a function of the physical parameters and relative velocity of the vehicle. Equations (3.62), (3.63), and (3.64) are constructed in M-file as shown in the Appendix. Then, the created functions are deployed in Simulink workspace to create the equation of motion subsystem as in Fig 4.2.

4.3 Observer Design

As shown in Fig 4.1, navigation process is followed by an observer stage to estimate the missing states of the system which cannot be obtained by the direct measurement tools. In this section, two different non-linear observers, based on HRC-AUV dynamic model for current velocity estimation, are represented using open loop observer and High Gain observer methods. It is assumed that the vehicle absolute velocities and Euler angle are measurable using the INS sensor and electronic compass. Generally, observation is used in AUVs with different purposes such as estimation of navigation parameters, enhancing the feedback parameters for the controller, or estimation of the missing ocean current data parameters. The following observers are used as a redundant or assistant estimation tool for measuring ocean currents and to support the guidance controller in tracking the desired path under environmental disturbance.

4.3.1 Open loop observer

Open loop observation is considered as a simple strategy for estimating the unmeasured states. However, the model uncertainty compensation is not available for this kind of estimation. The following assumptions have been considered in the observer design:

- The ocean current is irrotational and non-uniform but bounded with $V_c < V_{max}$
- The vehicle absolute velocity and Euler angles are measurable.
- The model uncertainty is very low.

By defining the system states:

$\mathbf{x}_1 = \eta$

$\mathbf{x}_2 = V$

Where $\mathbf{x}_2 = \dot{\mathbf{x}}_1$ and $\mathbf{y}$ is the measured output vector. Equation (4.1) could be written in the following form:

$$f(\mathbf{x}, \tau, V_c) = (M_{RB} + M_A)^{-1}.\left[\tau - C_{RB}(\mathbf{x}_2 - V_c)(\mathbf{x}_2 - V_c) - C_A\big((\mathbf{x}_2 - V_c)\big)((\mathbf{x}_2 - V_c) - g(\mathbf{x}_1)\right] \tag{4.2}$$

So, the dynamic equation of motion could be represented as:

$$\dot{\mathbf{x}}_2 = f(\mathbf{x}, \tau, V_c) + \dot{V}_c \tag{4.3}$$

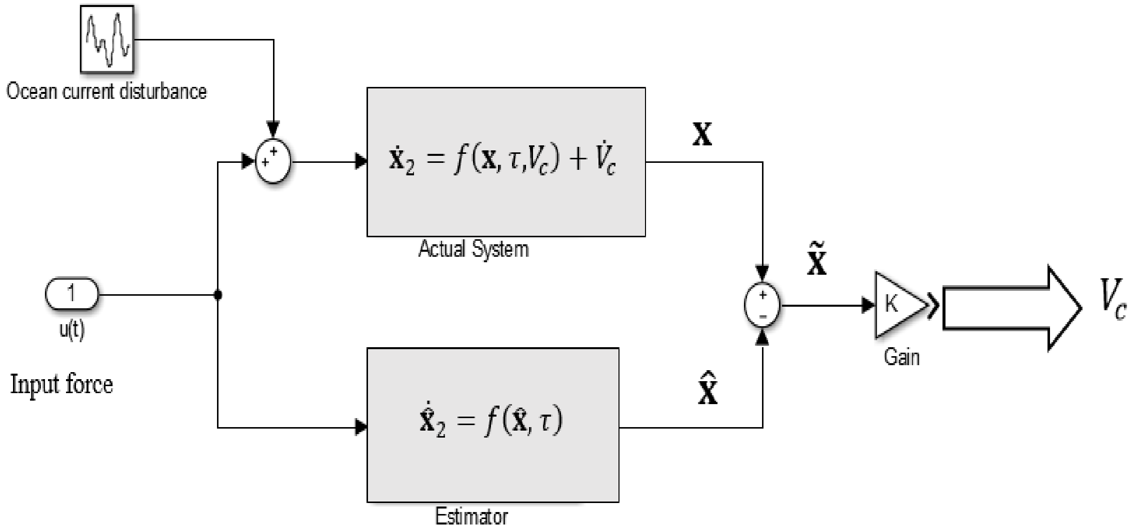

Fig 4.3 Block diagram of open loop observer

The observer consists of the dynamic model of the system which is simulated with the same actual input and the output is compared to the vehicle navigation output as shown in Fig. 4.3.

$$\dot{\hat{\mathbf{x}}}_2 = f(\hat{\mathbf{x}}, \tau) \tag{4.4}$$

Where $f(\hat{\mathbf{x}}, \tau)$ is the model of $f(\mathbf{x}, \tau, V_c)$ which V_c is the only system disturbance. So, the output of the observer is the relative velocity when the model disturbance is zero. Ocean current can be calculated from the difference between the absolute and relative velocities and multiplied by the rotation matrix $J(\eta)$ to express in the Earth fixed frame.

$$\dot{\tilde{\mathbf{x}}} = \dot{\mathbf{x}}_2 - \dot{\hat{\mathbf{x}}}_2 = f(\mathbf{x}, \tau, V_c) + \dot{V}_c - f(\hat{\mathbf{x}}, \tau) \tag{4.5}$$

So

$$V_c = k_o \tilde{\mathbf{x}}_2 \tag{4.6}$$

$$V_c^E = J(\eta). V_c \tag{4.7}$$

Where k_o is the observer gain and it is assumed to be unity as the current is the only uncertainty of the system.

4.3.2 High-Gain observer

On the other hand, the uncertainty of the model could affect the estimation process of the open loop observer in the real operation. So, the closed loop observers are required to compensate the uncertainty. In this case, the observer will include the compensating term given by the orientation measurements as describes in Fig 4.4. In which, the output measurement ($\mathbf{y}$) is given by the following equation:

$$\mathbf{y} = \mathrm{C}.\mathbf{x_1} \tag{4.8}$$

And $\mathrm{C} = \begin{bmatrix} 0 & 0 & 0 & 0 & 0 & 0 \\ 0 & 0 & 0 & 0 & 0 & 0 \\ 0 & 0 & 0 & 0 & 0 & 0 \\ 0 & 0 & 0 & 1 & 0 & 0 \\ 0 & 0 & 0 & 0 & 1 & 0 \\ 0 & 0 & 0 & 0 & 0 & 1 \end{bmatrix}$

$$\dot{\hat{\mathbf{x}}}_2 = f(\hat{\mathbf{x}}, \tau) + K_1(\mathbf{y} - C\,\hat{\mathbf{x}}_\mathbf{1}) \tag{4.9}$$

So, the estimation error from equations (4.3), (4.9) could be obtained from following:

$$\dot{\tilde{\mathbf{x}}} = \dot{\mathbf{x}}_2 - \dot{\hat{\mathbf{x}}}_2 = f(\mathbf{x}, \tau, V_c) + \dot{V}_c - f(\hat{\mathbf{x}}, \tau) - K_{o1}(\mathbf{y} - C\,\hat{\mathbf{x}}_\mathbf{1}) \tag{4.10}$$

$$\dot{\tilde{\mathbf{x}}} = \boldsymbol{\varepsilon}(\mathbf{x}, \hat{\mathbf{x}}, \boldsymbol{V_c}) + \dot{V}_c - K_{o1}(\mathbf{y} - C\,\hat{\mathbf{x}}_\mathbf{1}) \tag{4.11}$$

Where (K_{o1}) is the observer gain matrix and ($\boldsymbol{\varepsilon}$) is the difference between system dynamics and system model [$\boldsymbol{\varepsilon}(\mathbf{x}, \hat{\mathbf{x}}, \boldsymbol{V_c}) = f(\mathbf{x}, \tau, V_c) - f(\hat{\mathbf{x}}, \tau)$]. In the absence of system disturbance and uncertainty, the estimation error will be zero. In the presence of the system disturbance, the observer gain is designed in order to reject the effect of ($\boldsymbol{\varepsilon}$) and makes the observer robust to uncertainties in modelling the nonlinear functions. After rejecting the uncertainty term, the ocean current disturbance could be obtained using the same open-loop steps in equations (4.6), (4.7).

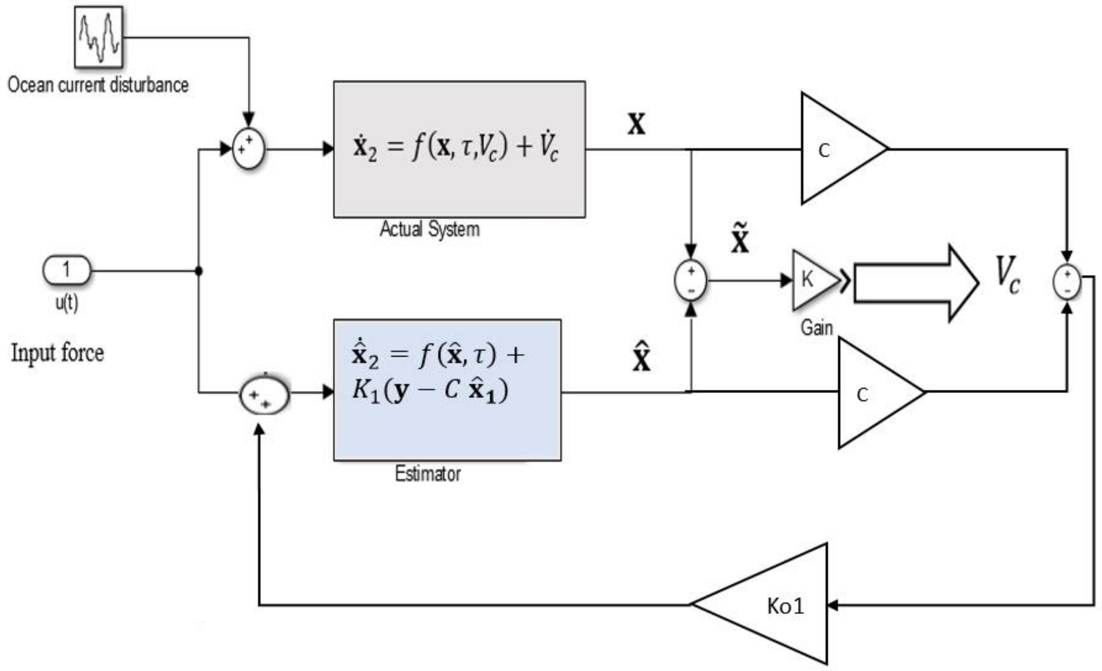

Fig 4.4 Block diagram of a high gain observer

4.4 Guidance controller

The guidance controller based on LOS is designed for a 2D straight line path following scenario where the autopilot has a decoupled motion control for heading and attitude motion. The system is applied to the heading controller which is similar to the attitude control. The speed of the vehicle is adjusted with constant value ($U_t > 0$) while steering angle is varied according to the path angle variation.

First, the guidance law is derived for the non-disturbed scenario and analysed before studying the guidance in ocean current disturbance scenario. The way points given by the planner are denoted as ($W_n = [W_{x_n}, W_{y_n}]^T$), and ($W_{n+1} = [W_{x_{n+1}}, W_{y_{n+1}}]^T$). The angle between any two waypoints (γ_p) could be calculated from:

$$\gamma_p = atan2\left(\frac{W_{y_{n+1}} - W_{y_n}}{W_{x_{n+1}} - W_{x_n}}\right) \tag{4.12}$$

The aim of the path following law is to converge the AUV towards the waypoint path. Hence, the cross track error (CE) is defined as the error between the vehicle position and the nearest path points. Also, the long track error (S) is defined as the difference between the AUV position and the waypoint along the track. According to Breivik and Fossen [11], the coordinates of the vehicle kinematics could be calculated from following equation:

$$\begin{bmatrix} S \\ CE \end{bmatrix} = J(\gamma_p)[P(t) - W_n] \tag{4.13}$$

Where ($P(t) = [x, y]^T$) is the instantaneous position of the AUV and $J(\gamma_p)$ is the transformation matrix between vehicle body fixed frame and path fixed frame:

$$J(\gamma_p) = \begin{bmatrix} \cos\gamma_p & -\sin\gamma_p \\ \sin\gamma_p & \cos\gamma_p \end{bmatrix} \tag{4.14}$$

From equations (4.13) and (4.14), the cross track error is expressed as following:

$$CE = -(x - W_{x_n})\sin\gamma_p + (y - W_{y_n})\cos\gamma_p \tag{4.15}$$

Then, the steering laws are aiming to minimize the cross track error.

$$\lim_{t\to\infty} CE(t) = 0 \tag{4.16}$$

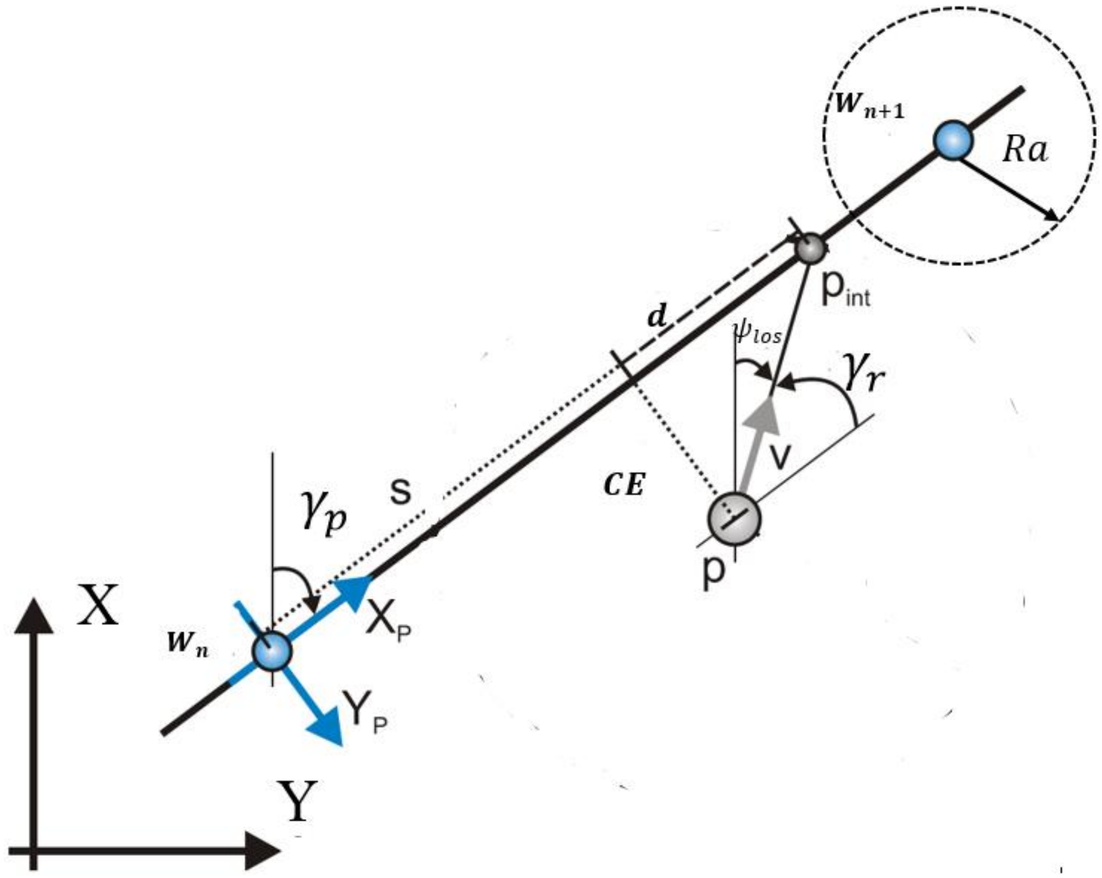

Fig 4.5 Geometrical representation of LOS guidance law

There are two main steering laws for the LOS guidance; enclosure based steering and look-ahead steering. The look-ahead steering has significant advantages over the enclosure based steering including less computationally intensive and valid for all cross- track errors. So, the look-ahead steering is discussed and selected for guiding the AUV. In Fig 4.5, the geometry of the steering is illustrated showing that the vehicle aiming to converge the line of sight between the reference and target way points. The vehicle is supposed to steer towards the point of interest (P_{int}) that located away from the projection of the vehicle position on the path by the look-ahead distance (d). So, the steering equation is:

$$\psi_{los} = \gamma_p + \tan^{-1}\frac{-CE}{d} \tag{4.17}$$

Where the (ψ_{los}) is deriving yaw angle for the vehicle and ($\gamma_r = \tan^{-1}\frac{-CE}{d}$).

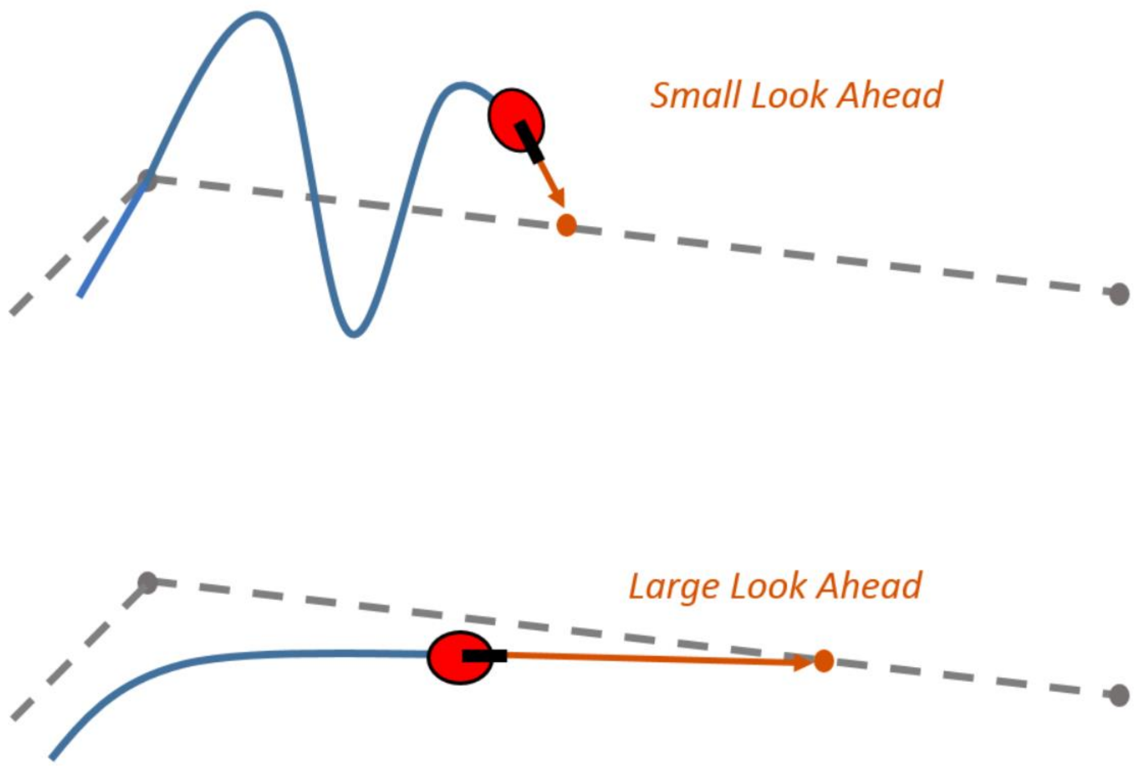

Fig 4.6 difference between small and large look-ahead distance

The look-ahead distance is a user specified value that control the converging behaviour. The small look-ahead distance makes the vehicle regain the path quicker between waypoints but it could cause oscillations along the path. However, the large look-ahead distance could cause slower converging to the path but with stable motion as in Fig 4.6. So, the look-ahead distance should be tuned in order to optimise the optimal tracking.

The criteria of switching between waypoints is based on Fossen's switching algorithm principle where the vehicle is shifted to the next point (W_{n+1}) if the vehicle is within the circle of acceptance of the current waypoint (W_n). Hence, the vehicle position must satisfy the following equation:

$$\left(W_{x_n} - x\right)^2 + (W_{y_n} - y)^2 \leq Ra_n^2 \tag{4.18}$$

Where Ra is the radius of the circle of acceptance.

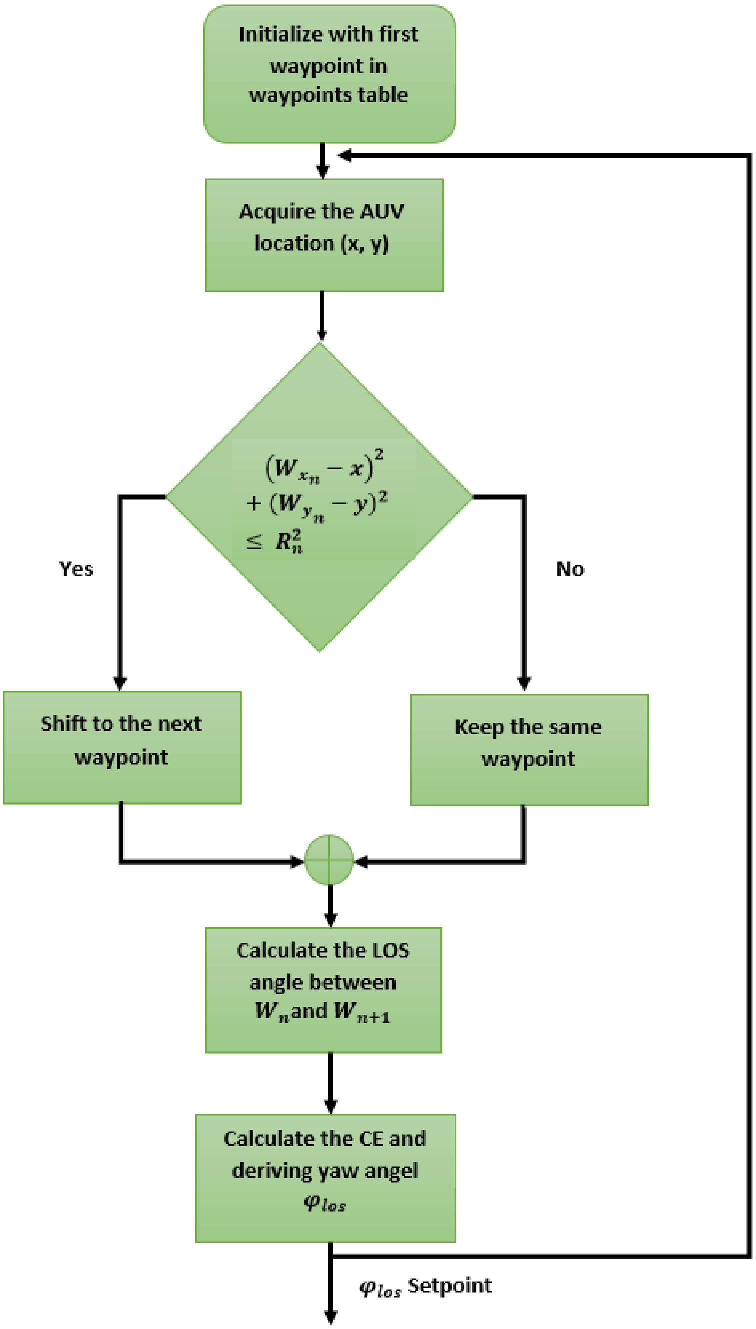

Fig 4.7 Guidance control algorithm flowchart

Fig 4.7 describes the process of guiding of vehicle along the waypoints path. The process starts with acquiring the position of the vehicle through the navigation system. Then, switching algorithm checks if the vehicle within the circle of acceptance of the desired waypoint to switch to next waypoint in the path. If the vehicle is not within the circle of acceptance of the waypoint, it will keep track that waypoint. Then, the guidance algorithm will calculate the angle of the line of sight between the reference waypoint and target waypoint. This angle is used to calculate the cross track error between the vehicle position and the desired path. Finally the LOS algorithm is used to generate the reference heading angle to the controller.

4.5 Guidance control in disturbance

In the previous section the conventional LOS algorithm was discussed. However, this algorithm is not designed to deal with the ocean current disturbance or any other environmental disturbances. This problem cannot be fixed by heading controller since the error is caused by the heading reference generator which is the LOS guidance law. So, several modifications are suggested to enhance the LOS algorithm to handle the disturbance problem. Generally, the modified algorithms are based on adding an integral action term to the guidance law as follows:

$$\psi_{los} = \gamma_p + \tan^{-1}\left(\frac{-CE - \alpha}{d}\right) \tag{4.19}$$

Here, $\alpha > 0$ is the integral term that responsible of making the (ψ_{los}) to be non-zero when the cross track error (CE=0) in presence of the ocean current when the vehicle on the desired path as shown in the Fig 4.8. The integral term (α) could be calculated by either ILOS or Adaptive ILOS methods as discussed in the next sections.

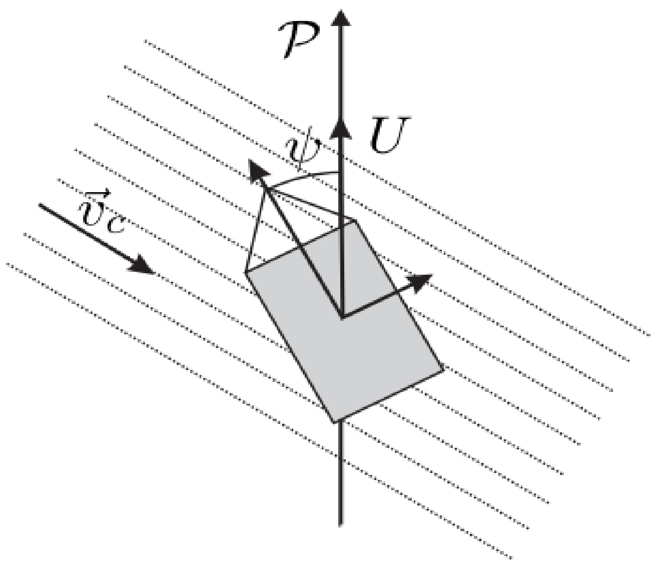

Fig 4.8 Guidance control in presence of ocean current disturbance

4.5.1 Integral line of sight algorithm

The ILOS was derived by Borhaug which is considered as a turning point principle in guidance control system not only for marine vessels but also for the any guided vehicle that has to follow a path in presence of environmental disturbances [48]. For underwater vehicles, this strategy is based on the following assumptions:

1. The real environmental disturbance is simplified where the ocean current is irrotational and constant.
2. To provide a stability criteria, the ocean current velocity has a known upper bound ($\sqrt{u_c^{E\ 2} + v_c^{E\ 2}} \leq V_{max} \leq \infty$).
3. The vehicle speed is greater than the ocean current velocity ($U > V_{max}$) to avoid losing control of the vehicle and drifting away with current.

Then, the integral term could be calculated from:

$$\alpha = \sigma \int \dot{CE}_{int}\, dt \tag{4.20}$$

Where ($\dot{CE}_{int}$) could be obtained from the following:

$$\dot{CE}_{int} = \frac{d.CE}{(CE + \sigma.CE_{int})^2 + d^2} \tag{4.21}$$

Where (σ) is the integral gain and must be greater than zero, and (d) is the look-ahead distance from the previous section. The concept behind this strategy is that the integral of cross track error (CE) will allow (ψ_{los}) to be non-zero when (CE=0) when the vehicle on the desired path in the presence of disturbance. So, the integral term will generate the necessary side-slip angle in equation (4.19) to maintain the desired path. The derivation of equation (4.21) has been proven in Caharija work in theorem 1 and also the stability of the system has been proven Lyapunov closed loop analysis to guarantee uniform global asymptotic stability (UGAS) and uniform local exponential stability (ULES) [88].

4.5.2 Adaptive Integral Line of sight algorithm

Another strategy used is the adaptive integral line of sight guidance law which differs from the ILOS in structure and based on the adaptive control theory. This strategy is simply constructed due to the formulation in kinematic level. It has been derived and analysed by Fossen and Lekkas who proved the stability of this guidance law and showed the global k exponential stability [49].

As in Fig 4.9, the vehicle kinematics in presence of ocean currents for 2D horizontal plane using the relative velocities according to Fossen[37] are as follows:

$$\dot{x} = u_r \cos(\psi) - v_r \sin(\psi) + u_c^E \tag{4.22}$$

$$\dot{y} = u_r \sin(\psi) + v_r \cos(\psi) + v_c^E \tag{4.23}$$

Where the (u_c^E, v_c^E) is the velocities of the ocean current in the Earth fixed frame and related to the velocities of the current in the body fixed frame (u_c, v_c) according to the following:

$$[u_c, v_c]^T = J^T(\psi)[u_c^E, v_c^E]^T \tag{4.24}$$

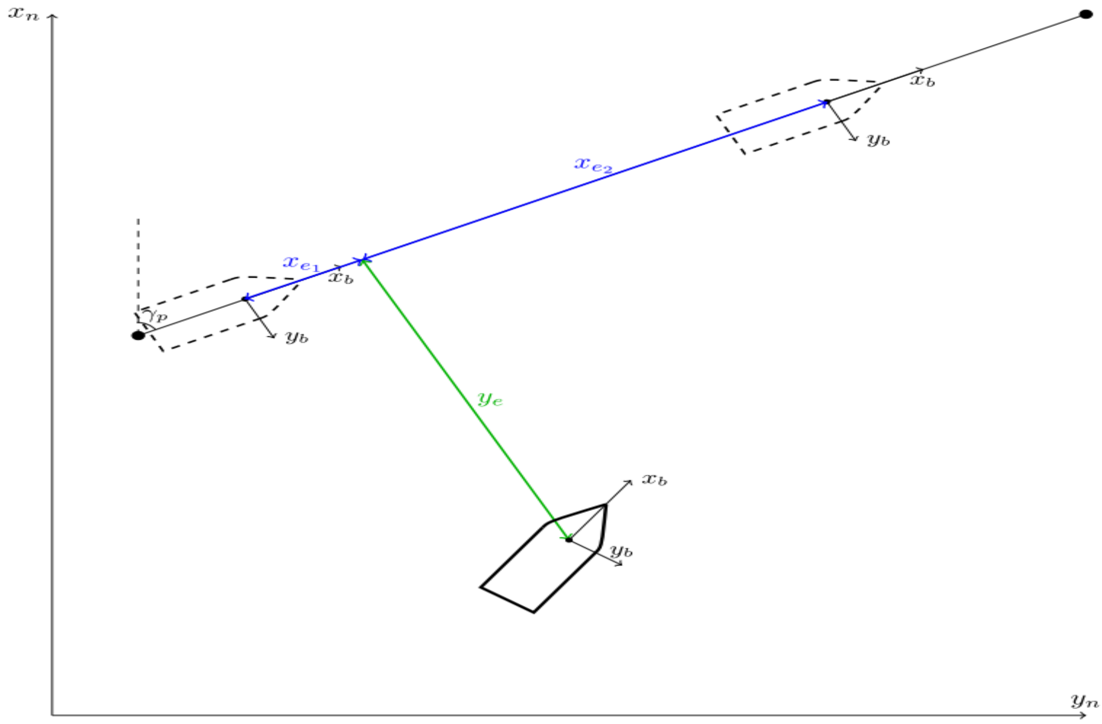

Fig 4.9 Vehicle kinematics representation under disturbance

Based on the cross track error equation (4.15), the time derivative of the (CE) is

$$\dot{CE} = -(\dot{x} - \dot{W}_{x_n}) \sin\gamma_p + \left(\dot{y} - \dot{W}_{y_n}\right) \cos\gamma_p - [(x - W_{x_n}) \cos\gamma_p + \left(y - W_{y_n}\right) \sin\gamma_p]\dot{\gamma}_p \tag{4.25}$$

For the straight line path following ($\dot{\gamma}_p = 0$) and the waypoint is fixed along the path which ($\dot{W}_n = 0$). Consequently, equations (4.22), (4.23), and (4.25) could be combined together and gives:

$$\dot{CE} = -\dot{x}\sin\gamma_p + \dot{y}\cos\gamma_p = -(u_r\cos(\psi) - v_r\sin(\psi) + u_c^E)\sin\gamma_p + (u_r\sin(\psi) + v_r\cos(\psi) + v_c^E)\cos\gamma_p \tag{4.26}$$

This formula could be written in the amplitude –phase form:

$$\dot{CE} = V_r\sin\left(\psi - \gamma_p\right) + V_c^E\sin(\beta_c - \gamma_p) \tag{4.27}$$

Combining equations (4.19) and (4.27) gives:

$$\dot{CE} = -\frac{V_r(CE + \alpha)}{\sqrt{d^2 + (CE + \alpha)^2}} + V_c^E\sin(\beta_c - \gamma_p) \tag{4.28}$$

The control objective is to drive the cross track error to zero ($CE \to 0$) and to cancel the effect of the ocean current disturbance ($V_c^E\sin(\beta_c - \gamma_p)$). So, from equation (4.28) the (α) could be obtained by the following:

$$\alpha = \frac{d.V_c^E\sin(\beta_c - \gamma_p)}{\sqrt{V_r^2 - (V_c^E\sin\left(\beta_c - \gamma_p\right))^2}} \tag{4.29}$$

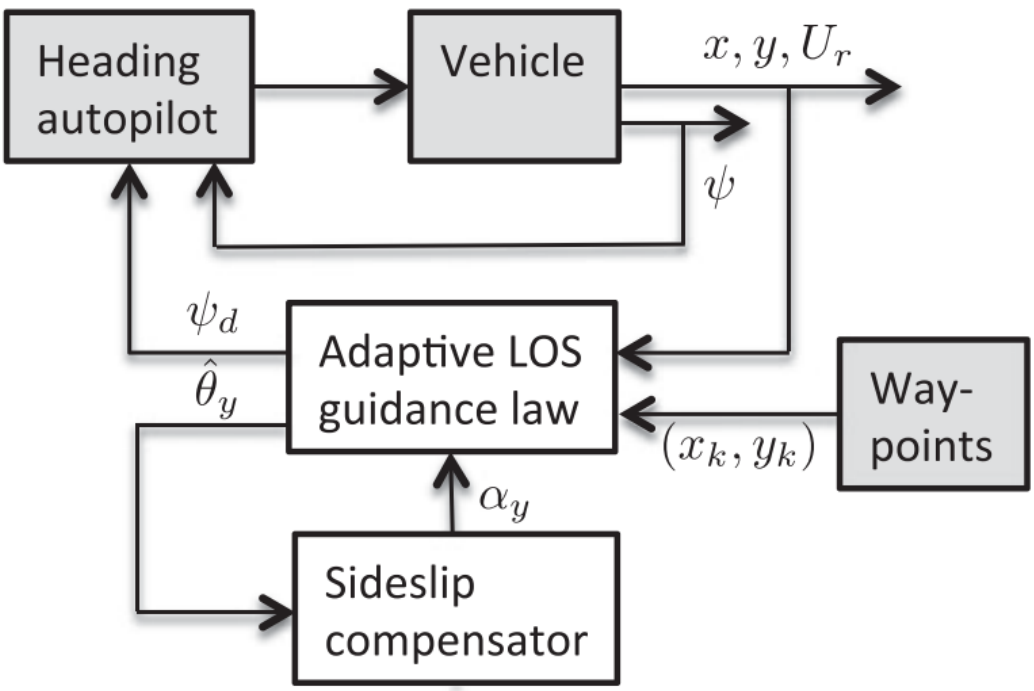

Fig 4.10 Adaptive LOS guidance architecture

However, this guidance strategy depends on the ocean current component to calculate the integral term (α). The ocean current value could be obtained from the observer estimation. The accuracy of guidance should depend on the accuracy of the estimation. The structure of the guidance law with observer and heading controller are illustrated in the Fig 4.10. The guidance system including switching algorithm and the three guidance laws are constructed in Simulink and M-file as shown in the Appendix.

4.6 Heading controller

The heading controller is responsible of driving the vehicle towards the path by turning the vehicle orientation to the guidance controller reference angle. The rudder angle (δ) is the controlled actuator that change the orientation of the vehicle (ψ) corresponding to the rudder position as shown in the Fig 4.11.

The controller designed is a conventional PID controller that performs the control signal depending on the reference yaw angle given by the guidance controller and the feedback given by the measured yaw given by the navigation system. this controller is a common control method that used in the literature and it is based on the Fossen representation of the vessels autopilot [23].

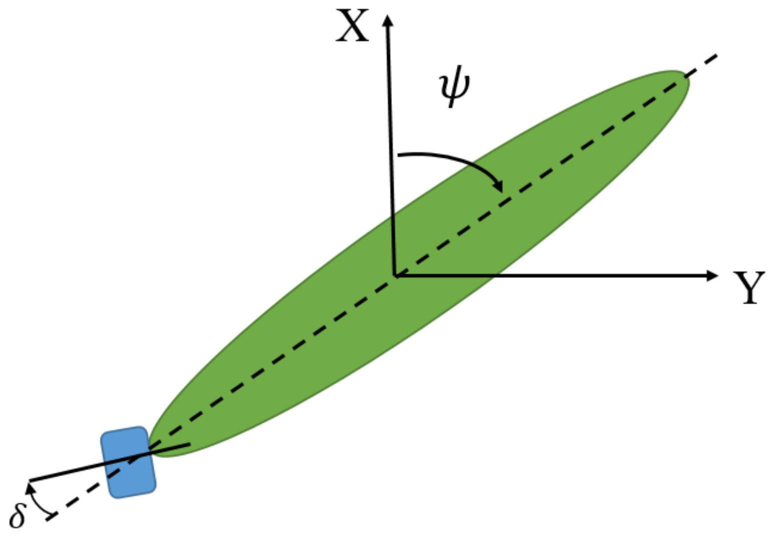

Fig 4.11 Rudder angle effect on the AUV heading

The PID gains are tuned by several optimisation methods or using manual tuning as described in the next chapter. PID heading controller is formulated as following:

$$\psi_e = \psi_{los} - \psi_m \tag{4.30a}$$

$$\delta(t) = K_p \psi_e + K_i \int \psi_e . dt + K_d \frac{d\psi_e}{dt} \tag{4.30b}$$

Where (ψ_m) is the measured yaw angle, (ψ_{los}) is the reference yaw angle provided by the guidance controller.

The same principle is applied for both the surge control and altitude (depth) control. However in this research the heading control is the focused issue and both surge and depth values are constant. The construction of the controller in Simulink is illustrated in Fig 4.12.

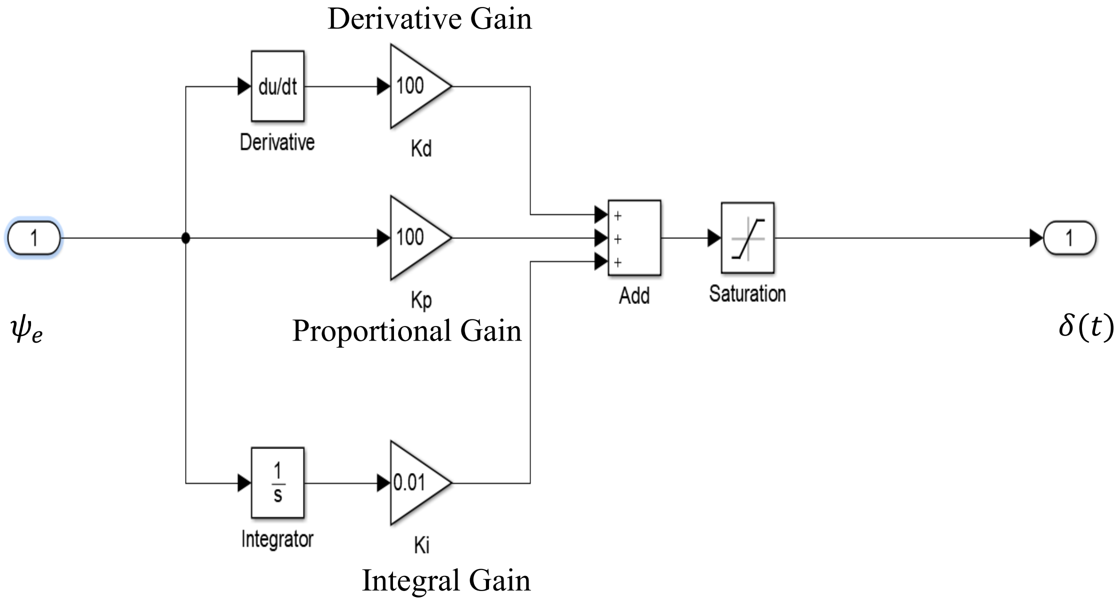

Fig 4.12 Heading PID controller

4.7 Summary

In this chapter, each subsystem of the AUV has been derived and constructed in Simulink to evaluate and test the performance of the full system. The full system is implemented in the Simulink as shown in Appendix. The parameters of the dynamic model are demonstrated in the software using the values obtained from the HRC-AUV model parameters which have been discussed in the AUV system model chapter. Next chapter, the constructed system will be tested in different simulation conditions to evaluate the observation and guidance systems behaviours and test the system ability to perform mapping missions under ocean current disturbances.

CHAPTER FIVE:

SIMULATION RESULT

5.1 Introduction

Simulation results of the HRC-AUV model explained in the previous chapter are presented and discussed. The simulation setup is firstly introduced reviewing the numerical method used to solve the system equations. Then, the performance of the heading controller is tested to view the response of the PID controller that is designed in previous chapter. The performance of the heading controller determines the maneuverability of the AUV which consequently affect the guidance of the vehicle. Moreover, the observer is tested with two cases to test the ocean current estimation. In first case the vehicle is subjected to constant ocean current while in the second case the vehicle is tested in random current disturbance and assigned to map the current along the covered area. Thereafter, the guidance controller is tested without disturbance and the look-ahead distance is tuned to improve the tracking performance. Furthermore, the integral and adaptive guidance laws are compared within constant and variable current disturbance. Finally, a case study is conducted using the better guidance strategy combined with mapping of ocean current to perform a surveillance mission in difficult environmental conditions.

5.2 Simulation setup

In Simulink platform where the model is implemented, the ODE45 solver is chosen to solve the system differential equations in matrix form. ODE45 solver is based on Runge-Kutta (4, 5) formula (the Dormand-Prince pair) for numerical integration and this method considered as a one of the accurate methods in solving differential equations. This method is recommended to solve problems in first trials due to its accuracy [87]. The selected sampling time is 0.1 sec and simulation runs for 400 sec except of one case study which runs for 1400 sec. Also, the environment disturbance of ocean currents is initialized with zero, constant, or random current data according to the type of test. The 2D ocean current velocity field is generated in script file for a specific area and stored in a lookup table as a function of location coordinated (x, y) which gives the corresponding velocity vector. Appendix shows different steady flow field scripts used in the model simulation. The random velocity field is loaded from Matlab stored wind field data. In addition, the initial positions and initial velocities are specified before the simulation test.

5.3 Controller performance results

The performance of the Heading controller is evaluated using step and square input to get the main characteristics of the controller. First, a step signal is applied to the controller to reach a heading angle ($\psi = 100°$). The PID controller parameters were tuned manually to give optimal performance with ($K_P = 100,\ K_I = 0.01, K_D = 100$). The aim of the controller is to converge the desired output with minimum rise time, overshoot, and steady state error. The results show an acceptable performance of the controller with rising time ($t_r = 20.09\, sec$), settling time ($t_s = 27.4028\, se$), and maximum overshoot of 1.1415% as shown in the Fig 5.1. For the pukse input signal, the heading angles are ($\psi = 0°, 180°$). The system response to these high manoeuvring angles is about $50\ sec$ as in the Fig 5.2. The response of the system depends on the actuator limitations which constrain the manoeuvring abilities of the AUV. To improve the manoeuvring, another actuator design is required.

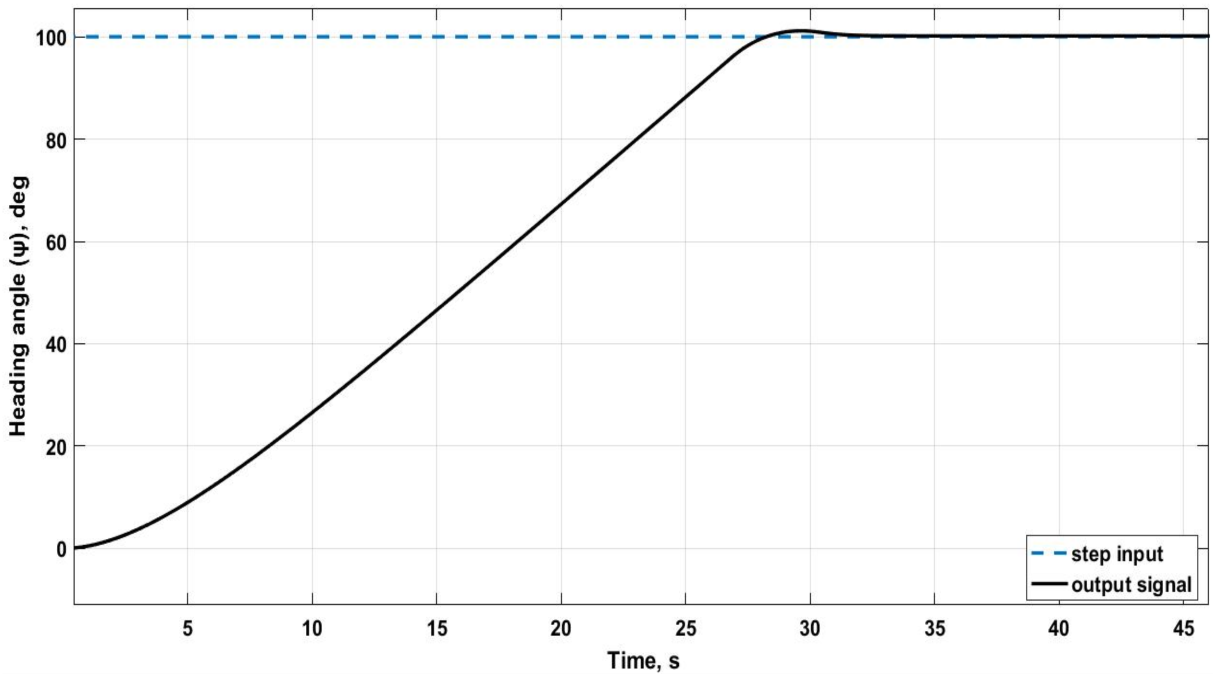

Fig 5.1 Step response of the yaw controller

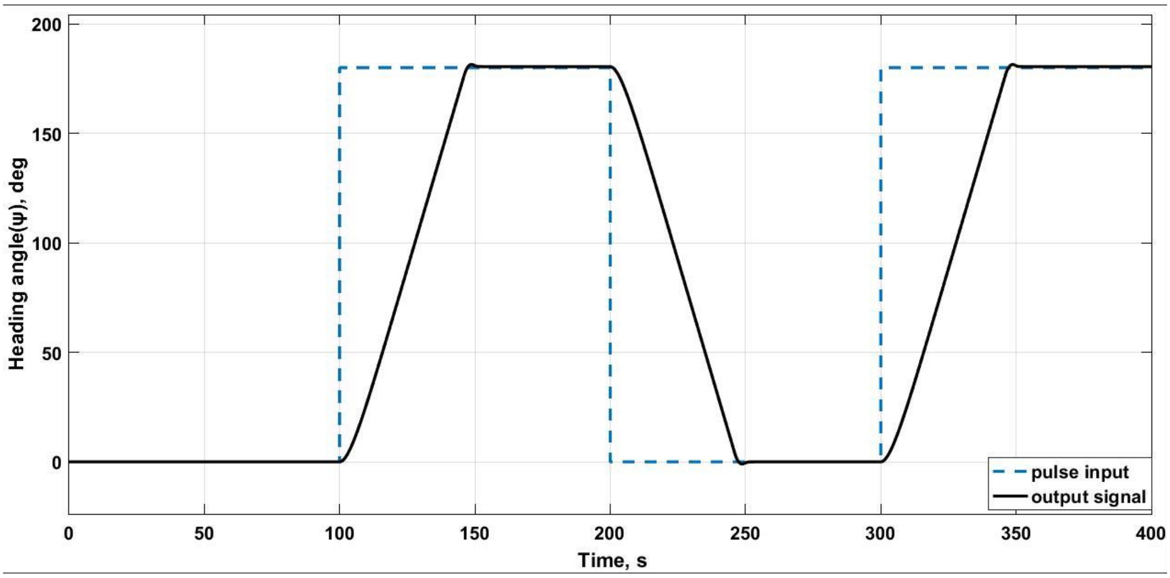

Fig 5.2 Pulse response of the yaw controller

5.4 Ocean current estimation results

To evaluate the ocean current estimation system, the model is tested at two disturbance cases. In the first case the system is subjected to a constant current disturbance. The initial conditions are constant rudder angle with 0.45 rad, population thruster at 490 rpm, and initial vehicle heading angle of 90º as illustrated in Fig 5.3.

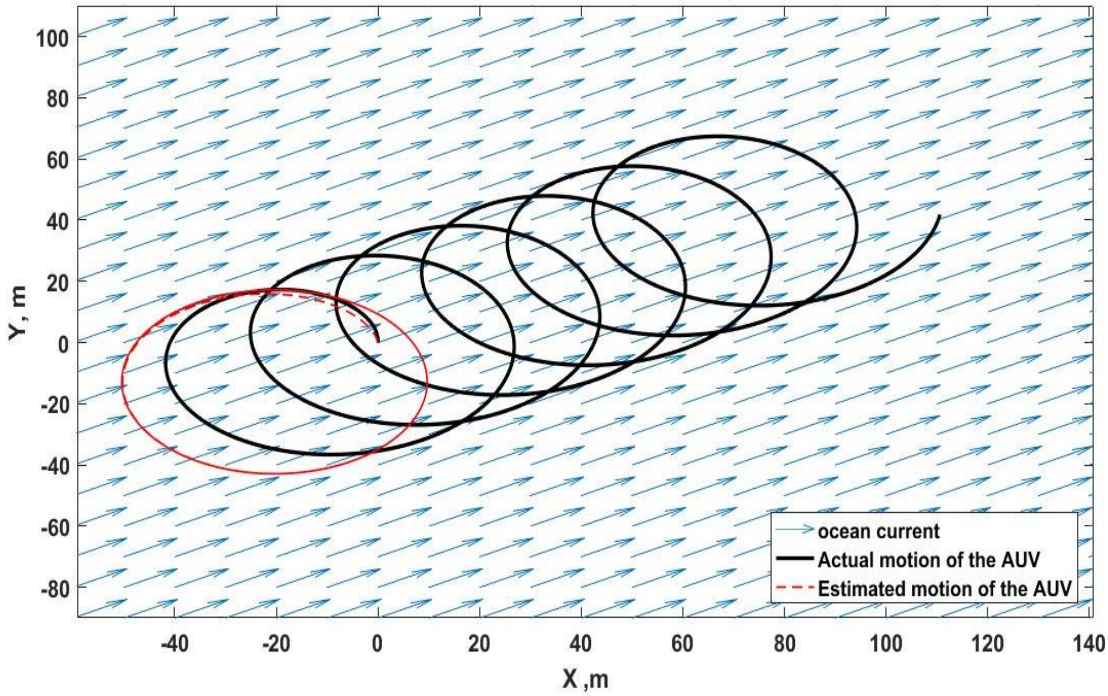

Fig 5.3 Vehicle motion within environmental ocean current disturbance

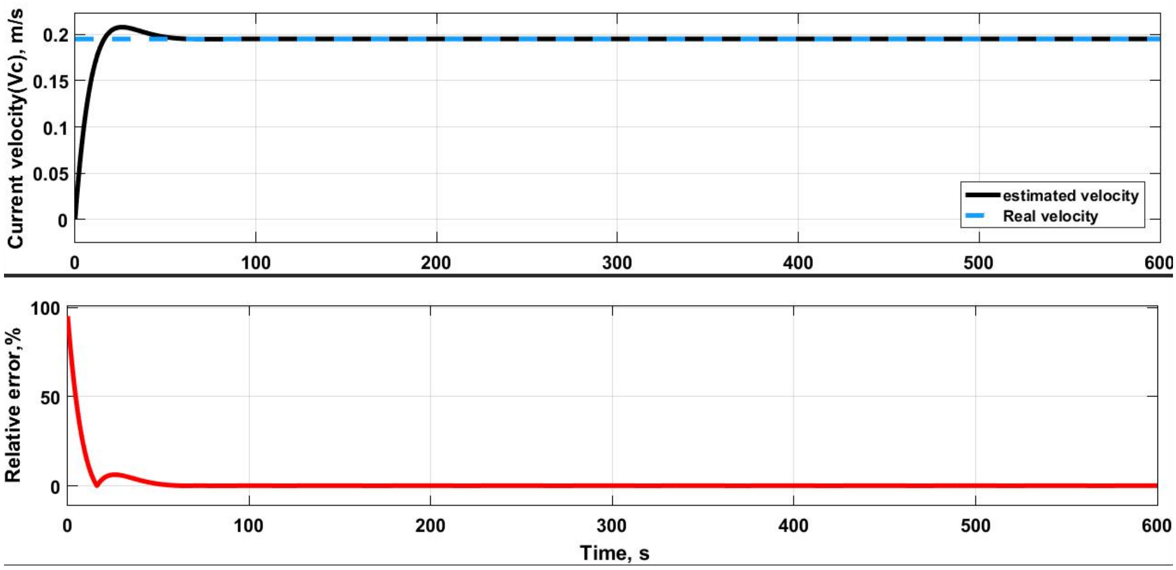

Fig 5.4 Estimated ocean current velocity vs. actual velocity

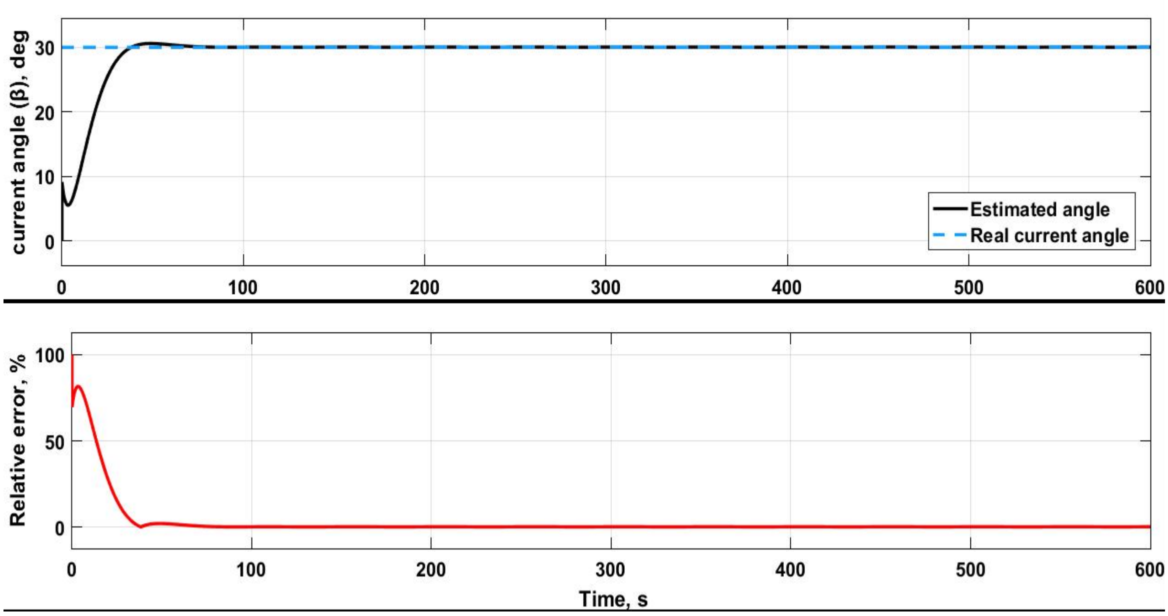

Fig 5.5 Estimated ocean current angle vs actual angle

Also, the average current speed Vc, is 0.195 m/s and current angle β, is 30º. Fig 5.3 shows the simulated behaviour of the AUV under upon mentioned conditions. The estimated current velocity and angle are shown in Fig 5.4 and Fig 5.5, where the settling time is about 30 seconds. Then, the collected data processed through interpolation equations to generate the estimated surrounding map of currents as shown in Fig 5.6.

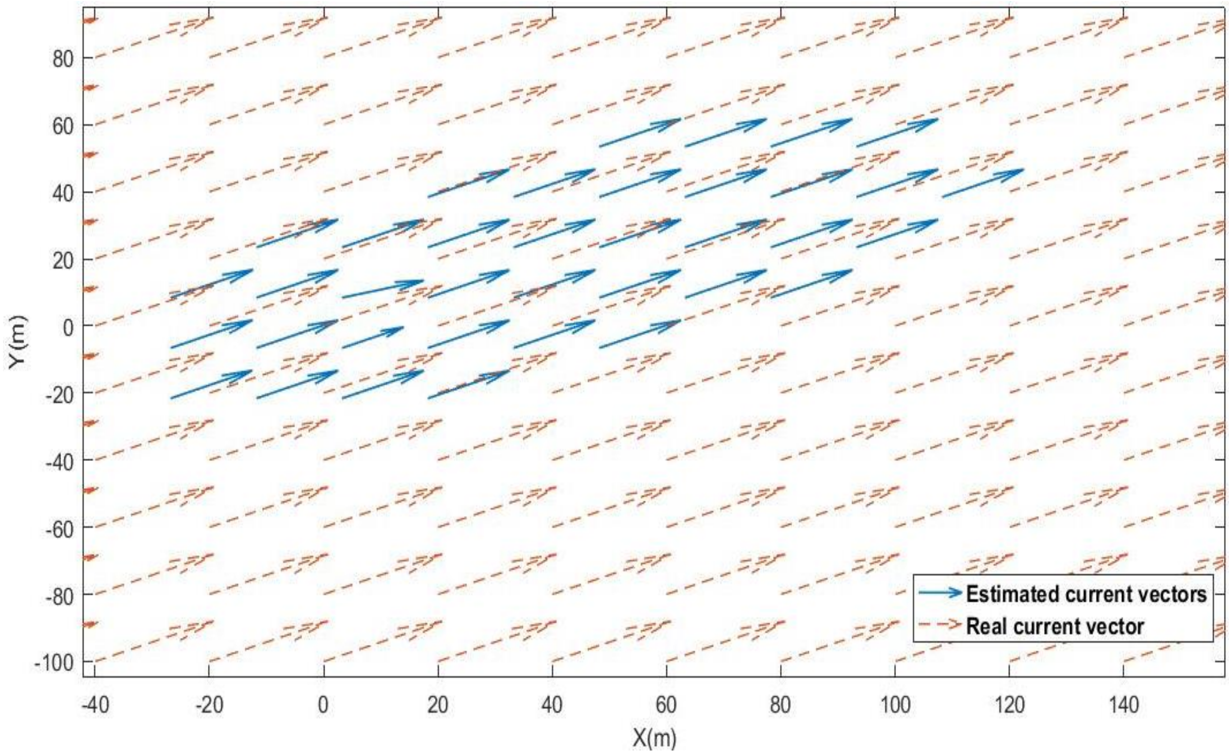

Fig 5.6 Estimated ocean current field vs. actual current field

The second case consists of random environmental disturbance with controlled vehicle motion over the controlled heading angle to cover the selected area. Velocity range of the ocean current ranges between 0.0134 and 1.216 m/s. The current angle is variable including vortices explained in Fig 5.7. The control signal consists of pulses inputs to the vehicle that is responsible of changing the direction of the vehicle over the simulation test. The tracked motion affected by the ocean current disturbance with the estimated current velocity and angle vectors is shown in Fig 5.8. Finally, Fig 5.9 shows that the generated contour map of the estimated ocean current indicates the vortices and high current field which is similar to the input current field map.

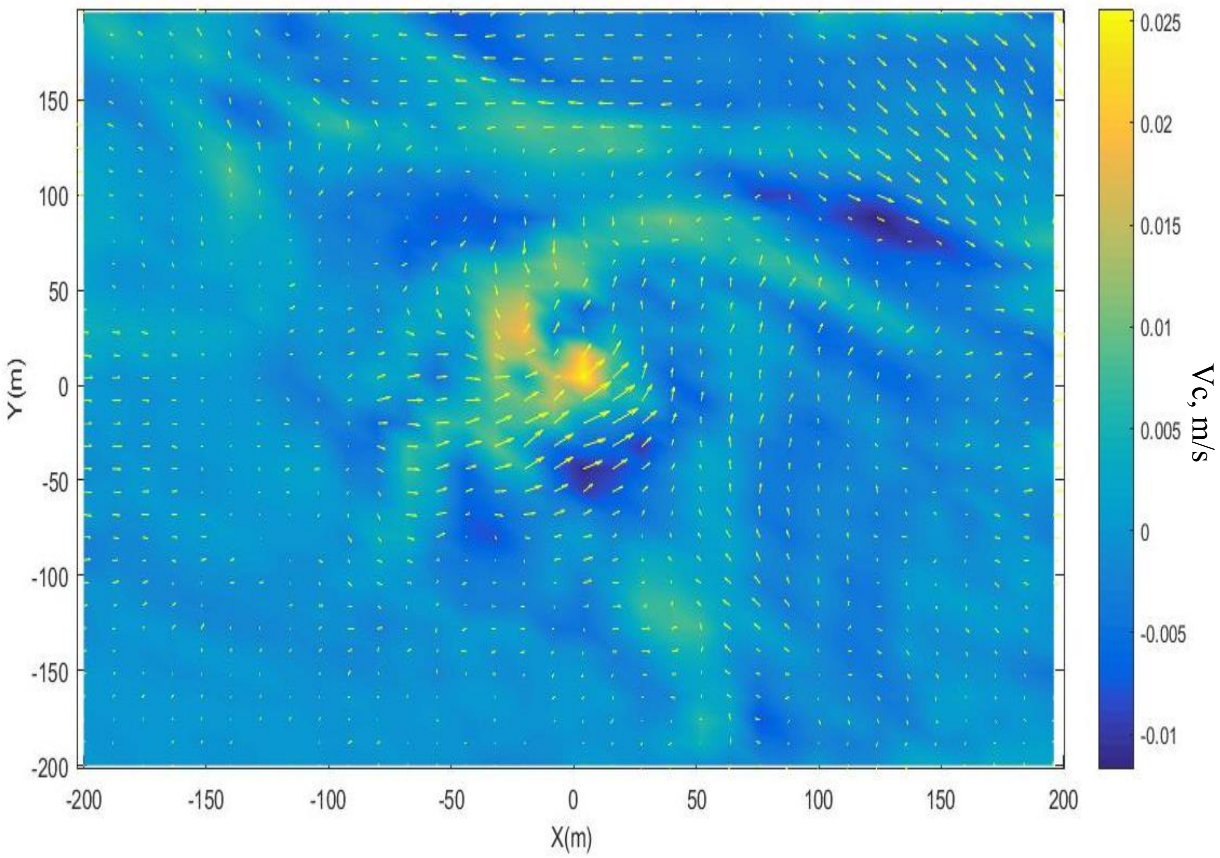

Fig 5.7 Input random ocean current field

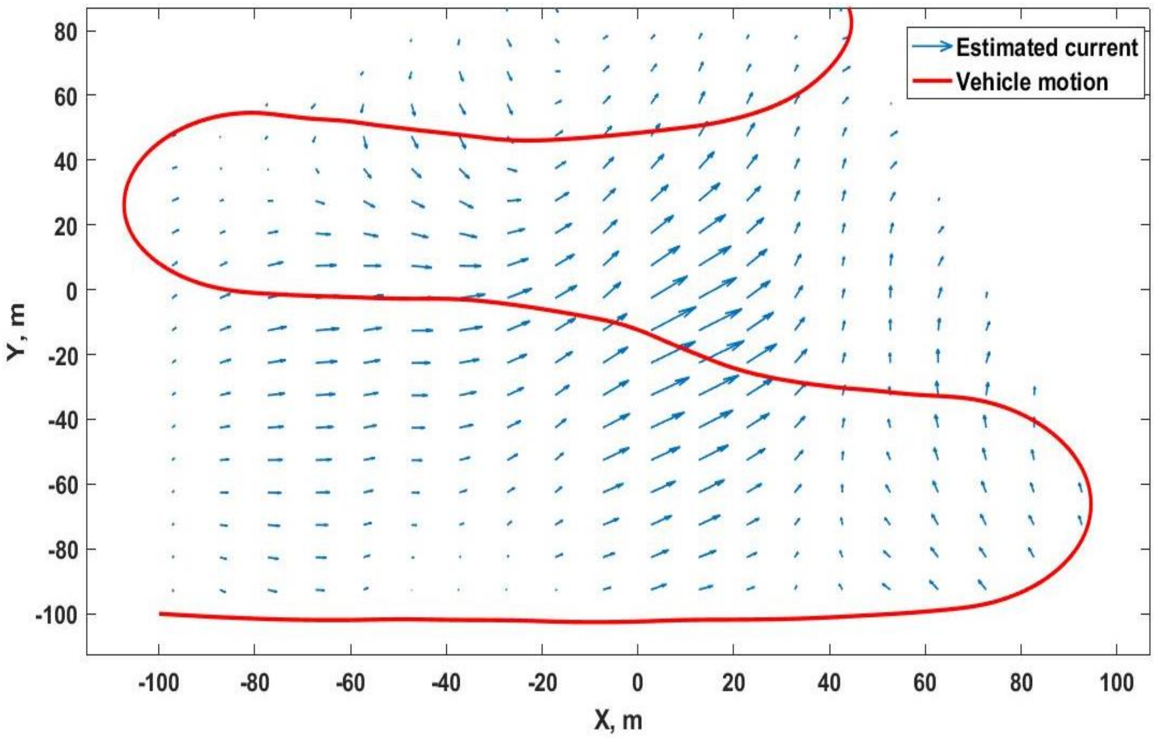

Fig 5.8 AUV motion and representation of the ocean current vector

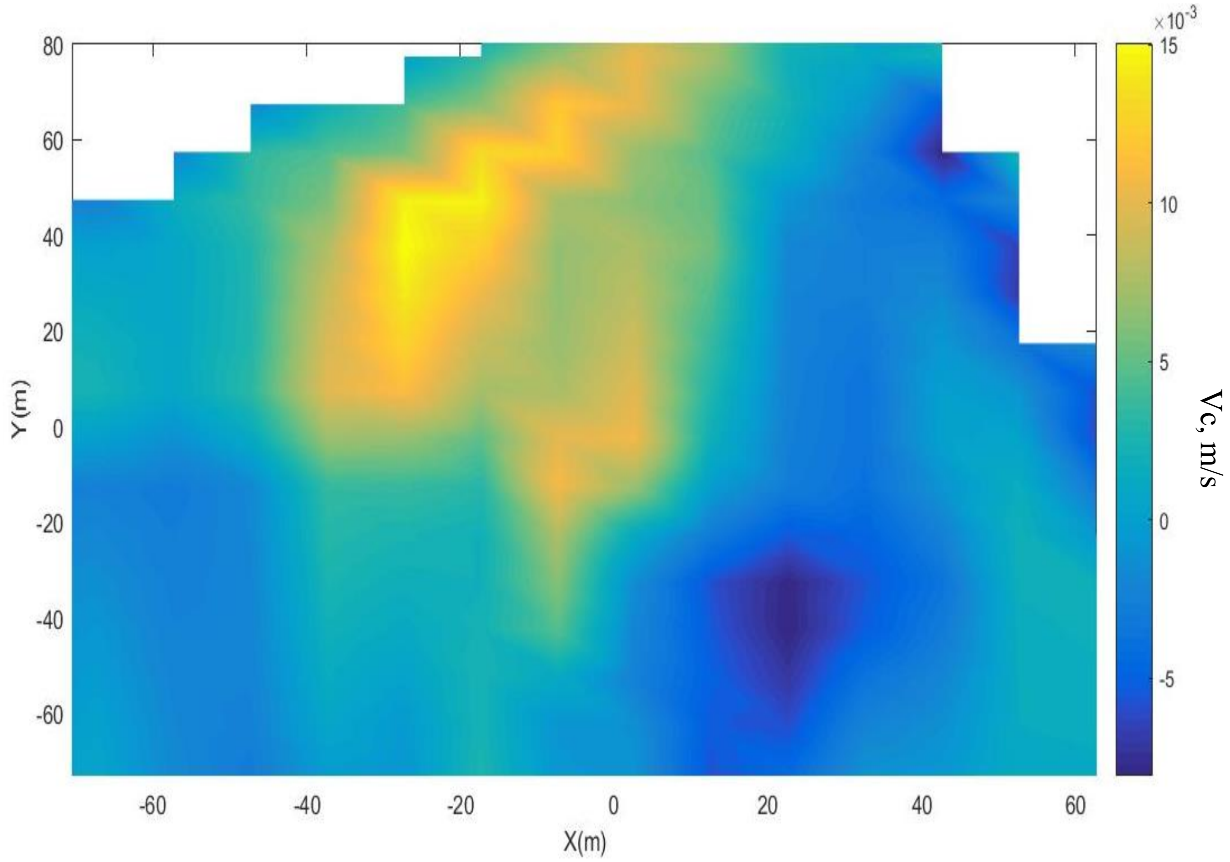

Fig 5.9 Generated contour map of the ocean current field

Fig 5.9 shows the mapping of the velocity field which based on interpolation equations. Triangulation-based linear interpolation is used to generate the 2D map from the collected data. In this methodology, the barycentric coordinates of the point are used to take a weighted average of the three observation values (associated with the three vertices of the triangle). The resulting interpolation function is continuous, but not differentiable across an edge.

5.5 Guidance without disturbance

After evaluating the yaw controller and the ocean current observer, the guidance system is tested at different scenarios to develop an autopilot that capable of executing given missions under the environmental disturbance. However, the guidance system is firstly simulated under no disturbance to select the suitable parameters that achieve high tracking performance. This case, the predefined path selected is:

$$W_{x,y} = \{(-96.0773, -94.9860), (8.2099, -94.9860), (75.3039, -61.6776), (125.6243, 22.5187), (131.4586, 104.8645), (62.1768, 155.7523), (-18.0442, 186.2850), (-118.6851, 186.2850)\},$$

The initial conditions of the test are shown in table 5.1 with simulation time of 330 sec. Fig 5.10, the AUV tracked the path with a maximum deviation of 16.877 meters, the average cross track error is $CE_{avg} = 1.1948\ m$, standard deviation is $SD = 2.7909\ m$, and integral absolute error is $IAE = 5.8364 \times 10^3 m.s$ as illustrated in the Fig 5.11.

Table 5.1 initial conditions of path following using LOS guidance scenario

Item	Description	value	Item	Description	value
η	initial position	$[100, -100,0,0,0,0]^T$	K_D	Derivative gain	100
n	thruster velocity	$490\ rpm$	d	look ahead distance	15 m
K_P	Proportional gain	100	Ra	waypoint radius of circle of acceptance	20 m
K_I	Integral gain	0.01	t_s	Sampling time	0.1 s

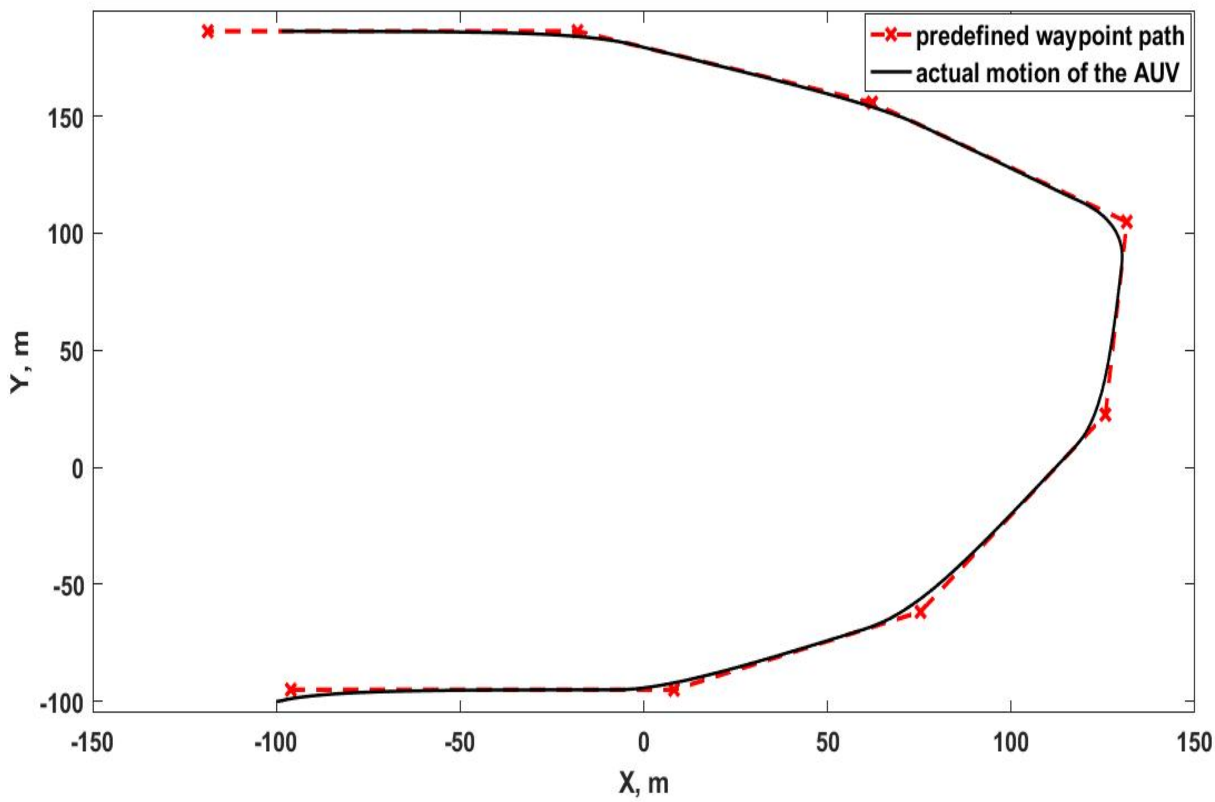

Fig 5.10 Simulation of the AUV path following using LOS guidance control

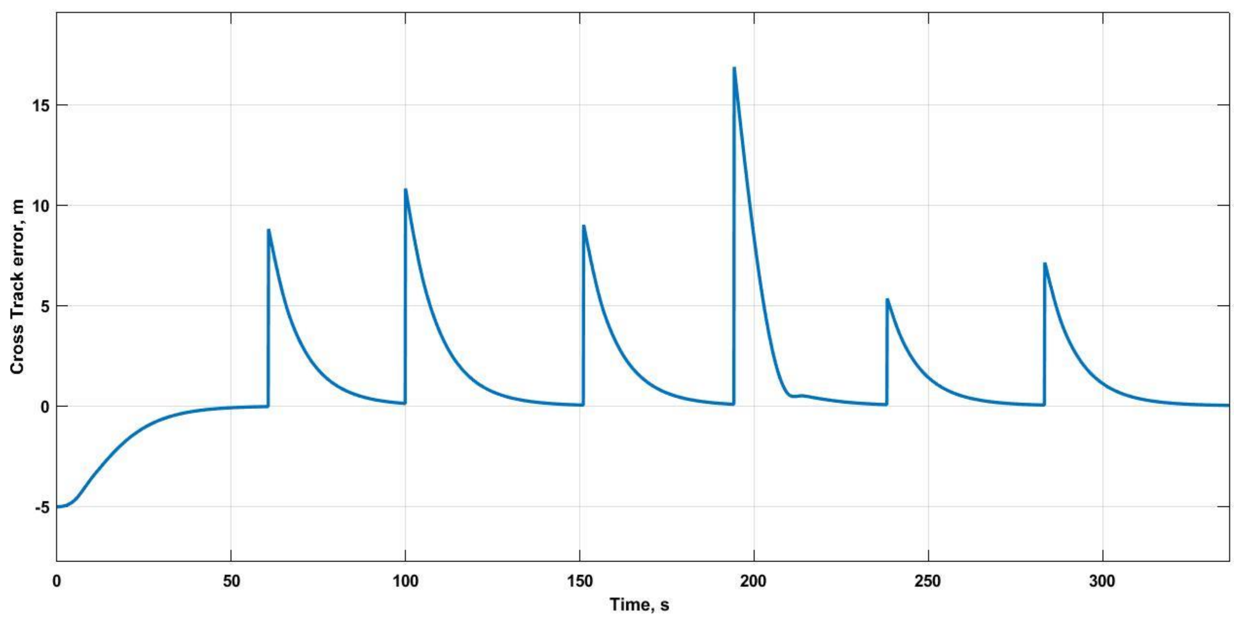

Fig 5.11 Cross track error along the path during the simulation

The deviation from the path is caused by switching between waypoints. It is noticed that the large manoeuvre as in the 5th waypoint generates a large cross track error.

According to the guidance equation (4.17), the tracking depends on the looking ahead distance that control the tracking performance. Large look ahead distance could cause slower tracking with bigger cross track error and small look ahead distance could cause a large fluctuation on the path. To tune the look ahead distance, several values are chosen and tested to optimise the performance. Using the same initial conditions and same waypoints in the previous case, the different look ahead distances were tested and simulated as in the Fig 5.12.

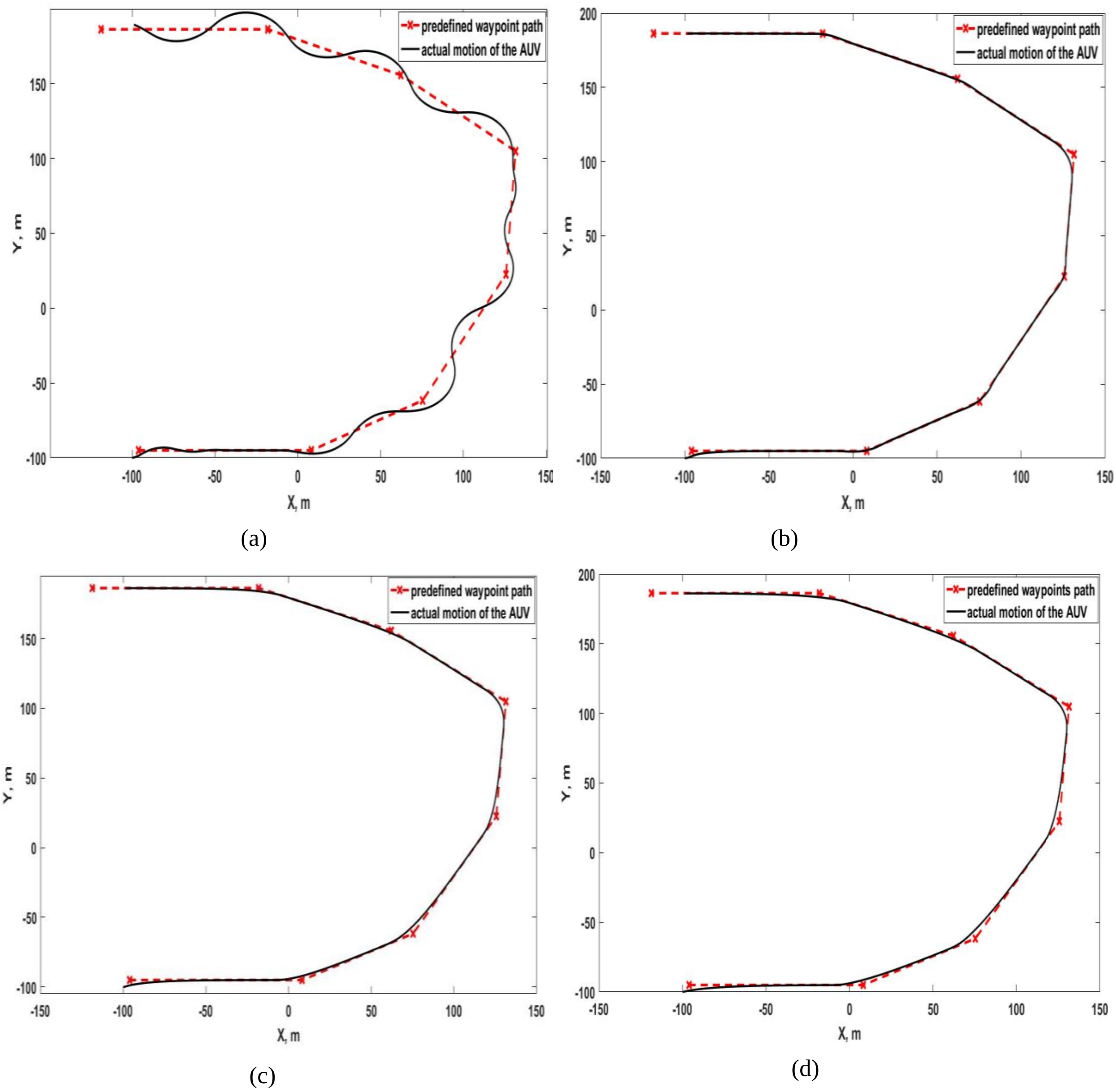

Fig 5.12 different look-ahead distance motion test; (a) d= 5m (b) d=10 m (c) d=15 m (d) d= 20 m

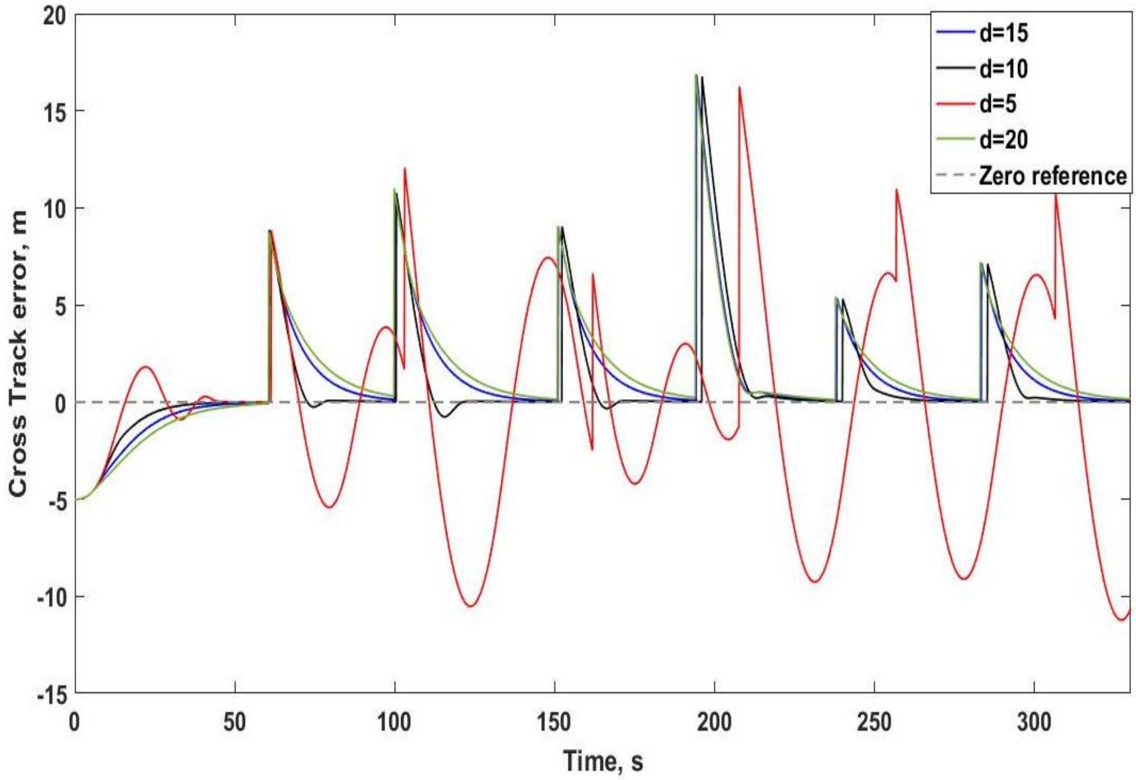

Fig 5.13 Comparison between cross track errors of the different look-ahead distances

Different cross track errors are compared to indicate the performance difference according to the change in look-ahead distances. As illustrated in the Fig 5.13, the small look-ahead distance has a less converging time and the increase in the distance increases the converging time. However, the smallest look-ahead distance has an oscillating performance along the path and has a high settling time that affect the tracking stability. On the other hand, the large look-ahead distance has a more converging time and slower response while switching between waypoints. Otherwise, large look-ahead distance are more stable and has a lower total cross track error. In each look-ahead distance case, a lot of parameters are calculated to evaluate the tracking performance including mean CE, maximum CE, standard deviation of the error, and Integral Absolute Error (IAE) of the CE as illustrated in Table 5.2.these parameters are calculated as following:

$$CE_{mean} = \frac{1}{\sum_0^{t_f} t} \int_0^t abs(CE).dt \tag{5.1}$$

$$\text{SD} = \sqrt{\frac{\sum (CE - CE_{mean})^2}{\sum_0^{t_f} t}} \tag{5.2}$$

Table 5.2 Statistical results of different look-ahead distance

Look-ahead distance	**Mean CE (m)**	**Max CE (m)**	**Standard deviation (m)**	**IAE (m.s)**
d=5	4.85	16.2539	5.4198	16.005×10^2
d=10	1.25	16.7723	2.6501	4.1286×10^2
d=15	1.768	16.8778	2.7907	5.8364×10^2
d=20	2.05	16.8792	2.8731	6.7834×10^2

$$IAE = \frac{1}{t_s}\int_0^t abs(CE).dt \tag{5.3}$$

Where t_f is the time of the simulation.

The 10 meters look-ahead distance has the lowest Integral Absolute Error (IAE) and lowest standard deviation among the four cases and indicate a good tracking performance. The look-ahead distance could be optimized using a suitable optimization technique to get better performance. So, it could be implemented in the future work.

5.6 Guidance with constant current disturbance

In this case, the ocean current disturbance is added to the system to increase the realistic conditions of the simulation and to view its effect on the guidance system. The input disturbance is a constant current velocity of 0.3 m/s and current angle of 30º. The predefined path waypoints of the test is: W_x = { -148.5856, 142.3978, 181.7790, 166.4641, -171.9227, -178.4862, -158.0663, 162.0884}

W_y = {-153.2757, -178.2570,-142.1729,-105.1636, 142.7991, 164.0794, 178.8832, 182.5841}.

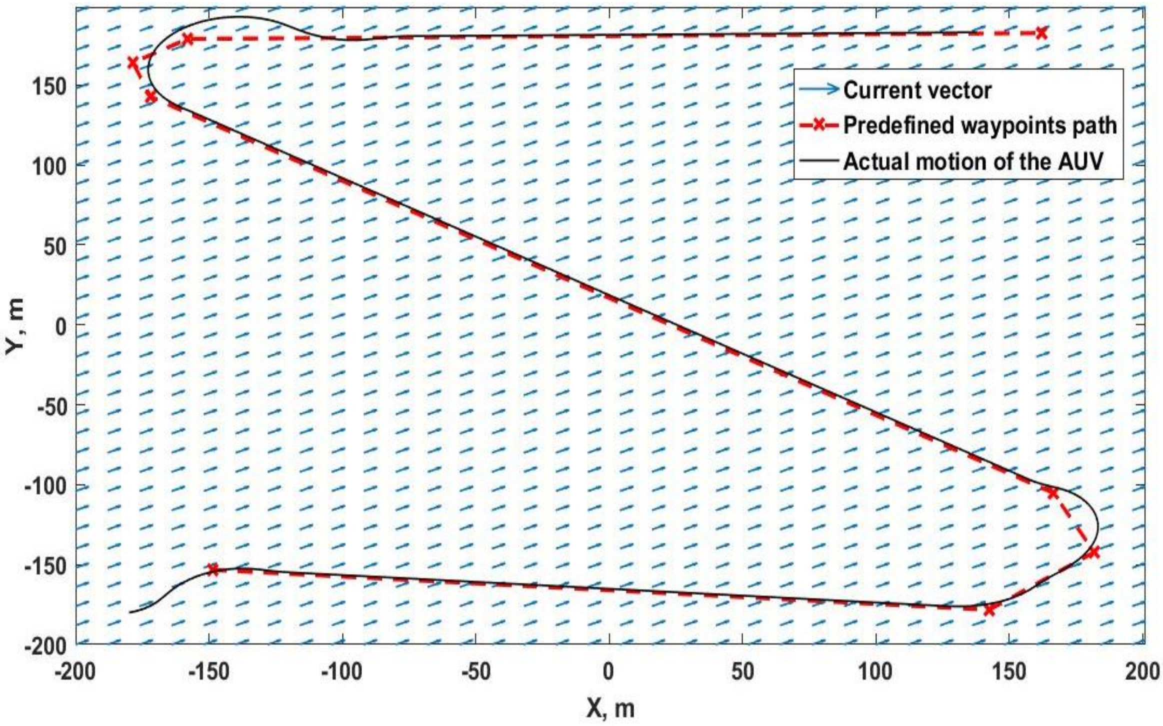

Fig 5.14 Simulation of the AUV path following using LOS guidance control under constant ocean current disturbance

Table 5.3 Initial conditions of guidance under constant disturbance scenario

Item	**Description**	**value**	**Item**	**Description**	**value**
η	initial position	$[180, -180,0,0,0,0]^T$	K_D	Derivative gain	100
n	thruster velocity	490 rpm	d	look ahead distance	10 m
K_P	Proportional gain	100	Ra	waypoint radius of circle of acceptance	20 m
K_I	Integral gain	0.01	t_s	Sampling time	0.1 s

The initial conditions of the simulation is shown in table 5.3 with simulation time of 630 sec. The LOS guidance law is applied to guide the vehicle along the determined path.

Fig 5.14 shows the tracking performance of the AUV with standard deviation of 5.98 m and an integral absolute error of 1.9455×10^3 .These values is expected to increase according to the increment of the ocean current magnitude. So, the ILOS and adaptive LOS guidance laws are used to minimize the deviation and increase the accuracy of tracking performance. With the same initial conditions, the ILOS guidance law is applied and motion of the vehicle is simulated taking to account the integral gain ($\sigma = 0.5$). The integral gain is tuned to get the optimal value that will enhance the tracking performance. Simulation results show an improvement of the tracking which the guidance controller compensate the ocean current disturbance effect as shown in the Fig 5.15(a). From Table 4, the IAE is decreased by 18.8% while the standard deviation increased by 1%.

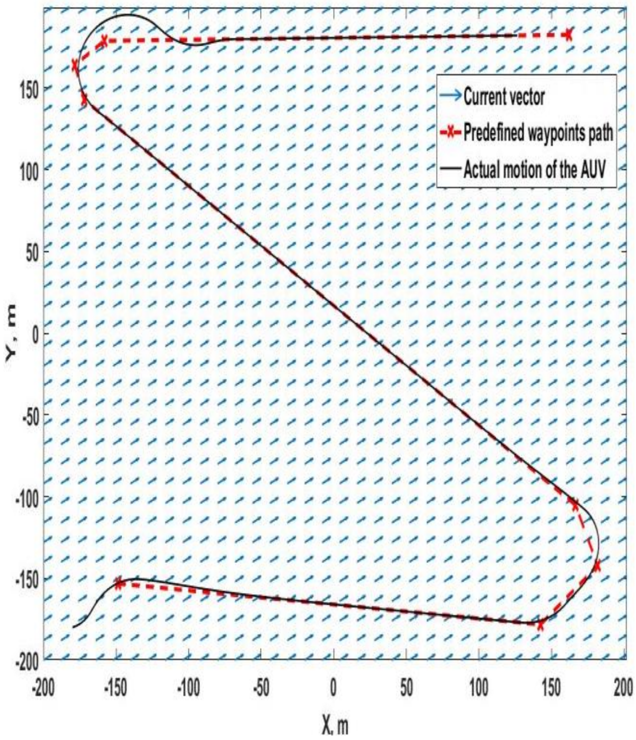

(a)

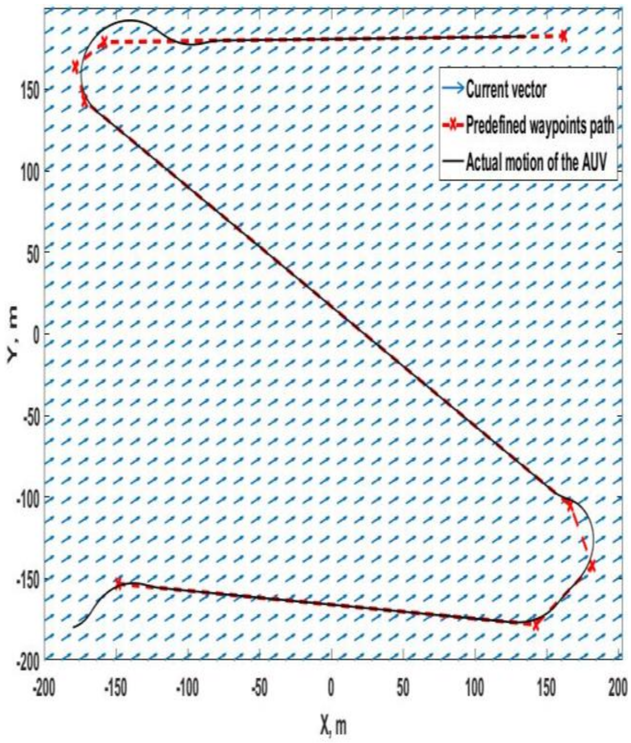

(b)

Fig 5.15 (a) ILOS guidance motion simulation (b) Adaptive LOS motion simulation

Although the minimisation of the CE of the tracking but this method suffer from the slower path convergence and the great deviations while switching the waypoints.

However, the adaptive LOS shows a slight better tracking performance as illustrated in Fig 5.15 that shows a smooth and stable tracking. Compared to the ILOS guidance, the adaptive LOS guidance decreased the IAE by 28.5% and the SD by 2.5% from the conventional LOS guidance as shown in Table 5.4. In Fig 5.16 the cross track error of each guidance method is plotted to compare the main differences between each method. The two strategies of compensating the disturbance cause increase of the tracking performance significantly. Although the ILOS has a large overshoots but it minimise the steady state error. The characteristics of ILOS cross track error indicate a winding up response to the switching between waypoints and slower converging to the path that makes the ILOS ineffective solution to the guidance control under disturbance.

Table 5.4 Statistical results of different guidance laws under constant disturbance case

Look-ahead distance	**Mean CE (m)**	**Max CE (m)**	**Standard deviation (m)**	**IAE(m.s)** $\times 10^3$	**Decrement percentage of IAE from LOS**
LOS	3.088	-29.3134	5.9842	1.9455	-
ILOS	2.507	-29.3134	6.0456	1.5799	18.8%
Adaptive LOS	2.207	-29.3134	5.8367	1.3910	28.5 %

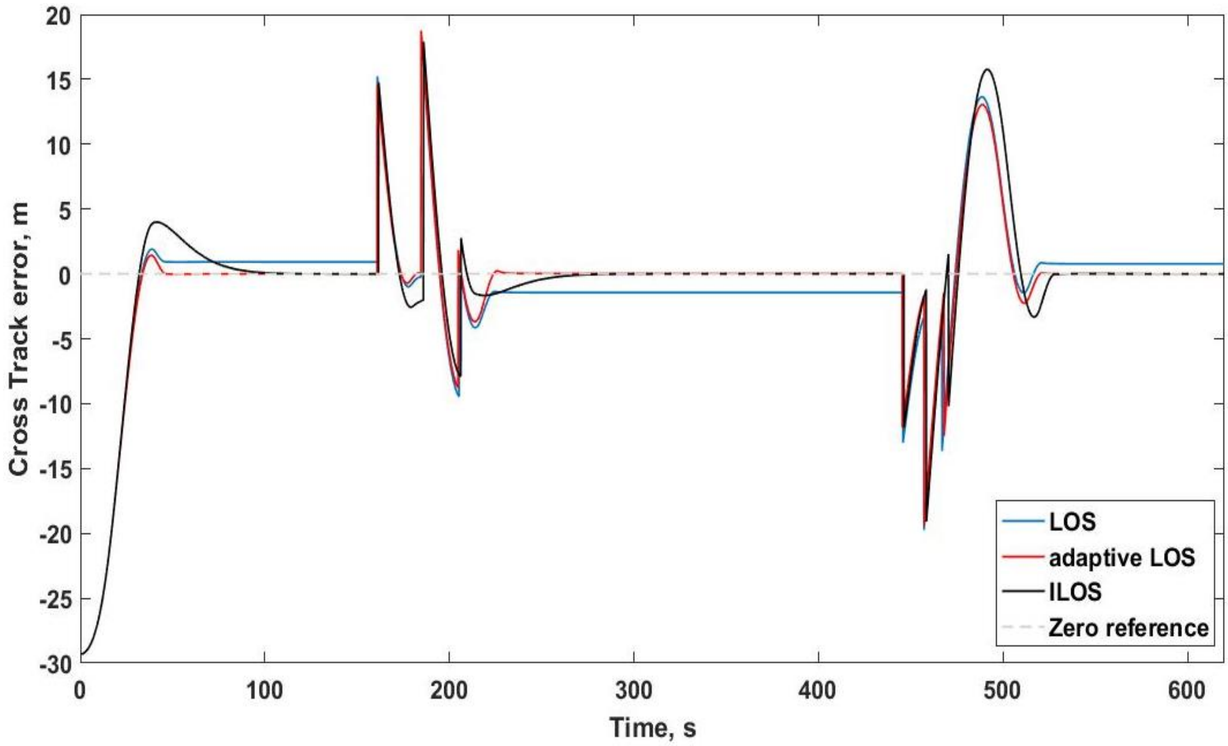

Fig 5.16 Comparison of guidance laws cross track errors

On the other hand, adaptive LOS guidance shows a good behaviour during the tracking and also provide a high converging time with lower overshoots that gives the guidance controller a robustness performance in manoeuvring within disturbance.

5.7 Guidance in random current disturbance

To increase the realistic conditions, the AUV is applied to a random disturbance is applied to the AUV to test the guidance strategies. The ocean current velocity field is loaded from Matlab velocity field library in which the magnitude of velocity ranges from 0.0268 m/sec to 2.432m/s. This high ocean disturbance with vortices is set to test the performance of guidance controller in complex environment. The initial conditions of the simulation are similar to the previous test and with the same predefined path waypoints. Firstly, the conventional LOS is applied to control the AUV in this case to monitor the response of the Vehicle motion. Fig 5.17 illustrate the motion of the AUV which is slightly deviated from the path especially at the highly disturbed zones. In Fig 5.18, the cross track error clears the behaviour of the vehicle under the LOS guidance and indicate the oscillating unstable performance of the controller.

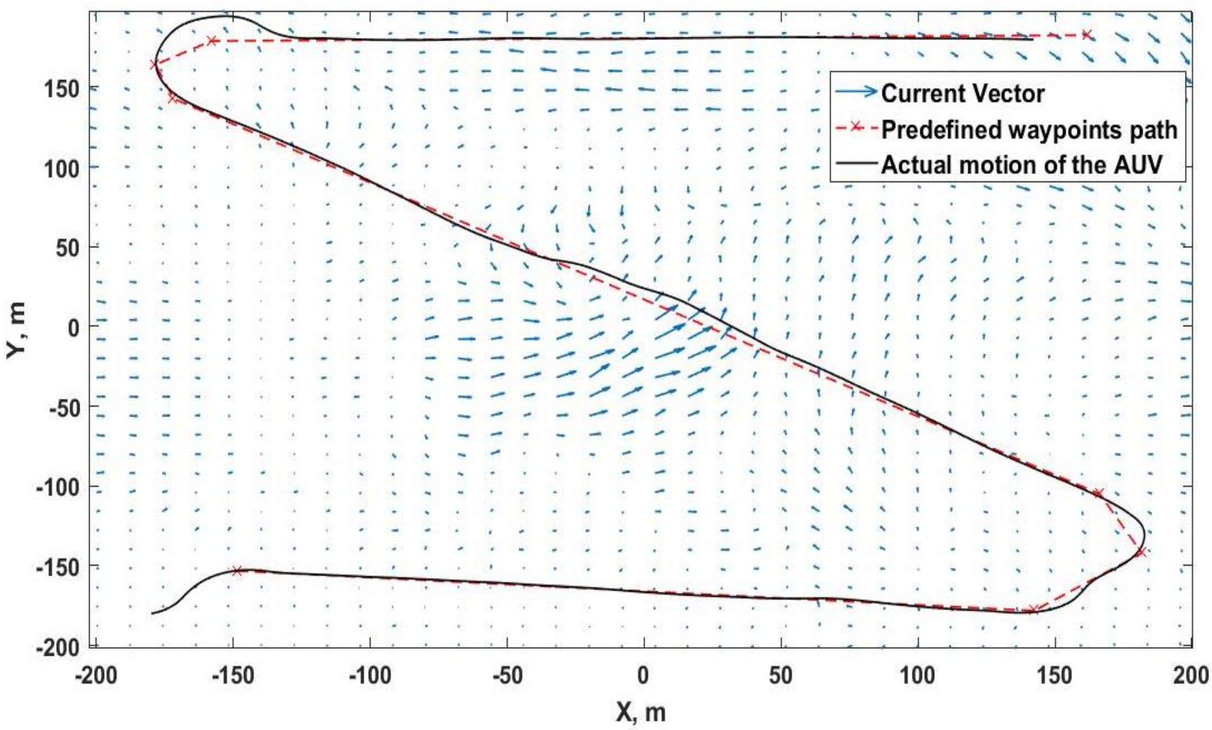

Fig 5.17 Simulation of the AUV path following using LOS guidance control under random ocean current disturbance

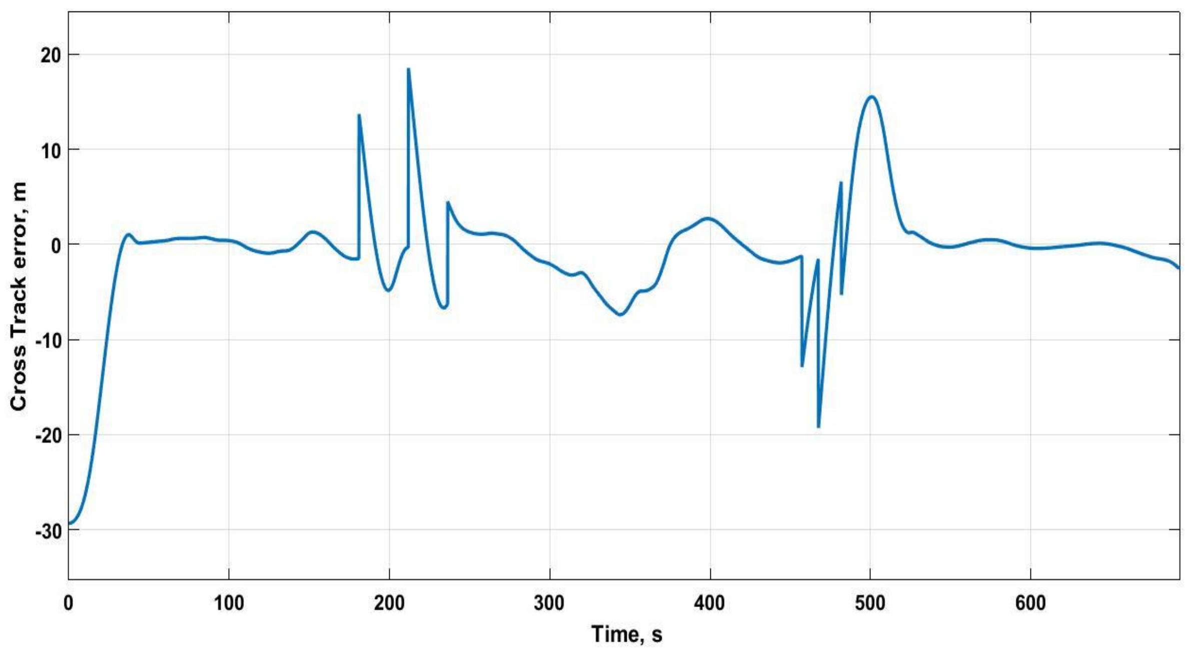

Fig 5.18 Cross track error of the LOS guidance in random ocean current disturb-ance

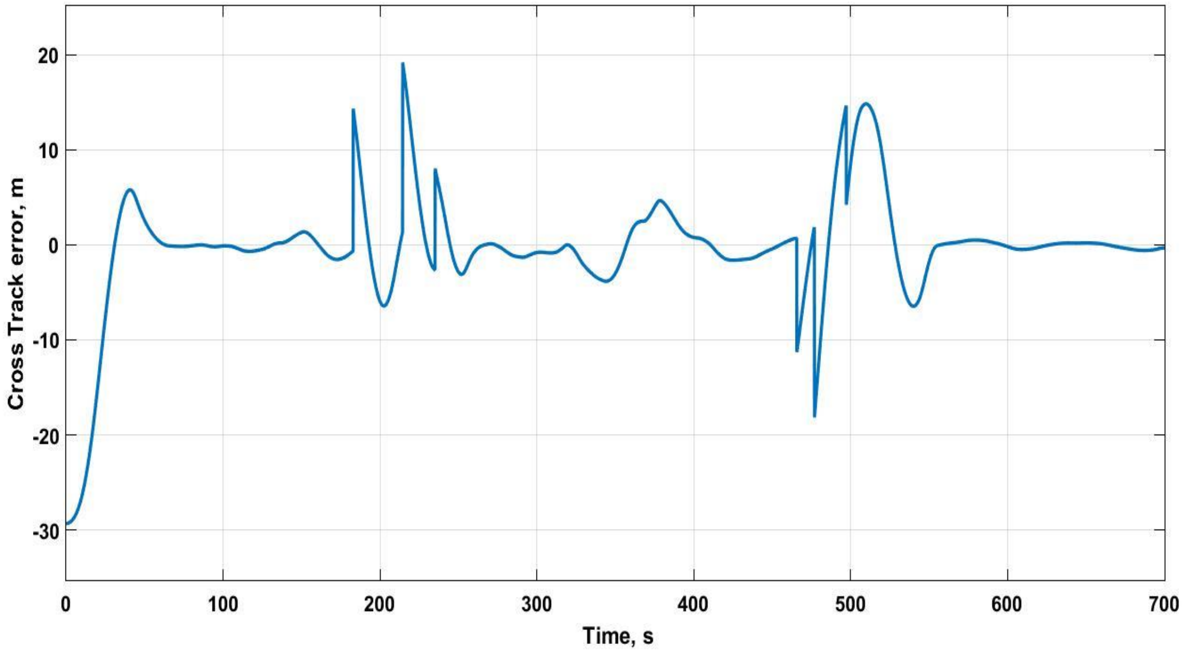

Fig 5.19 Cross track error of the ILOS guidance in random ocean current disturbance

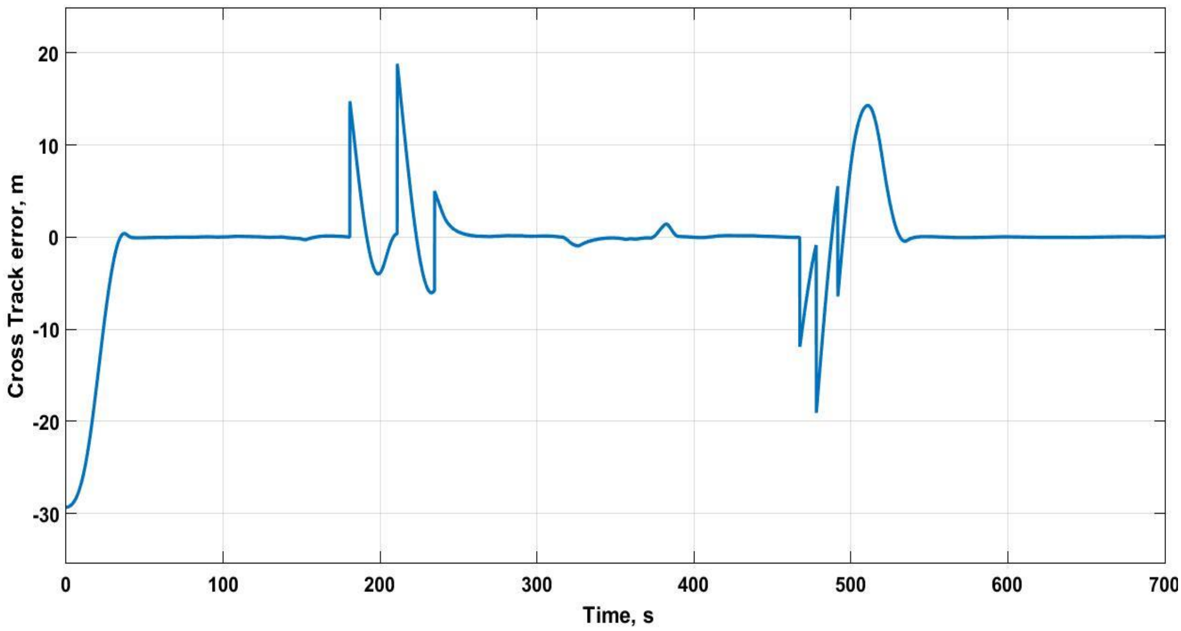

Fig 5.20 Cross track error of the LOS guidance in random ocean current disturbance

Then, the ILOS is applied to monitor the performance of this enhanced strategy of guidance. All the initial conditions are applied to the simulation and the integral gain is tuned to optimise the guidance controller performance. As shown in Fig 5.19, the performance of the tracking has a slight improvement although the winding up problem appeared in switching between waypoints.

Table 5.5 Statistical results of different guidance laws under random disturbance case

Look-ahead distance	Mean CE (m)	Max CE (m)	Standard deviation (m)	IAE(m.s) $\times 10^3$	Decrement percentage of IAE from LOS
LOS	3.0711	-29.3134	5.9142	2.1498	-
ILOS	2.9922	-29.3134	5.9560	2.0946	2.5%
Adaptive LOS	-2.08	-29.3134	5.5618	1.4560	32.27%

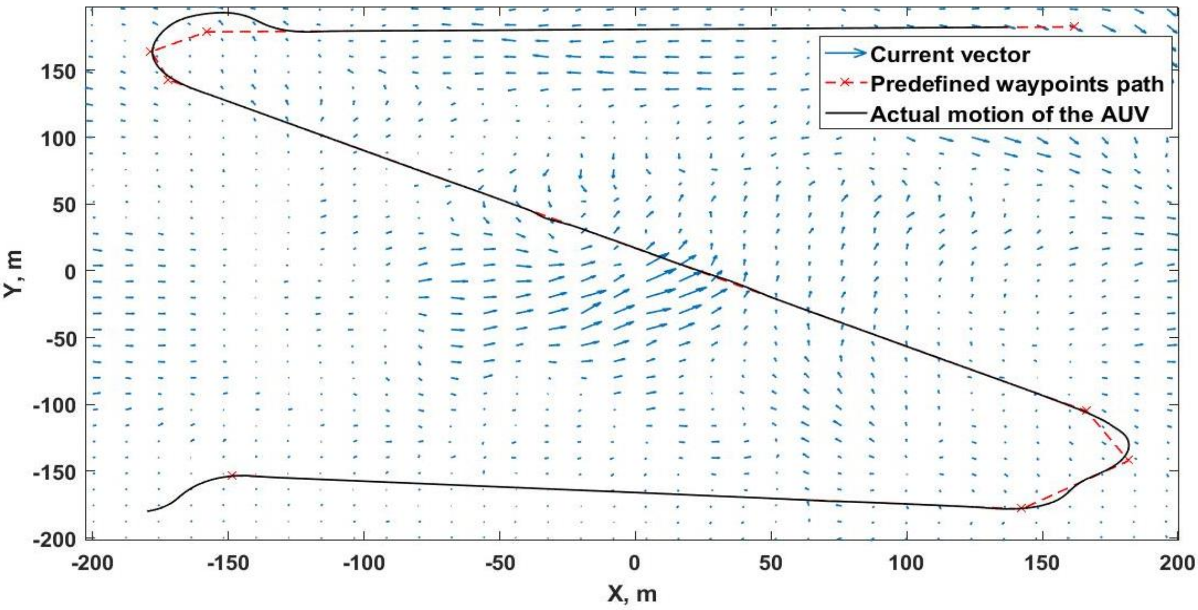

Fig 5.21 Simulation of the AUV path following using Adaptive LOS guidance control under random ocean current disturbance

The adaptive LOS guidance is finally applied with the same initial conditions and disturbance. In Fig 5.20, the tracking response of the adaptive LOS guidance has a significant enhancement in tracking and shows a great stability and robustness within the disturbance. Compared to the previous guidance approaches, the adaptive LOS track the predefined path and capable of performing the required mission without oscillations or deviation from the path as illustrated in Fig 5-21. Statistical data of each guidance strategy represent the performance of the tracking and indicate that the ILOS enhanced the tracking performance with 2.5% of IAE and decreased the standard deviation with less than 1% compared to the conventional LOS guidance. While, the adaptive LOS increased the tracking performance with 32.27% of IAE and 6% of standard deviation compared to the conventional LOS guidance as shown in Table 5. SO, the adaptive LOS improves the tracking with 30.5% compared to the ILOS guidance and provide a suitable strategy to path following missions under the environmental disturbances.

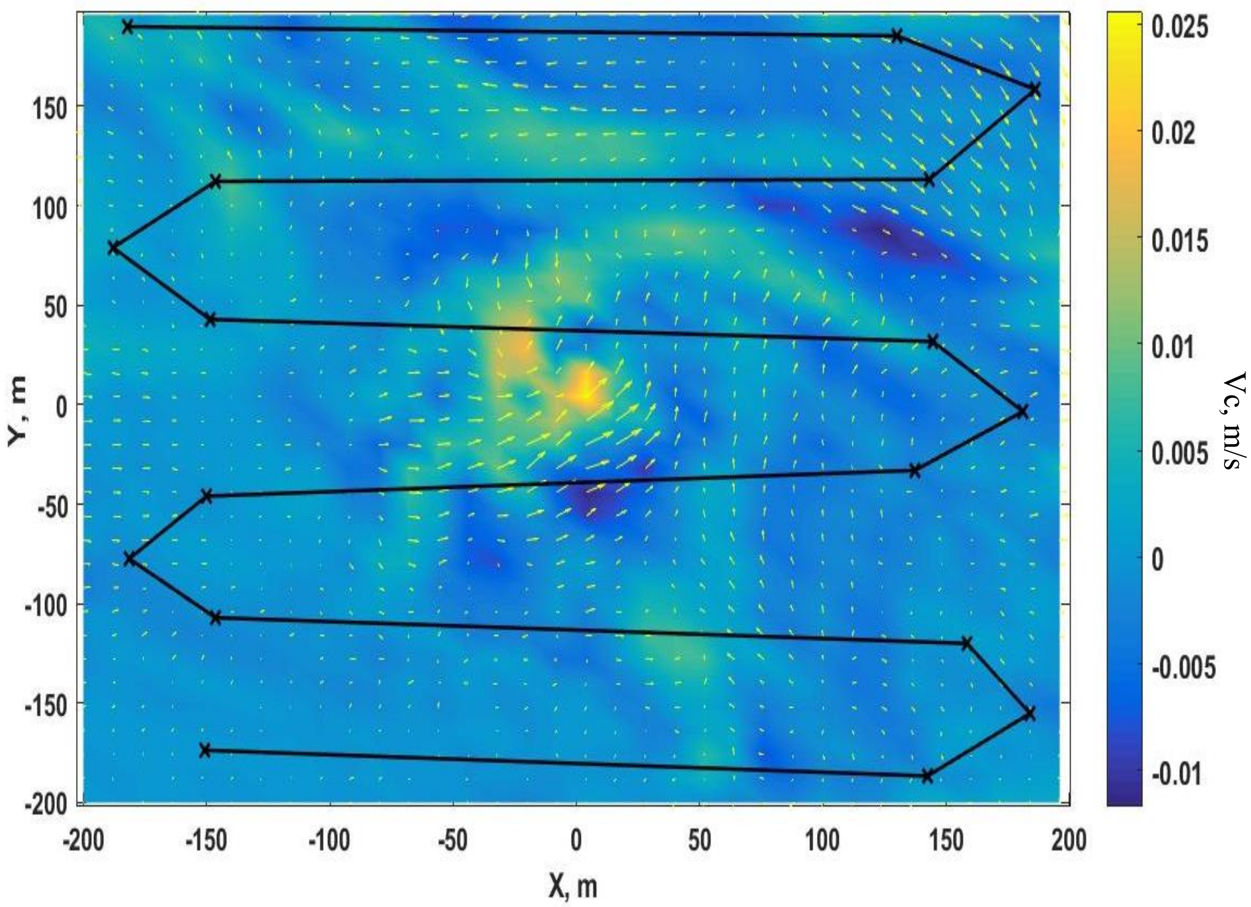

Fig 5.22 Input map environment with mission path way points

5.8 Case study

After evaluating the system components, the HRC-AUV is provided with a mission to test the overall system performance. In this case study, the AUV is required to scan a specific area and to provide a contour map of the ocean current disturbance. The planner provide a maze path to cover the selected area as shown in Fig 5-22. The path waypoints are:

$\mathrm{W}_x = \{$ -150.7735, 142.3978,183.9669,158.4420, -146.3978, -181.4033, -150.0442, 137.2928, 181.0497,144.5856, -148.5856, -187.9669, -146.3978, 143.1271,186.1547, 130.0000, -182.1326 },

$\mathrm{W}_y = \{$-173.6308, -186.5841, -155.1262, -119.9673, -107.0140, -77.4065, -45.9486, -32.9953,-3.3879,31.7710,42.8738,78.9579,112.2664,113.1916, 158.5280,185.3598,190.00$\}$.

The initial conditions of the test are initial position of ($\eta = [-180, -180,0,0,0]^{\mathrm{T}}$), thruster velocity of ($n = 490\, rpm$), controller gains with ($K_P = 100,\ K_I = 0.01, K_D = 100$), look ahead distance of ($d = 10\ m$), and waypoint radius of circle of acceptance ($R = 20\ m$). The system is simulated for 1263 sec with sampling time of 0.1sec. The ocean current disturbance has a velocity range between 0.0134 and 1.216 m/s. the adaptive LOS guidance control is selected to perform the path following task due its effectiveness and stability which has been proved in previous sections. The simulation of the provided mission shows that the vehicle has maintained the predefined path and performed the large manoeuvres with a minimum deviation under the random disturbance as shown in Fig 5-23. The performance of the tracking is showing a good tracking with ($IAE = \ 2.2781 \times 10^3 m.s$), average cross track error ($CE_{mean} = 1.8037\ m$), standard deviation (SD = 4.4691 m), and maximum overshoot ($CE_{max} = 22.6058\, m$). The AUV performance affected greatly with the difficulty of the provided path rather than the applied disturbance.

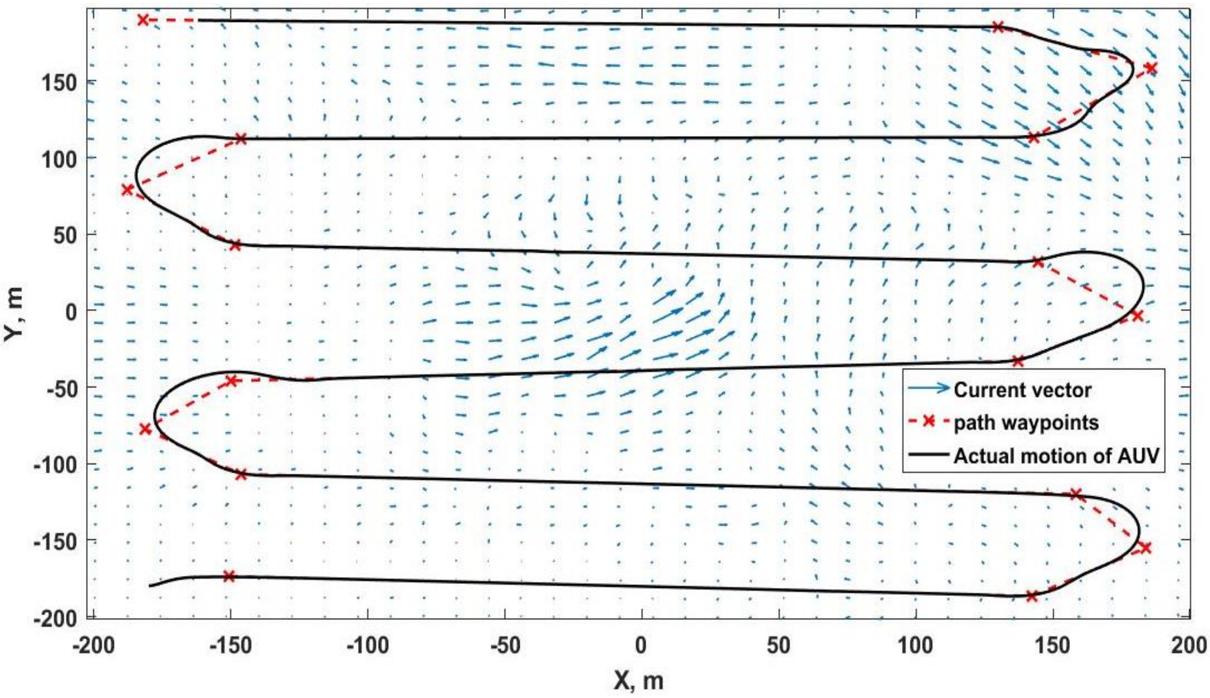

Fig 5.23 Simulation of the AUV motion under current disturbance while performing a path following mission

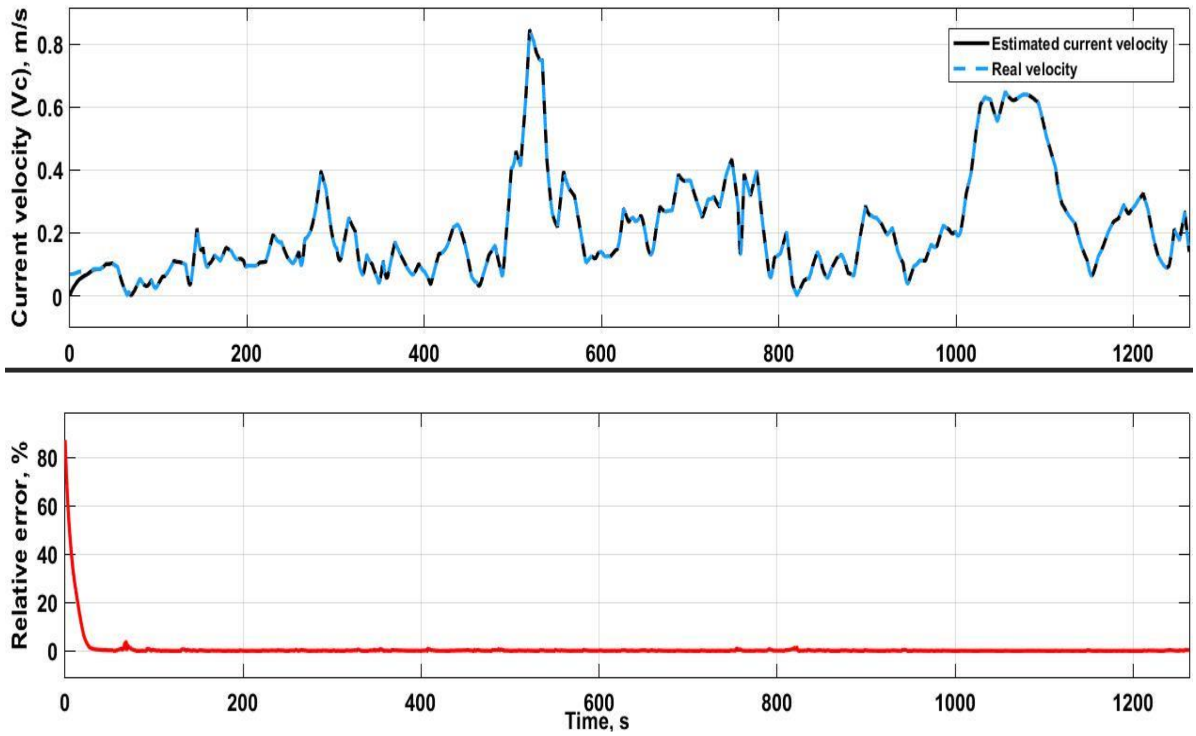

Fig 5.24 Comparison of estimated ocean current velocity and actual velocity along the mission path

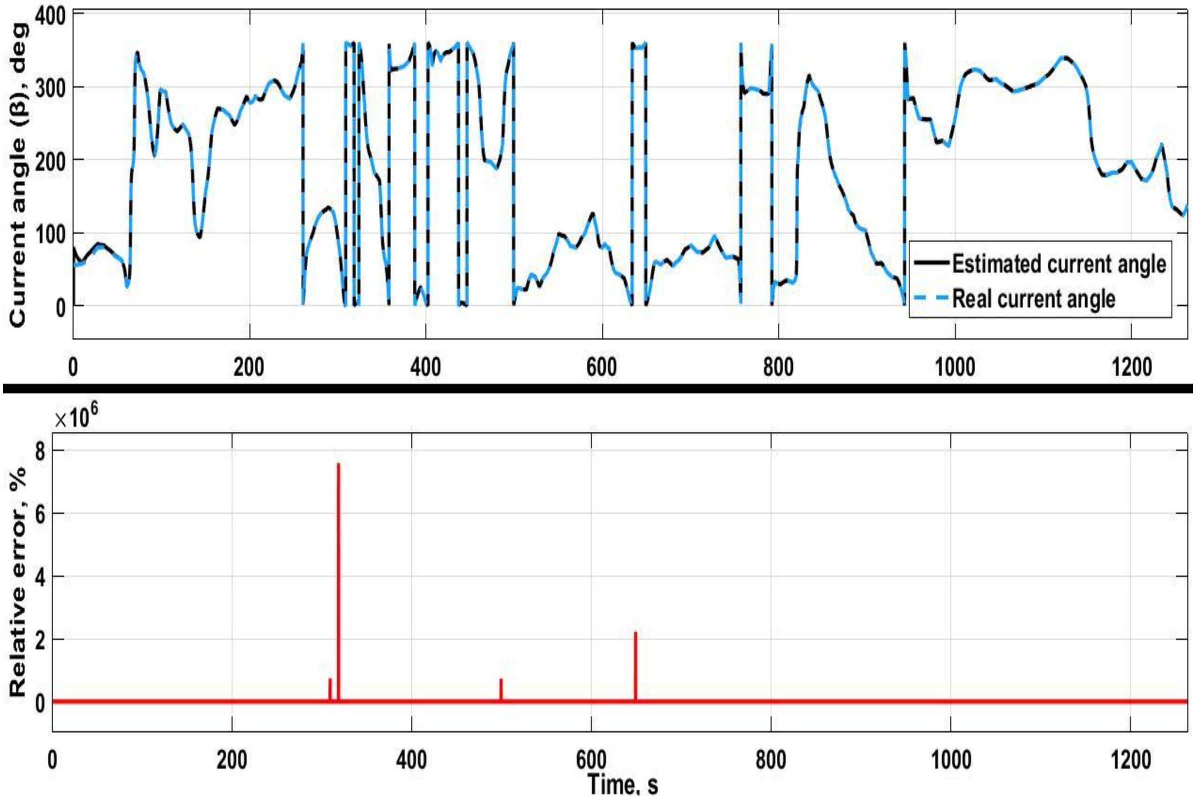

Fig 5.25 Comparison of estimated ocean current angle and actual angle along the mission path

So, the straight line path following is not the preferred type of paths that the vehicle could track easily with large manoeuvres. Curved paths could be easier and suitable in manoeuvring missions. The ocean current estimation mission is provided by this simulation test and the velocity and direction are calculated along the actual path that the vehicle travel on. In Fig 5.24 and Fig 5.25, the ocean current velocity and direction are estimated online showing an accurate estimation. From the graph figures, the estimation shows a sensitive response to the change in current field values.

Then, the collected data are used to predict ocean current data in the full scanned area. The triangulation-based linear interpolation is used to predict the full map velocities indicating high and low current fields as shown in the generated contour map in Fig 5.26.

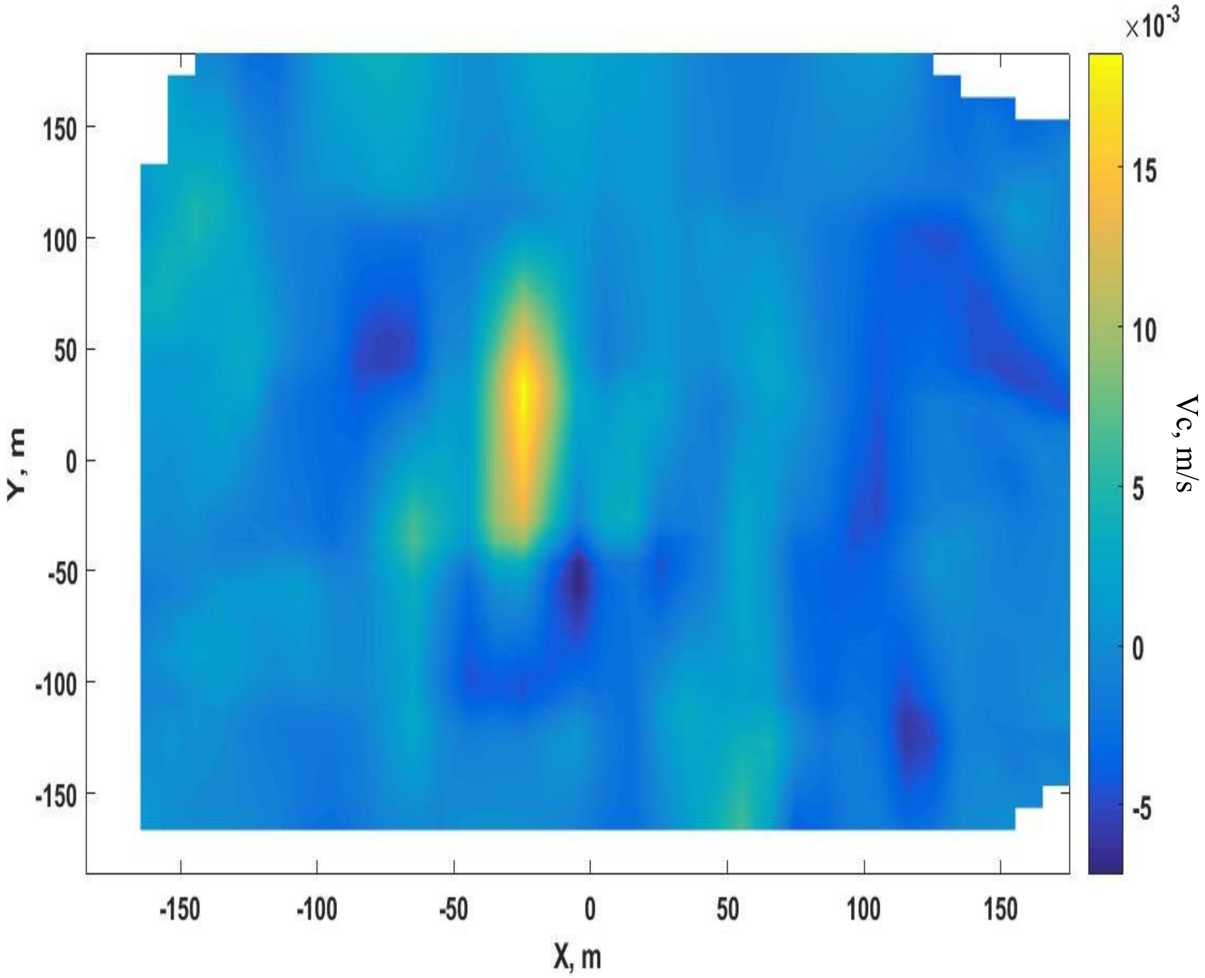

Fig 5.26 Generated contour map of the ocean current disturbance using AUV

The generated map is close to the input map and indicates the highly disturbed regions in the scanned area. To enhance the prediction results, the AUV has to follow a path with more layers to provide a more interpolation accuracy.

5.9 Summary

In this chapter, the simulation of HRC-AUV has been configured and viewed in different scenarios. The simulation setup for Matlab software is shown and the solving technique is reviewed. Then, the performance of the heading PID controller is tested to obtain the controllability of the heading controller which shows a good performance characteristics. Then, the ocean current estimation is tested using constant and random current scenarios. The performance of the observer shows functionality in the estimation for both cases. Then, the guidance system is tested using the LOS. ILOS, and adaptive LOS laws under the ocean current disturbance. Guidance laws are compared to obtain the robust and efficient controller under environmental disturbance. Finally, a surveillance mission under random ocean current disturbance is simulated to evaluate the mission handling ability of the system. The results obtained in this chapter is used in concluding the research in next chapter and the recommendations to enhance the system are also discussed.

CHAPTER SIX:

CONCLUSION AND RECOMMENDATIONS

In this work, the main problem was to allow the AUV to work under ocean current disturbance. The motion of AUV had been used to estimate the ocean currents during the autonomous motion of AUV. An observer have been designed in order to compare the actual motion trajectory to the estimated trajectory from the model, to derive ocean current magnitude and direction. These currents had not been explicitly dealt with in the literature but treated as a disturbance. By keeping log of the current and vehicle location, a map can be constructed and is quite beneficial for at least two reasons. The first is that knowledge of ocean current can be used in planning the motion to reduce error and save vehicle energy. Secondly the map is dynamic and it can show dangerous vortices to avoid or other environmental data that can be used for environmental monitoring, fishing and survey industry. In addition, a guidance system was designed to compensate the ocean current disturbance using the estimated current data in order to maintain the predefined mission path. From the results of this study, the following can be concluded:

1. The performance of the heading controller is quite accepted but the actuator design needs to be modified and optimized in order to achieve higher maneuverability.
2. The nonlinear observer design was successful to build a dynamic map of the ocean currents in several cases ranging from fixed direction current to complex vortices.
3. Traditional LOS guidance law showed an accurate tracking performance in non-disturbed environment when the look-ahead distance was tuned.
4. ILOS enhanced the guidance system in the constant environmental disturbances by decreasing the path error with 18% compared to the traditional LOS but it has a significant drawbacks in overshooting, oscillation, and higher transient time. In addition, the ILOS was not efficient in the random disturbance cases.
5. Adaptive LOS guidance that depends on the current estimation improved the tracking performance in random environmental disturbances with 32.27% compared to the tradition LOS guidance and 30.5% compared to the ILOS guidance.

6. A mission of mapping the ocean current in specific area under random current disturbance was successfully performed and the generated contour map of the current gave a good indication of high and low velocities in the scanned current field area.

Moreover, the results achieved make a recommendations to the AUV system in different ways such as:

1. Evaluate the control system experimentally by testing the AUV in real environmental disturbance and comparing the results with the simulation data.
2. Apply the designed system in 3D which the depth control will be included and also convert the straight line path tracking in curved line to avoid the overshoot problem in switching between waypoints.
3. Upgrade the path following mission to a trajectory tracking scenario which the speed of the vehicle will be included.
4. Use a multi vehicles to map the ocean current data for specific region which will increase the mapping performance and make a large area monitoring. Technologies such as Underwater Internet of Things (UIoT) could be used to collect the ocean current data from different vehicles and sensors to enhance the ocean monitoring.
5. Design a planner system that re-plans the mission path according to the estimation of ocean current to avoid the dangerous vortices and violent current. Also, an artificial intelligence (AI) could be used to make a risk analyses of the predicted mission path using the estimated map.

Finally, ocean current disturbance considered as one of the main challenges that prevent the AUVs from working in complex locations. In this work, a solution in estimating the disturbance and compensate its effect in tracking control have been suggested to improve the AUV autonomy. The improvement in the autonomy of the AUVs will not only enhance the ocean monitoring, industry and exploration but also it will inspire the autonomous vehicles generally by providing the developments reached

List of Publications

Omar H. Rashed, Mohamed Abdellatif, S.Shaaban, Abdulaziz Morgan (2018) "Online Ocean Current Estimation and Mapping for Autonomous Underwater Vehicle", Proceedings of the 16th Mechatronics International Conference University of Strathclyde, Glasgow, UK 19th – 21st September 2018.

References

[1] "Global Autonomous Underwater Vehicle Market 2017-2021," *technavio*, 2017. [Online]. Available: https://www.technavio.com/report/global-autonomous-underwater-vehicle-market. [Accessed: 07-May-2018].

[2] A. Shukla and H. Karki, "Application of robotics in offshore oil and gas industry — A review Part II," *Rob. Auton. Syst.*, vol. 75, pp. 508–524, 2016.

[3] "UTEC Awarded Contract with Saipem To Support in Zohr Field Development," 2017. [Online]. Available: https://utecsurvey.com/utec-awarded-contract-with-saipem-to-support-in-zohr-field-development/. [Accessed: 20-Aug-2018].

[4] "SCOPUS," 2018. [Online]. Available: https://www.scopus.com/sources. [Accessed: 20-Aug-2018].

[5] A. J. Sørensen and M. Ludvigsen, "Towards integrated autonomous underwater operations," *IFAC-PapersOnLine*, vol. 28, no. 2, pp. 107–118, 2015.

[6] M. Ludvigsen and A. J. Sørensen, "Towards integrated autonomous underwater operations for ocean mapping and monitoring," *Annu. Rev. Control*, vol. 42, pp. 145–157, 2016.

[7] X. Du, H. Cui, and Z. Zhang, "Dynamics model and maneuverability of a novel AUV with a deflectable duct propeller," *Ocean Eng.*, vol. 163, no. June, pp. 191–206, 2018.

[8] K. M. Ã, "Pulsatile vortex generators for low-speed maneuvering of small underwater vehicles," vol. 33, pp. 2209–2223, 2006.

[9] S. A. Gafurov and E. V. Klochkov, "Autonomous Unmanned Underwater Vehicles Development Tendencies," *Procedia Eng.*, vol. 106, pp. 141–148, 2015.

[10] J. Erling and G. Refsnes, "Nonlinear Model-Based Control of Slender Body AUVs," Norwegian University of Science and Technology, 2007.

[11] M. Breivik and T. I. Fossen, "Guidance Laws for Autonomous Underwater Vehicles," in *Underwater Vehicles*, no. December, A. V. Inzartsev, Ed. InTech, 2009, p. 582.

[12] R. Wernli and R. Christ, *The ROV Manual: A User Guide for Remotely Operated Vehicles*, 2nd Editio. Butterworth-Heinemann, 2014.

[13] T. Kwasnitschka, T. H. Hansteen, C. W. Devey, and S. Kutterolf, "Doing fieldwork on the seafloor : Photogrammetric techniques to yield 3D visual models from ROV video," *Comput. Geosci.*, vol. 52, pp. 218–226, 2013.

[14] V. A. I. Huvenne, K. Robert, L. Marsh, C. Lo Iacono, T. Le Bas, and R. B. Wynn, "ROVs and AUVs," in *Submarine Geomorphology*, Springer, Cham, 2018, pp. 93–108.

[15] R. B. Wynn *et al.*, “Autonomous Underwater Vehicles (AUVs): Their past, present and future contributions to the advancement of marine geoscience,” *Mar. Geol.*, vol. 352, pp. 451–468, 2014.

[16] M. Tang, Z. Zhang, and Y. Xing, “Analysis of new developments and key technologies of autonomous underwater vehicle in marine survey,” in *Procedia Environmental Sciences*, 2011, vol. 10, pp. 1992–1997.

[17] “Autonomous Underwater Vehicle, HUGIN.” [Online]. Available: https://www.km.kongsberg.com/ks/web/nokbg0240.nsf/AllWeb/B3F87A63D8E419E5C1256A68004E946C?OpenDocument. [Accessed: 05-Jun-2018].

[18] P. E. Hagen and N. Stcrrkersen, “The HUGIN 1000 Autonomous Underwater Vehicle for Military Applications,” no. 2027, pp. 1141–1145, 2003.

[19] “REMUS 6000 for Defense Applications,” 2018. [Online]. Available: https://www.hydroid.com/remus-6000-defense-applications.

[20] Y. Valeriano-Medina, A. Martinez, L. Hernandez, H. Sahli, Y. Rodriguez, and J. R. Canizares, “Dynamic model for an autonomous underwater vehicle based on experimental data,” *Math. Comput. Model. Dyn. Syst. Methods, Tools Appl. Eng. Relat. Sci.*, vol. 19, no. 2, pp. 175–200, 2012.

[21] Wood and Stephen, “Autonomous Underwater Gliders,” in *Underwater Vehicles*, 2008, pp. 505–530.

[22] NIST, “Autonomy Levels For Unmanned Systems,” 2016. [Online]. Available: https://www.nist.gov/el/intelligent-systems-division-73500/cognition-and-collaboration-systems/autonomy-levels-unmanned. [Accessed: 05-Jun-2018].

[23] T. I. Fossen, *Marine control systems: guidance, navigation and control of ships, rigs and underwater vehicles*. Springer, 2002.

[24] M. Gertler and G. R. Hagen, “STANDARD EQUATIONS OF MOTION FOR SUBMARINE SIMULATION,” *Nav. Sh. Res. Dev. Ctr. (NSRDC), Bethesda, MD*, 1967.

[25] T. I. Fossen, “Guidance and Control of Ocean Vehicles,” *Automatica*, vol. 32, no. 8. p. 1235, 1994.

[26] C. W. Chen, J. S. Kouh, and J. F. Tsai, “Modeling and simulation of an AUV simulator with guidance system,” *IEEE J. Ocean. Eng.*, vol. 38, no. 2, pp. 211–225, 2013.

[27] C. Wang, F. Zhang, and D. Schaefer, “Dynamic modeling of an autonomous underwater vehicle,” 2014.

[28] Z. Zeng, K. Sammut, L. Lian, F. He, and A. Lammas, “A comparison of optimization techniques for AUV path planning in environments with ocean currents,” *Rob. Auton. Syst.*, vol. 82, pp. 61–72, 2016.

[29] M. D. Pedersen and T. I. Fossen, *Marine Vessel Path Planning & Guidance Using*

Potential Flow, vol. 45, no. 27. IFAC, 2012.

[30] K. Ma, L. Liu, and G. S. Sukhatme, “An Information-Driven and Disturbance-Aware Planning Method for Long-Term Ocean Monitoring,” pp. 2102–2108, 2016.

[31] C. S. Draper, “Guidance is Forever,” *Navigation*, vol. 1, no. 18, pp. 26–50, 1971.

[32] Z. F. Sfahani, “Pure Pursuit Guidance and Sliding Mode Control of an Autonomous Underwater Vehicle for Pipeline Tracking,” pp. 279–283, 2017.

[33] M. Breivik, V. E. Hovstein, and T. I. Fossen, “Straight-Line Target Tracking for Unmanned Surface Vehicles,” no. June 2014, 2008.

[34] K. Ytterstad, C. Paliotta, S. Member, E. Lefeber, K. Y. Pettersen, and I. J. Pinto, “Trajectory tracking and path following for underactuated marine vehicles,” 2018.

[35] T. I. Fossen and M. Breivik, “Line-of- sight path following of underactuated marine craft,” in *Maneuvering and Control of Marine Crafts*, 2003, pp. 244–249.

[36] A. J. Healey and D. Lienard, “Multivariable Sliding-Mode Control for Autonomous Diving and Steering of Unmanned Underwater Vehicles,” *IEEE J. Ocean. Eng.*, vol. 18, no. 3, pp. 327–339, 1993.

[37] T. I. Fossen, *Handbook of Marine Craft Hydrodynamics and Motion Control*. 2011.

[38] A. M. Lekkas and T. I. Fossen, “Minimization of cross-track and along-track errors for path tracking of marine underactuated vehicles,” *2014 Eur. Control Conf. ECC 2014*, no. October 2015, pp. 3004–3010, 2014.

[39] M. Breivik and T. I. Fossen, “Path Following for Marine Surface Vessels,” in *Oceans ’04 MTS/IEEE Techno-Ocean ’04 (IEEE Cat. No.04CH37600)*, 2004, pp. 2282–2289.

[40] T. I. Fossen and K. Y. Pettersen, “On uniform semiglobal exponential stability (USGES) of proportional line-of-sight guidance laws ☆,” vol. 50, no. July, pp. 2912–2917, 2014.

[41] S. Moe, W. Caharija, K. Y. Pettersen, and I. Schjølberg, “Path Following of Underactuated Marine Surface Vessels in the Presence of Unknown Ocean Currents,” no. 2, pp. 3856–3861, 2014.

[42] M. Maghenem, D. J. W. Belleter, C. Paliotta, and K. Y. Pettersen, “Observer Based Path Following for Underactuated Marine Vessels in the Presence of Ocean Currents: A Local Approach,” *IFAC-PapersOnLine*, vol. 50, no. 1, pp. 13654–13661, 2017.

[43] S. Moe, K. Y. Pettersen, T. I. Fossen, and J. T. Gravdahl, “Line-of-sight curved path following for underactuated USVs and AUVs in the horizontal plane under the influence of ocean currents,” *24th Mediterr. Conf. Control Autom. MED 2016*, no. 978, pp. 38–45, 2016.

[44] M. Breivik, “Principles of Guidance-Based Path Following in 2D and 3D,” in *Proceedings of the 44th IEEE Conference on Decision and Control*, 2005, pp. 627–

634.

[45] C. Yu, X. Xiang, L. Lapierre, and Q. Zhang, "Nonlinear guidance and fuzzy control for three-dimensional path following of an underactuated autonomous underwater vehicle," *Ocean Eng.*, vol. 146, no. October, pp. 457–467, 2017.

[46] A. P. Aguiar and A. M. Pascoal, "Modeling and control of an autonomous underwater shuttle for the transport of benthic laboratories," *Ocean. IEEE/MTS Conf. Exhib.*, vol. 2, pp. 888–895, 1997.

[47] V. Bakaric, Z. Vukic, and R. Antonic, "Improved basic planar algorithm of vehicle guidance through waypoints by the line of sight," *First Int. Symp. Control. Commun. Signal Process. 2004.*, vol. 2, no. 2, pp. 541–544, 2004.

[48] E. Børhaug, A. Pavlov, and K. Y. Pettersen, "Integral LOS Control for Path Following of Underactuated Marine Surface Vessels in the Presence of Constant Ocean Currents," pp. 4984–4991, 2008.

[49] T. I. Fossen and A. M. Lekkas, "Direct and indirect adaptive integral line-of-sight path-following controllers for marine craft exposed to ocean currents," no. March 2015, pp. 445–463, 2017.

[50] A. M. Lekkas and T. I. Fossen, "Trajectory Tracking and Ocean Current Estimation for Marine Underactuated Vehicles," 2014.

[51] J. Zeng, L. Wan, Y. Li, and Z. Dong, "Adaptive line-of-sight path following control for underactuated autonomous underwater vehicles in the presence of ocean currents," no. December, pp. 1–14, 2017.

[52] P. G. Thomasson and C. A. Woolsey, "Vehicle motion in currents," *IEEE J. Ocean. Eng.*, vol. 38, no. 2, pp. 226–242, 2013.

[53] S. Fan and C. a Woolsey, "Underwater Vehicle Control and Estimation in Nonuniform Currents," pp. 1402–1407, 2013.

[54] M. Hedayati and K. Saeed, "Modeling and control of autonomous underwater vehicle (AUV) in heading and depth attitude via self-adaptive fuzzy PID controller," *J. Mar. Sci. Technol.*, pp. 559–578, 2015.

[55] P. Herman, "Decoupled PD set-point controller for underwater vehicles," *Ocean Eng.*, vol. 36, no. 6–7, pp. 529–534, 2009.

[56] S. Soylu, B. J. Buckham, and R. P. Podhorodeski, "A chattering-free sliding-mode controller for underwater vehicles with fault-tolerant infinity-norm thrust allocation," *Ocean Eng.*, vol. 35, no. 16, pp. 1647–1659, 2008.

[57] X. Qi, "Adaptive coordinated tracking control of multiple autonomous underwater vehicles," *Ocean Eng.*, vol. 91, pp. 84–90, 2014.

[58] M. Zeinali and L. Notash, "Adaptive sliding mode control with uncertainty estimator for robot manipulators," *Mech. Mach. Theory*, vol. 45, no. 1, pp. 80–90, 2010.

[59] S. Mohan and J. Kim, "Indirect adaptive control of an autonomous underwater vehicle-manipulator system for underwater manipulation tasks," *Ocean Eng.*, vol. 54, pp. 233–243, 2012.

[60] X. Xiang, "Survey on Fuzzy-Logic-Based Guidance and Control of Marine Surface Vehicles and Underwater Vehicles," *Int. J. Fuzzy Syst.*, vol. 20, no. 2, pp. 572–586, 2018.

[61] P. W. J. V. D. V. Ã, C. Flanagan, and D. Toal, "Neural network control of underwater vehicles," vol. 18, pp. 533–547, 2005.

[62] P. E. Hagen, Ø. Hegrenæs, B. Jalving, Ø. Midtgaard, M. Wiig, and O. K. Hagen, "Making AUVs Truly Autonomous," no. December, 2008.

[63] L. Paull, S. Saeedi, M. Seto, and H. Li, "AUV Navigation and Localization : A Review," vol. 39, no. 1, pp. 131–149, 2014.

[64] A. Kim, S. Member, R. M. Eustice, and S. Member, "Real-Time Visual SLAM for Autonomous Underwater Hull Inspection Using Visual Saliency," *IEEE Trans. Robot.*, vol. 29, no. 3, pp. 719–733, 2013.

[65] C. Lyon *et al.*, "Model aided navigation with sea current estimation for autonomous underwater vehicle," *Int. J. Adv. Robot. Syst. Model*, pp. 1–9, 2015.

[66] Ø. Hegrenaes and O. Hallingstad, "Model-aided INS with sea current estimation for robust underwater navigation," *IEEE J. Ocean. Eng.*, vol. 36, no. 2, pp. 316–337, 2011.

[67] J. D. Boyd, "EVALUATION OF ADCP WAVE MEASUREMENTS," University of Kansas, 2006.

[68] P. Rogowski and E. Terrill, "Mapping velocity fields in coastal waters using an autonomous underwater vehicle," in *2015 IEEE/OES 11th Current, Waves and Turbulence Measurement, CWTM 2015*, 2015.

[69] M. Muste, K. Yu, T. Pratt, and D. Abraham, "Practical aspects of ADCP data use for quantification of mean river flow characteristics; Part II: Fixed-vessel measurements," *Flow Meas. Instrum.*, vol. 15, no. 1, pp. 17–28, 2004.

[70] K. Ogatta, *Modern control engineering*, 5th ed. Pearson Education, 2010.

[71] A. Martínez, Y. Rodríguez, L. Hernández, C. Guerra, and H. Sahli, "Hardware and software architecture for AUV based on low-cost sensors," *11th Int. Conf. Control. Autom. Robot. Vision, ICARCV 2010*, vol. 1428, no. December, pp. 1428–1433, 2010.

[72] Ø. Hegrenæs, O. Hallingstad, and B. Jalving, "A framework for obtaining steady-state maneuvering characteristics of underwater vehicles using sea-trial data," in *2007 Mediterranean Conference on Control and Automation, MED*, 2007.

[73] S. Fan, W. Xu, Z. Chen, and F. Zhang, "Nonlinear observer design for current estimation based on underwater vehicle dynamic model," in *OCEANS 2016 -*

Shanghai, 2016.

[74] N. Mahmoudian and C. Woolsey, “DYNAMICS & CONTROL OF UNDERWATER GLIDERS II: MOTION PLANNING AND CONTROL N. Mahmoudian & C. Woolsey,” *2008 47th IEEE Conf. Decis. Control*, pp. 552–557, 2010.

[75] H. K. Khalil and L. Praly, “High-gain observers in nonlinear feedback control,” no. July 2013, pp. 993–1015, 2014.

[76] A. P. Aguiar and A. M. Pascoal, “Dynamic positioning and way-point tracking of underactuated AUVs in the presence of ocean currents,” *Int. J. Control*, vol. 80, no. 7, pp. 1092–1108, 2007.

[77] J. E. Refsnes, A. J. S??rensen, and K. Y. Pettersen, “Robust observer design for underwater vehicles,” *Proc. IEEE Int. Conf. Control Appl.*, pp. 313–319, 2006.

[78] J. E. Refsnes, K. Y. Pettersen, and A. J. Sorensen, “Control of slender body underactuated AUVs with current estimation,” *Proc. 45th IEEE Conf. Decis. Control*, pp. 43–50, 2006.

[79] O. Hallingstad and K. Maritime, “Comparison of Mathematical Models for the HUGIN 4500 AUV Based on Experimental Data Commonsfor dervabiov menfotionetepenotations hed so-led hdodmnamice depries . ntheionseis are oces andimomets . os the,” no. 7491, pp. 17–20, 2007.

[80] M. Sangekar, M. Chitre, and T. B. Koay, “Hardware architecture for a modular autonomous underwater vehicle STARFISH,” *Ocean. 2008*, no. October, 2008.

[81] S. of N. A. and M. E. (U. S.). T. and R. C. H. Subcommittee, *Nomenclature for Treating the Motion of a Submerged Body Through a Fluid: Report of the American Towing Tank Conference*. Society of Naval Architects and Marine Engineers, 1950.

[82] O. Faltinsen, *Sea Loads on Ships and Offshore Structures*. Cambridge University Press, 1990.

[83] G. Antonelli, *Underwater Robots: Motion and Force Control of Vehicle-Manipulator Systems*, Second Ed. Springer, 2006.

[84] J. N. Newman, “Marine Hydrodynamics,” in *Marine Hydrodynamics*, MITP, 1977.

[85] T. I. Fossen and A. Ross, “Nonlinear Modelling, Identi…cation and Control of UUVs Thor,” in *Guidance and Control of Unmanned Marine Vehicles*, no. 1, 2006, pp. 23–42.

[86] S. Lyashevskiy and L. A. Abel, “NONLINEAR SYSTEMS IDENTIFICATION USING THE,” *IFAC Proc. Vol.*, vol. 27, no. 8, pp. 271–276, 1994.

[87] T. I. Fossen, T. A. Johansen, and T. Perez, “A Survey of Control Allocation Methods for Underwater Vehicles,” no. January, 2009.

[88] W. Caharija *et al.*, “Integral line-of-sight guidance and control of underactuated

marine vehicles: Theory, simulations and experiments," *IEEE Trans. Control Syst. Technol.*, vol. 24, no. 5, pp. 1623–1642, 2016.

APPENDIX

MATLAB M-FFILES

Physical parameters of the HRC-AUV declaration

```
function V1= HRC()

V1.m=4094.56;
V1.L=9.46;
V1.R=0.4;
V1.BG=[0 0 22*10^-3]';
V1.BGz=22*10^-3;

V1.Ixx=450.1;
V1.Iyy=21010.4;
V1.Izz=20816;
V1.Ixz=275.44;

V1.Xud=-250.84;
V1.Yvd=-3834;
V1.Zwd=-3834;
V1.Kpd=0;
V1.Mqd=-15572;
V1.Nrd=-15572;

V1.Xu=-181.45;
V1.Yv=-1219.8;
V1.Zw=-1219.8;
V1.Kp=-126.62;
V1.Mq=-9096.9;
V1.Nr=-9096.9;
V1.Mrb=[V1.m 0 0 0 V1.m*V1.BGz 0;
    0 V1.m 0 -V1.m*V1.BGz 0 0;
    0 0 V1.m 0 0 0;
    0 -V1.m*V1.BGz 0 V1.Ixx 0 -V1.Ixz;
    V1.m*V1.BGz 0 0 0 V1.Iyy 0;
    0 0 0 -V1.Ixz 0 V1.Izz];
V1.Ma=-diag([V1.Xud V1.Yvd V1.Zwd V1.Kpd V1.Mqd
V1.Nrd]);
V1.M=V1.Mrb+V1.Ma;

V1.M3=[V1.m-V1.Xud 0 0;
    0 V1.m-V1.Yvd 0;
    0 0 V1.Izz-V1.Nrd];
```

```
veh=V1;
```

Coriolis of rigid body

```
function Crb=cor_rb(nu)
V1=HRC();
Crb=[0 0 0 V1.m*V1.BGz*nu(6) V1.m*nu(3) -V1.m*nu(2);
    0 0 0 -V1.m*nu(3) V1.m*V1.BGz*nu(6)  V1.m*nu(1);
    0 0 0 V1.m*nu(2)-V1.m*V1.BGz*nu(4) -V1.m*nu(1)-
V1.m*V1.BGz*nu(5) 0;
    -V1.m*V1.BGz*nu(6) V1.m*nu(3) -
V1.m*nu(2)+V1.m*V1.BGz*nu(4) 0 -
V1.Ixz*nu(4)+V1.Izz*nu(6) -V1.Ixz*nu(4)+V1.Izz*nu(6);
    -V1.m*nu(3) V1.m*V1.BGz*nu(6)
V1.m*nu(1)+V1.m*V1.BGz*nu(5) V1.Ixz*nu(4)-V1.Izz*nu(6) 0
V1.Ixz*nu(4)-V1.Izz*nu(6);
    V1.m*nu(2) -V1.m*nu(1) 0 V1.Iyy*nu(5) -
V1.Ixx*nu(4)+V1.Ixz*nu(6) 0];
```

Added Coriolis

```
function Ca=cor_a(nu)
V1=HRC();
Ca=[0 0 0 0 -V1.Zwd*nu(3) V1.Yvd*nu(2);
    0 0 0 V1.Zwd*nu(3) 0 -V1.Xud*nu(1);
    0 0 0 -V1.Yvd*nu(2) V1.Xud*nu(1) 0;
    0 -V1.Zwd*nu(3) V1.Yvd*nu(2) 0 -V1.Nrd*nu(6)
V1.Mqd*nu(5);
    V1.Zwd*nu(3) 0 -V1.Xud*nu(1) V1.Nrd*nu(6) 0 -
V1.Kpd*nu(4);
    -V1.Yvd*nu(2) V1.Xud*nu(1) 0 -V1.Mqd*nu(5)
V1.Kpd*nu(4) 0;];
```

Damping term

```
function D=damp(nu)
V1=HRC();
Dl=-diag([V1.Xu V1.Yv V1.Zw V1.Kp V1.Mq V1.Nr]);
Dc=-diag([-47.49*abs(nu(1)) 0 0 0 0 0]);
D=Dl+Dc;
```

Hydrostatic term

```
function g=g_f(p)
V1=HRC();
g=[0 0 0 V1.m*9.81*V1.BGz*cos(p(5))*sin(p(4))
V1.m*9.81*V1.BGz*sin(p(5)) 0]';
```

Guidance system Simulink

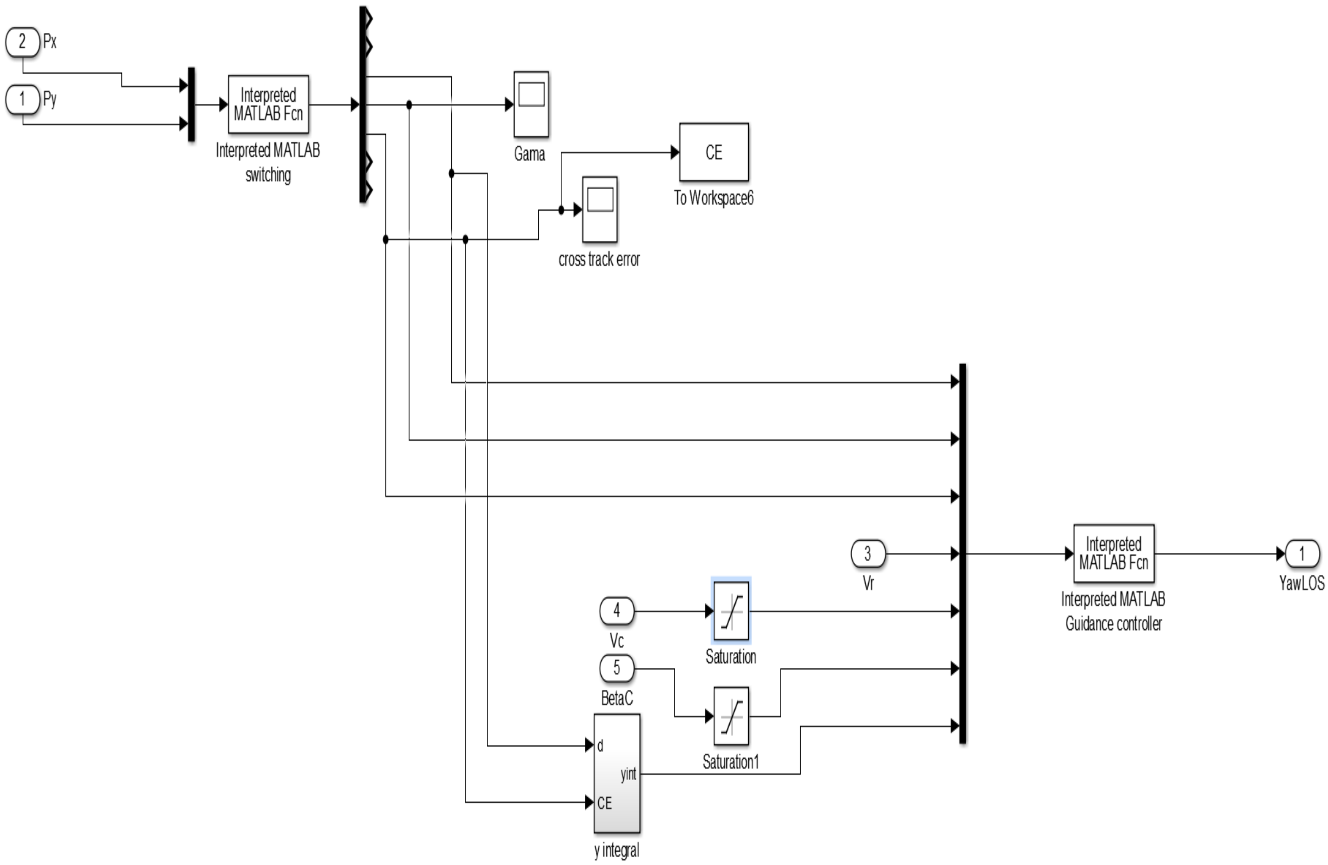

Switching algorithm

```
function SW=switching(position)
Px=position(1,:);
Py=position(2,:);
global n
global Wx
global Wy
Rk=20;
```

```
d=10;
Rx=Wx(n);
Ry=Wy(n);
Tx=Wx(n+1);
Ty=Wy(n+1);
value=((Px-Tx)^2+(Py-Ty)^2);

if(value < (Rk^2))
    n=n+1;
else
    n=n;
end
Rx=Wx(n);
Ry=Wy(n);
Tx=Wx(n+1);
Ty=Wy(n+1);

Gama=atan2d(Ty-Ry,Tx-Rx);
CE=-((Px-Rx)*sind(Gama))+((Py-Ry)*cosd(Gama));
LE=((Px-Rx)*cosd(Gama))+((Py-Ry)*sind(Gama));
PSY=atan2d(-CE,d)+Gama;
SW=[Tx-Rx;Ty-Ry;d;Gama;CE;LE;PSY];
```

Guidance laws controller

```
function PSY=Guidance_controller(input)
d=input(1,:);
Gama=input(2,:);
CE=input(3,:);
Vr=input(4,:);
Vc=input(5,:);
BetaC=input(6,:);
yint=input(7,:);
Vcy=Vc*sind(-Gama+BetaC);
global segma
global s


if(Vr==0)
    Vr=0.005;
else
    Vr=Vr;
end
```

```
alfa=(d*Vcy)/(sqrt(Vr^2-Vcy^2)+0);


if(s==1)     %traditional guidance without disturbance
PSY=atan2d(-CE,d)+Gama;

elseif(s==2)     %adaptive LOS guidamce
    PSY=atan2d(-CE-alfa,d)+Gama;
elseif(s==3)     %integral LOS guidamce
    PSY=atan2d(-CE-(segma*yint),d)+Gama;
else
    PSY=0;
end
```

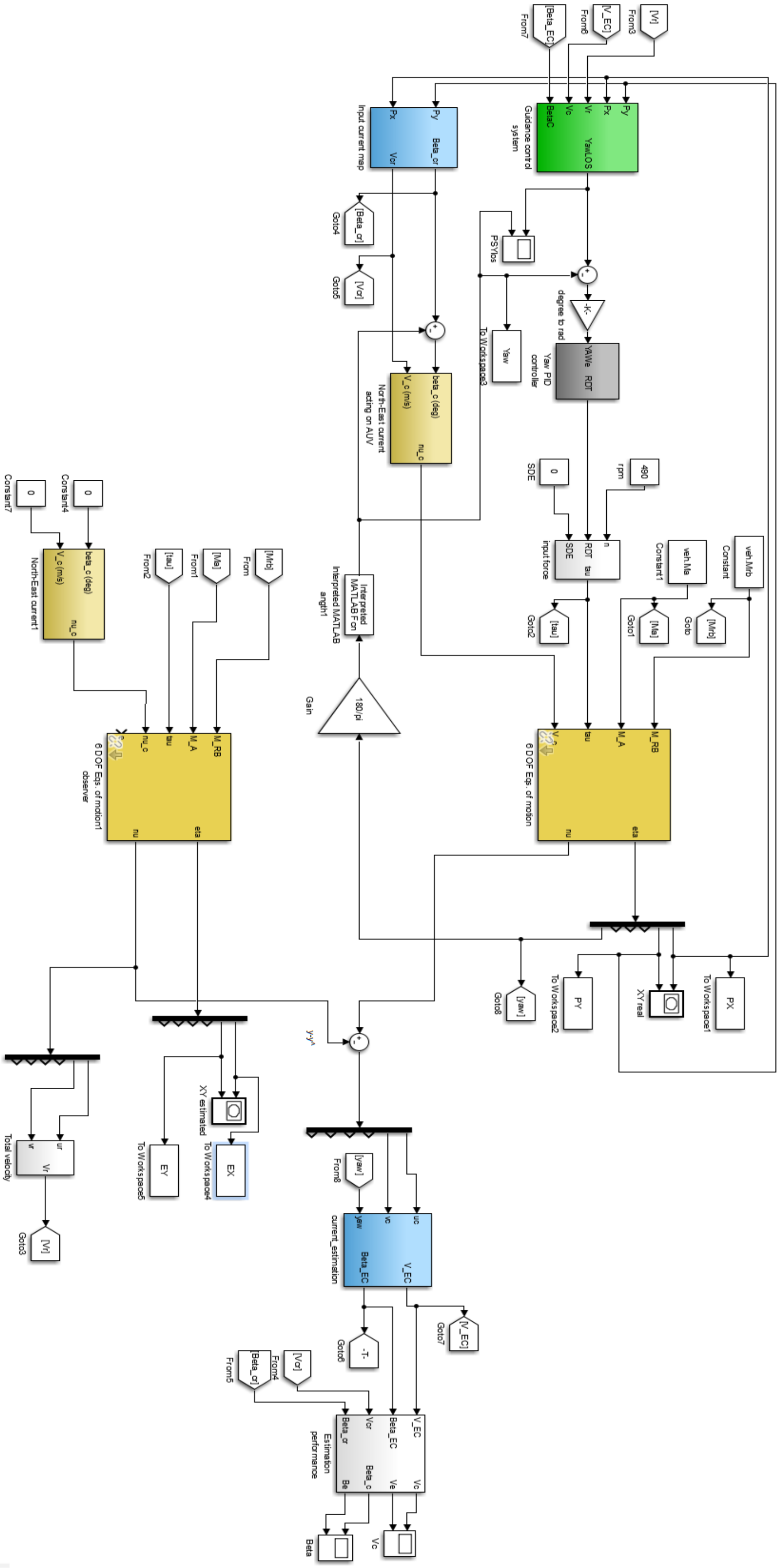
Guidance control system
Input current map
Yaw PID controller
North-East current acting on AUV
input force
6 DOF Eqs. of motion
6 DOF Eqs. of motion1 observer
North-East current1
Interpreted MATLAB Fcn angle1
Gain
To Workspace1
To Workspace2
To Workspace3
To Workspace4
To Workspace5
XY real
XY estimated
Total velocity
current_estimation
Estimation performance
degree to rad
PSYbs
Beta
Vc

الملخـــــص

تعتبر الغواصات ذاتية الحركة من مجالات البحث الرائجة فى العقود الثلاث الاخيرة نظرا لتطبيقاتها الواسعة و المتنوعة كاعلوم البحار و المحيطات و العلوم الجيولوجيا و صناعة البترول و اعمال البحث و الاستكشاف و التطبيقات العسكرية. لذلك فان التكنولوجيا المصاحبة لتلك الغواصات اصبحت اكثر ذكائا و تطورا لتنفيذ المهام المعقدة بدون تدخل بشرى. ومن التحديات الرئيسية لهذه التكنولوجيا هى الاضطرابات البيئية كاتيارات المياه و الامواج والرياح و التى قد تتسبب فى عدم تنفيذ الغواصات مهمتها على النحو الامثل بل و قد يتم فقد الغواصة فى بعض الاحيان و فشل المهمة مع شدة هذه الاضطرابات. فى هذا البحث تم التعامل مع احد هذه الاضطرابات و هو تيارات المياه و اعتبارها المصدر الوحيد المؤثر على الغواصة حيث ان الهدف هو تقدير و حساب هذه التيارات و العمل فى ظل تأثيرها بدون الانحراف عن مسار المهمة. لذلك تم استخدام مراقب (observer) لحساب قيمة و اتجاه هذه التيارات و رسم خريطة بهذه القيم فى نطاق عمل الغواصة. و بنائا على قيم التيارات المحسوبة تم تزويد نظام التوجيه الخاص بالغواصة بهذه المعلومات لاعطاء الاشارات المناسبة للمتحكم حتى يستطيع مكافأة تأثير التيارات و المحافظة على المسار المحدد بدون الانجراف مع التيار.ومن ناحية اخرى , الخرائط الخاصة بالتيارات المعطاه تساعد اجهزة التخطيط فى الغواصة لتجنب المناطق الخطرة كما ان هذه الخرائط قد تساعد فى علوم البحار و تنبؤات الطقس. لتنفيذ هذا التصميم، تم استنباط النموذج الرياضى الغير خطى للغواصة و نموذج التيارات المائية و تنفيذهما فى برنامج المحاكاة (Matlab). بعد ذلك ، تم تصميم مراقب التيارات المحيطة بالغواصة ثم تصميم نظام التوجيه الخاص بالغواصة (LOS) لتوجيه الغواصة فى مسار معين. و من أجل التعامل مع التيارات، تم تعديل نظام التوجيه و جعله متكيف (Adaptive) مع التيارت ثم مقارنته بالنظام الاقدام و هو نظام التوجيه المكمل(ILOS). و قد تم تطبيق العديد من التجارب و الاختبارات لمحاكاة حركة المركبة فى ظل وجود التيارات المائية كما تم تقيم النظام المستخدم فى الظروف المختلفة. و قد نتج عن هذا نجاح نظام المراقبة فى حساب التيارات المائية و تم عمل خرائط بهذه التيارات بالاضاف لتحسين نظام التوجيه مقارنتا بالاساليب الاخرى.

قرار لجنة التحكيم والمناقشة

تم مناقشة هذه الرسالة وإجازتها بتاريخ: / /

أعضاء اللجنة

الأساتذة المشرفون على الرسالة:

الاسم : التوقيع: ....

الوظيفة : أ

الاسم. : التوقيع: ....

الوظيفة :

الأساتذة المحكمون:

الاسم : التوقيع: ....

الوظيفة :أ

الاسم : التوقيع : ....

الوظيفة :

الاسم : التوقيع: ....

الوظيفة : أستا

أودعت هذه الرسالة بالمكتبة بتاريخ / /

الأكاديميــة العربيــة للعلوم و التكنولوجيـا و النقل البحري

كلية الهندســــة و التكنولوجيــا – قسم الهندسة الميكانيكية

تقدير و رسم خرائط تيارات المياه باستخدام غواصة الية الحركة

إعداد

عمر هشام احمد عزت راشد

بكالوريوس الهندسة الميكانيكية

الاكاديمية العربية للعلوم والتكنولوجيا والنقل البحرى

رسالة مقدمة لقسم الهندسة الميكانيكية لإستكمال متطلبات نيل درجة

الماجستير

فى

الهندسة الميكانيكية

إشراف

الاستاذ الدكتور/ عبدالعزيز مرجان
استاذ بكلية الهندسة – قسم الهندسة الميكانيكية
جامعة عين شمس

الاستاذ الدكتور/ محمد عبداللطيف
استاذ بكلية الهندسة – قسم الهندسة الميكانيكية
جامعة المستقبل

الاستاذ الدكتور/ سامح شعبان
استاذ بكلية الهندسة – قسم الهندسة الميكانيكية
الاكاديمية العربية للعلوم و التكنولوجيا

2019